MATHEMATICAL MODELING FOR THE CO-INFECTION OF COFFEE BERRY DISEASE AND COFFEE LEAF RUST WITH OPTIMAL CONTROL AND COST-EFFECTIVENESS ANALYSIS

HALSON OGETO NYABERI (M.Sc.)

I84/21410/2021

A thesis submitted in fulfilment of the requirements for the award of the degree of Ph.D. in Applied Mathematics in the School of Pure and Applied Sciences of Kenyatta University

JUNE 2025

Declaration

This thesis is my original work and has not been presented for a degree in any other University or any other award.

Signature: ..... Date: 15/6/2025
Halson Ogeto Nyaberi (BSc, MSc)

We confirm that the candidate carried out the work reported in this thesis under our supervision.

Signature: ..... Date .....
Prof. Winifred Mutuku,
Department of Mathematics and Actuarial Science,
Kenyatta University.

Signature ..... Date 17-06-2025
Prof. David M. Malonza,
Department of Mathematics and Actuarial Science,
South Eastern Kenya University.

Signature ..... Date 16-06-2025
Dr. Grace Gachigua,
Department of Industrial and Engineering Mathematics,
Technical University of Kenya.

Dedication

I dedicate this thesis to my mother Doris, my wife Jemimah, my daughter Shillomy, and my son Cayden for their love, support, and encouragement.

Acknowledgement

Thanks to Almighty Father, the Greatest, the Most Merciful and the most Gracious, Whose countless blessings bestowed upon me kind, talented, and wise lecturers, who provided me sufficient opportunities and enlightened me towards this research work.

I would like to extend my deepest thanks to my supervisors, Prof. Malonza, Prof. Mutuku, and Dr. Gachigua, for allowing me to undertake this research work under their determined directions. Their support, dedication, encouragement, excellent supervision, and guidance made this thesis possible.

Acknowledgment is also extended to my uncle Zephaniah Oinde for his prayers, support, and encouragement throughout my academic work. I extend special thanks to my mother Doris Kwamboka, my wife Jemimah Kwamboka, my daughter Shillomy, and my son Cayden, whose prayers, dedication, support, and love are the most precious assets I had (and I have) during my research and for all of my endeavors.

Table of Contents

Declaration . . . ii
Dedication . . . iii
Acknowledgement . . . iv
List of Tables . . . viii
List of Figures . . . ix
Nomenclature . . . x
Abstract . . . xi

1 Introduction **1**
1.1 Background Information . . . 1
1.1.1 World coffee production . . . 1
1.1.2 Coffee production in Kenya . . . 2
1.1.3 Coffee Berry Disease . . . 2
1.1.3.1 Effects of CBD on Coffee production . . . 3
1.1.4 Coffee Leaf Rust (CLR) . . . 4
1.1.4.1 The effects of CLR on coffee production . . . 5
1.2 Statement of the Problem . . . 5
1.3 Objectives . . . 5
1.3.1 General Objective . . . 5
1.3.2 Specific Objectives . . . 6
1.4 Justification of the study . . . 6
1.5 Significance of the Study . . . 6

2 Literature Review **8**
2.1 Etiology of plant disease . . . 8
2.2 General models on plant diseases . . . 9
2.3 CBD models . . . 9
2.4 CLR models . . . 10
2.5 Co-infection of CBD and CLR . . . 11

3 Method of Solution **12**
3.1 Formulation of the model . . . 12
3.1.1 Flow Among the Classes . . . 12
3.1.2 Model Assumptions . . . 13
3.1.3 Model Flow Chart . . . 14
3.1.4 Model Flow Equations . . . 14
3.2 Co-infection model analysis . . . 15
3.2.1 Basic Properties of the co-infection model . . . 15
3.2.1.1 Positivity of the solutions of the co-infection model . . . 15
3.2.1.2 Boundedness of the solutions of the co-infection model . . . 16
3.2.2 Equilibrium points of the Co-infection model . . . 18

3.2.2.1 Disease Free Equilibrium point (DFE) . . . 18
3.2.2.2 Endemic Equilibrium point ($\mathscr{E}^*_{kv}$) . . . 19
3.2.3 Reproduction number ($\mathscr{R}_{kv0}$) due co-infection Model . . . 21
3.2.4 The Impact of CBD on CLR . . . 24
3.2.5 Local stability of the Disease Free equilibrium (DFE) . . . 25
3.2.6 Bifurcation Analysis . . . 25
3.3 CBD Model . . . 32
3.3.1 CBD Disease Free Equilibrium point (DFE) . . . 33
3.3.2 Reproduction number ($\mathscr{R}_{k0}$) due to the CBD Model . . . 33
3.3.3 Local Stability of the DFE . . . 34
3.3.4 Global stability of disease-free equilibrium . . . 36
3.3.5 Existence of Endemic Equilibrium ($\mathscr{E}^*_k$) of Coffee Berry Disease . . . 37
3.3.6 Local Stability of Endemic Equilibrium . . . 37
3.3.7 Global Stability of the Endemic Equilibrium Point . . . 38
3.3.8 Bifurcation Analysis . . . 40
3.4 CLR disease model . . . 44
3.4.1 CLR Disease Free Equilibrium point (DFE) . . . 44
3.4.2 Reproduction number ($\mathscr{R}_{v0}$) due to the CLR Model . . . 44
3.4.3 Stability analysis of the CLR model . . . 45
3.4.4 Local Stability of the DFE . . . 45
3.4.5 Global stability of disease-free equilibrium . . . 47
3.4.6 Existence of Endemic Equilibrium ($\mathscr{E}^*_v$) of Coffee Leaf Rust . . . 48
3.4.7 Local Stability of Endemic Equilibrium . . . 48
3.4.8 Global Stability of the Endemic Equilibrium Point . . . 49
3.5 Numerical Simulation . . . 51

4 Optimal Control and cost effectiveness analysis of the co-infection model 58

4.1 Optimal Control Analysis . . . 58
4.1.1 Introduction . . . 58
4.1.2 Co-infection model with controls . . . 58
4.1.3 The Hamiltonian and Optimality System . . . 61
4.1.4 Numerical Simulation . . . 67
4.1.4.1 Strategy 1: Control with prevention of CBD and CLR infections (u_1, u_2) . . . 69
4.1.4.2 Strategy 2: Control with treatment of CBD, CLR and CBD-CLR co-infection (u_3, u_4, u_5) . . . 72
4.1.4.3 Strategy 3: Control with elimination of *Colletotrichum kahawae* and *Hemileia vastatrix* pathogens (u_6, u_7) . . . 72
4.1.4.4 Strategy 4: Control with prevention of CBD and CLR infections and Treatment of CBD, CLR and CBD-CLR co-infection (u_1, u_2, u_3, u_4, u_5) . . . 74
4.1.4.5 Strategy 5: Control with prevention of CBD and CLR infections and elimination of *Colletotrichum kahawae* and *Hemileia vastatrix* pathogens (u_1, u_2, u_6, u_7) . . . 74

4.1.4.6 Strategy 6: Control with the treatment of CBD, CLR and CBD-CLR co-infection and elimination of *Colletotrichum kahawae* and *Hemileia vastatrix* pathogens ($u_3,\ u_4,\ u_5,\ u_6,\ u_7$) 77
4.1.4.7 Strategy 7: Using all interventions ($u_1,\ u_2,\ u_3,\ u_4,\ u_5,\ u_6,\ u_7$) 77
4.2 Cost effectiveness analysis 77

5 Conclusion and Recommendations **83**
5.1 Conclusion 83
5.2 Recommendations 84
REFERENCES 85

List of Tables

3.1 Parameter values 52

4.1 Costs associated with minimizing infected plants 68
4.2 Number of infections averted and total cost of each strategy 80
4.3 First iteration for ICER Computations 80
4.4 Second iteration for ICER Computations 81
4.5 Third iteration for ICER Computations 81
4.6 Fourth iteration for ICER Computations 82
4.7 Fifth iteration for ICER Computations 82
4.8 Sixth iteration for ICER Computations 82

List of Figures

3.1 Flow chart 14
3.2 Graphs showing the dynamics of model system (3.1) when $\mathscr{R}_{kv0} < 1$ . . . 53
3.3 Graphs showing the dynamics of model system (3.1) when $\mathscr{R}_{kv0} > 1$ 56

4.1 Graphs showing the effect of prevention of CBD and CLR infections ($u_1,\ u_2$) on CBD and CLR co-infection model 70
4.2 Graphs effect of treatment of CBD, CLR, and CBD-CLR co-infection ($u_3,\ u_4,\ u_5$) on CBD and CLR co-infection model 71
4.3 Graphs showing the elimination of *Colletotrichum Kahawae* and *Hemileia vastatrix* pathogens ($u_6,\ u_7$) 73
4.4 Graphs showing the effect of prevention of CBD and CLR infections and Treatment of CBD, CLR, and CBD-CLR co-infection ($u_1,\ u_2,\ u_3,\ u_4,\ u_5$) on CBD and CLR co-infection model 75
4.5 Graphs showing the effect of prevention of CBD and CLR infections and elimination of *Colletotrichum kahawae* and *Hemileia vastatrix* pathogens ($u_1,\ u_2,\ u_6,\ u_7$) on CBD and CLR co-infection model 76
4.6 Graphs showing the effect of treatment of CBD, CLR and CBD-CLR co-infection and elimination of *Colletotrichum kahawae* and *Hemileia vastatrix* pathogens ($u_3,\ u_4,\ u_5,\ u_6,\ u_7$) on CBD and CLR co-infection model . . . 78
4.7 Graphs showing the effect of all interventions ($u_1,\ u_2,\ u_3,\ u_4,\ u_5,\ u_6,\ u_7$) on CBD and CLR co-infection model 79

Nomenclature

Abbreviation	**Meaning**
CBD	Coffee berry disease
CLR	Coffee Leaf Rust
ICER	Incremental Cost-Effectiveness Ratio
ICO	International Coffee Organization
Variable	**Definition**
$S(t)$	Susceptible coffee plants at time t
$E_k(t)$	Coffee plants exposed to *Colletotrichum kahawae* (CBD) but not yet symptomatic
$E_v(t)$	Coffee plants exposed to *Hemileia vastatrix* (CLR) but not yet symptomatic
$E_{kv}(t)$	Coffee plants co-exposed to both *Colletotrichum kahawae* and *Hemileia vastatrix*
$I_k(t)$	Coffee plants infected with coffee berry disease (CBD)
$I_v(t)$	Coffee plants infected with coffee leaf rust (CLR)
$I_{kv}(t)$	Coffee plants co-infected with both CBD and CLR
$R(t)$	Recovered coffee plants
$P_k(t)$	Pathogen population of *Colletotrichum kahawae* (CBD) at time t
$P_v(t)$	Pathogen population of *Hemileia vastatrix* (CLR) at time t
$N(t)$	Total number of coffee plants at time t, given by $N(t) = S(t) + E_k(t) + E_v(t) + E_{kv}(t) + I_k(t) + I_v(t) + I_{kv}(t) + R(t)$
Parameter	**Definition**
Λ	Recruitment rate of susceptible coffee trees
ϖ_k	Infection rate of coffee trees with CBD through contact with *Colletotrichum kahawae*
ϖ_v	Infection rate of coffee trees with CLR through contact with *Hemileia vastatrix*
μ	Natural death rate of coffee trees
δ_k	Death rate of coffee trees due to CBD
δ_v	Death rate of coffee trees due to CLR
δ_1	Decay rate of P_k pathogen in the environment
δ_2	Decay rate of P_v pathogen in the environment
q_k	Proportion of coffee trees in $E_v(t)$ that progress to $I_{kv}(t)$ after getting exposed to CBD
q_v	Proportion of coffee trees in $E_k(t)$ that progress to $I_{kv}(t)$ after getting exposed to CLR
ξ_k	Proportion of coffee trees in $E_{kv}(t)$ move to $I_v(t)$ after recovering from CBD only
ξ_v	Proportion of coffee trees in $E_{kv}(t)$ move to $I_k(t)$ after recovering from CLR only
ω_k	Rate at which coffee trees in $E_{kv}(t)$ recover from CBD only
ω_v	Rate at which coffee trees in $E_{kv}(t)$ recover from CLR only
π_k	Recovery rate of coffee trees in $I_{kv}(t)$ from CBD
π_v	Recovery rate of coffee trees in $I_{kv}(t)$ from CLR
η_k	Progression rate of coffee trees in $E_k(t)$ to $I_k(t)$
η_v	Progression rate of coffee trees in $E_v(t)$ to $I_v(t)$
η_{kv}	Progression rate of coffee trees in $E_{kv}(t)$ to $I_{kv}(t)$
ρ_k	Recovery rate of coffee trees in $I_k(t)$ from CLR
ρ_v	Recovery rate of coffee trees in $I_v(t)$ from CBD
ρ_{kv}	Recovery rate of coffee trees in $I_{kv}(t)$ from both CLR and CBD
α_k	Progression rate of coffee trees from $I_k(t)$ to $R(t)$
α_v	Progression rate of coffee trees from $I_v(t)$ to $R(t)$
α_{kv}	Progression rate of coffee trees from $I_{kv}(t)$ to $R(t)$
γ_1	Contribution rate of $E_k(t)$ trees to the increase of P_k pathogen in the environment
γ_2	Contribution rate of $I_k(t)$ trees to the increase of P_k pathogen in the environment
γ_3	Contribution rate of $E_{kv}(t)$ trees to the increase of P_k pathogen in the environment
γ_4	Contribution rate of $I_{kv}(t)$ trees to the increase of P_k pathogen in the environment
τ_1	Contribution rate of $E_v(t)$ trees to the increase of P_v pathogen in the environment
τ_2	Contribution rate of $I_v(t)$ trees to the increase of P_v pathogen in the environment
τ_3	Contribution rate of $E_{kv}(t)$ trees to the increase of P_v pathogen in the environment
τ_4	Contribution rate of $I_{kv}(t)$ trees to the increase of P_v pathogen in the environment

Abstract

In the 1980s, Kenya's coffee production peaked at an average of 1.7 million bags annually. However, this production has declined to below 0.9 million bags annually due to the effects of Coffee Berry Disease (CBD) and Coffee Leaf Rust (CLR). A significant challenge in managing these diseases is the insufficient knowledge of optimal and cost-effective control strategies for their co-infection.

In this thesis, we derive a system of ODEs from a mathematical model for the co-infection of CBD and CLR. Additionally, we demonstrate that when the sub-model reproduction numbers are smaller than unity, the equilibria points of the co-infection sub-models are both locally and globally asymptotically stable. The outcomes of numerical simulations show that CBD-CLR co-infection would die out when it is less than one and persist when the reproduction number is greater than one. An optimal control problem is formulated and solved using Pontryagin's maximum principle. Numerical simulations using fourth-order Runge-Kutta are also conducted, and different combinations of intervention strategies are evaluated to ascertain the optimal strategy for managing the CBD-CLR co-infection. The results indicate that combining all controls would be the best strategy for slowing the spread of the co-infection. A cost-effectiveness analysis is carried out using the incremental cost-effectiveness ratio, and the computations revealed that strategy 5 is the most cost-effective of all strategies for controlling CBD-CLR co-infection. These findings provide valuable insights for policymakers and farmers in optimizing disease control strategies while minimizing costs.

Chapter 1: Introduction

1.1 Background Information

Coffee is a significant cash crop in the economies of various East and Central African countries. It's a substantial source of revenue through foreign exchange gains and employment opportunities, which raises living standards (Rutherford, 2006). According to Mussatto *et al.* (2011), coffee is one of the most popular beverages in the world.

Coffee was discovered in Ethiopia in about AD 850. After that, it spread to different parts of the world like Persia, South India, America, and northern Africa despite the imposition of fines by the Islamic religious leaders of Cairo in Mecca (Smith, 1985).

1.1.1 World coffee production

Coffee is produced in different parts of the world in two species, Arabica and Robusta species of coffee. According to Coffee and Health (2021), Arabica coffee is produced in Latin America, Eastern Africa, and Arabia, and Robusta coffee is produced in South America, Southeast Asia, and Western and Central Africa.

Szenthe (2019) reports that Brazil has been the leading coffee-producing country in the world for more than 150 years; in 2016, it produced 2.595 million metric tonnes of coffee beans. Ethiopia is Africa's top coffee-producing country and the world's fifth-largest coffee producer.

According to Fairtrade (2021), 80% of coffee is produced by 25 million small-scale farmers worldwide. Coffee production has created employment opportunities since approximately 125 million people depend heavily on it worldwide. In reference to Souza (2008), in Brazil, 7 million people are employed to cultivate, harvest, process, market, and transport coffee.

1.1.2 Coffee production in Kenya

Coffee is one of the major cash crops in Kenya. According to the Coffee Research Institute of Kenya, coffee is grown in large and small-scale farms, whereby 70% of coffee production is from small-scale farms. The regions where coffee is grown in Kenya are: Mt. Kenya, Rift Valley, Nyanza, and Western. These comprise 32 counties out of a total of 47 counties in Kenya (ICO, 2019).

According to ICO (2019), there are around 700 thousand coffee farmers in Kenya, and it is estimated that 5 million Kenyans were hired to work in the production chain of coffee. Thus, coffee production earns a living for several Kenyans and contributes to the economy's growth through foreign exchange earnings amounting to an average of US$ 230 million annually.

In the 1980s, coffee production in Kenya peaked at an average of 1.7 million bags annually (Condliffe *et al.*, 2008). Since then, this production has declined to the current output of below 0.9 million bags annually due to several factors like climate change leading to erratic rainfall and droughts, high production costs due to rising labor and input prices, poor market structures with low farmer returns, pests and diseases, aging coffee plantations, lack of access to improved technologies, a shift by farmers towards more profitable crops, land use changes (uprooting of coffee bushes), trade imbalances, nutritional deficiencies, and management (ICO, 2019). For instance, Coffee Berry Disease (CBD) and Coffee Leaf Rust (CLR) are some of the diseases that have contributed to the decline of coffee production in Kenya.

1.1.3 Coffee Berry Disease

Coffee Berry Disease is a fungal disease caused by *Colletotrichum kahawae*. The first documentation of CBD dates back to 1922 in western Kenya. The disease led to the severe destruction of coffee plantations in the region (McDonald, 1926). After that, the disease spread to all Arabica coffee-producing countries in Africa like Angola, Malawi,

Zimbabwe, and Cameroon (Silva, 2010).

The fungus *Colletotrichum kahawae* infects all stages of the coffee crop, from flowers to mature coffee berries, causing premature fruit drop and berry rot (Giddisa , 2016). The primary sources of inoculum for the disease are dead branches, twig bark, and mummified berries. Germination of *Colletotrichum conidium* can occur 24 hours after conidia come into contact with the host plant tissues. Then, the elongation of the germ tubes occurs, and the apical segment is later differentiated into an appressorium. The hyphae infection arising from these appressoria then colonizes the fruit, causing tissue necrosis on which new acervuli develop (Silva, 2010). Most infected coffee berries fall prematurely, but as a source of secondary inoculum, they remain attached to infected berries. Rainfall disperses most conidia. What portion of the pathogen persists in the seasons is uncertain. There is a sexual phase, but in spreading coffee berry disease, it does not play a role (Mouen *et al.*, 2010).

CBD has two different symptoms termed "active lesion" and "scab lesion" on green berries. Active lesions are visible as tiny dark sunken spots that quickly spread to consume as much as the entire berry. The pathogen sporulates quickly and is shown on the lesion's surface by a pale pink coating. The scab lesion visible as cocky, tiny pale tan sunken, is evidenced on young and mature berries (Masaba and Van Der Vossen, 1982). When infection occurs early and climatic conditions promote disease production, berries' growth is delayed, leading to mummified berries (Mouen *et al.*, 2010).

1.1.3.1 Effects of CBD on Coffee production

Coffee berry disease infects coffee berries, the harvestable portion of the crop. This causes direct yield loss even if it cannot reduce the plant's vegetative vigor or subsequent productive capacity. Also, CBD causes the pulp to adhere to the coffee bean, hence making it more challenging to process, and it may lower the quality of processed coffee (Waller, 1985).

CBD is a significant constraint to coffee production in Kenya and Africa. The impact of CBD in Kenya was strongly felt during the 1962/1963 and 1967/1968 crop years, when losses in coffee production increased to 80% (Gichimu and Omondi, 2010).

According to ICO (2019), there are around 700 thousand coffee farmers in Kenya, and it is estimated that 5 million Kenyans were hired to work in the coffee production chain. This implies that CBD threatens the livelihood of millions because direct losses of the crop reduce the income.

1.1.4 Coffee Leaf Rust (CLR)

Coffee leaf rust (CLR), which is caused by the fungus *Hemileia vastatrix*, is one of the most common diseases affecting coffee worldwide. It is actually Kenya's second most serious after CBD (Gichuru *et al.*, 2012).

CLR was first discovered in Kenya in 1912 (Gichuru *et al.*, 2021), but records show that it was first discovered on uncultivated coffee in Western Kenya near Lake Victoria in 1861 (Ferreira and Boley, 1991), suggesting that the disease could have occurred earlier in Eastern Africa.

Spores spread the CLR Infection. Uredospore germination occurs on the underside of the leaf through germ holes in the spore. When the hole passes over or near a stoma, appressoria are formed, producing vesicles used by hyphae to gain access to the substomatal cavity and continue their growth within the leaf tissues (Nutman and Roberts, 1964) .

A tiny, lighter patch forms on the leaf three weeks after infection, followed by the bright orange uredospores a few days later. These are budded off from the terminals of fine hyphae that have protruded through the stomata by this time, and the entire spore-producing region forms the distinctive "pustule" (Nutman and Roberts, 1964).

CLR is dispersed by water. This dispersal only works over very short distances. After and during dispersal, germination, and infection must occur (Nutman and Roberts, 1964).

1.1.4.1 The effects of CLR on coffee production

CLR impacts coffee production in both direct and indirect ways. Direct consequences include a reduction in the quantity and quality of harvested crops. According to Alworah and Gichuru (2014), CLR may lead to loss of berries up to 70% and foliage up to 50%. Indirect effects include higher costs to monitor and combat the disease, such as stumping and replacing diseased plants.

1.2 Statement of the Problem

The co-infection of CBD and CLR remains endemic due to a lack of sufficient knowledge about their dynamics and the absence of optimal, cost-effective control strategies. Since 1913 and 1922, when CLR and CBD were respectively reported in Kenya, efforts by the government, several development partners, and the private sector have been geared toward fighting the diseases. Although these efforts have gathered a lot of steam in the last decade, coffee production volumes do not seem to respond as expected. Thus, we need to address this problem. This research seeks to formulate a mathematical model for the co-infection of CBD and CLR and use the model to quantify the magnitude of the interventions, such as prevention of CBD infection, prevention of CLR infection, the treatment of CBD-infected coffee plants, the treatment of CLR-infected coffee plants, the treatment of CBD-CLR Co-infected coffee plants, elimination of *Colletotrichum kahawae* pathogens, and elimination of *Hemileia vastatrix* pathogens, so that an optimal control and cost-effective strategy for the co-infection of CBD and CLR is obtained.

1.3 Objectives

1.3.1 General Objective

To obtain an optimal control strategy for Coffee Berry Disease and Coffee Leaf Rust co-infection through mathematical modeling using prevention of CBD infection, prevention of CLR infection, the treatment of CBD-infected coffee plants, the treatment of CLR-infected coffee plants, the treatment of CBD-CLR Co-infected coffee plants, elimination

of *Colletotrichum kahawae* pathogens, and elimination of *Hemileia vastatrix* pathogens as the interventions.

1.3.2 Specific Objectives

The specific objectives of this study are to;

i. Formulate a deterministic mathematical model for Coffee Berry Disease and Coffee Leaf Rust co-infection.

ii. Perform stability analysis of the model's disease-free and endemic equilibrium points.

iii. Perform numerical simulation of the model

iv. Determine the optimal control strategy for CBD and CLR.

v. Perform cost-effectiveness analysis.

1.4 Justification of the study

Much work has been done to understand the properties and management of CBD and CLR. However, a cost-effective and optimal control strategy must be implemented to control CBD and CLR effectively. To our knowledge, no CBD and CLR research with an optimal cost-effective control strategy has been conducted. Our research aims to bridge this information gap.

1.5 Significance of the Study

The study covers the co-infection of coffee berry disease and coffee leaf rust with a cost-effective optimal control strategy. This will be of great benefit to coffee farmers, the Coffee Research Institute, and the Ministry of Agriculture, Livestock and Fisheries in planning, budgeting resource allocation, policy formulation, sensitizing farmers, and making informed decisions relating to the control of co-infection of coffee berry disease and coffee leaf rust. It will help the Kenya Coffee Producers Association (KCPA) and Kenya Plant Health Inspectorate Service (KEPHIS) in health inspection and regulatory frameworks.

The study also contributes to the current mathematical studies on the co-infection dynamics of coffee berry disease and coffee leaf rust.

Chapter 2: Literature Review

2.1 Etiology of plant disease

The etiology of plant disease refers to the study of its causes, which can be classified into biotic (living) and abiotic (nonliving) factors. Biotic causes include pathogens such as fungi, bacteria, viruses, nematodes, protozoa, and parasitic plants. These organisms invade plant tissues, disrupt physiological processes, and lead to symptoms such as wilting, yellowing, and necrosis (Agrios, 2005). Fungal pathogens, for example, cause rusts, blights, and mildew, while bacterial infections result in leaf spots and wilts. Viral diseases often manifest as mosaics and stunting, whereas nematodes attack plant roots, reducing water and nutrient uptake. In contrast, abiotic factors such as nutrient imbalances, extreme temperatures, drought, waterlogging, soil pH variations, and chemical pollutants can also cause plant disorders without the involvement of infectious agents (Schumann and D'Arcy, 2012).

The disease triangle explains plant disease development, which highlights the interaction between a susceptible host, a virulent pathogen, and favorable environmental conditions. If these components are absent, the disease may not develop or be less severe (Agrios, 2005). Pathogens spread through various means, including airborne spores, movement of soil and water, infected planting materials, insect vectors, and mechanical transmission through contaminated tools or human activity (Schumann and D'Arcy, 2012). Managing plant diseases involves an integrated approach, including cultural practices such as crop rotation and sanitation, biological control using beneficial microorganisms, chemical treatments such as fungicides, and the use of resistant plant varieties (Strange, 2003).

Understanding plant disease etiology is crucial for developing sustainable agricultural practices and improving food security. By identifying the causes and mechanisms of plant diseases, researchers and farmers can implement preventive and control measures to

maintain healthy crops and improve productivity. Mathematical models have been used to study human, animal, and plant disease dynamics, (Nannyonga, 2015).

2.2 General models on plant diseases

Several mathematical models have been created to investigate the effects of preventive and control techniques on the dynamics of plant disease spread. A study for the dynamics of the transmission of plant diseases with and without a roguing mechanism was carried out by (Chan and Jeger, 1994). The study's results demonstrated that roguing mechanisms help prevent the transmission of plant diseases.

The mathematical model of induced resistance to plant disease presented by (Latif and Syaza, 2014) divides the plant population into three compartments: susceptible, resistant, and diseased. The model outcomes showed that when the elicitor application is done on plants before the inoculation of pathogens, plants are less severely affected by the diseases.

In addition, a model to study the optimal control of Rice Tungro Disease with biological agents and insecticides was proposed by (Suryaningrat *et al.*, 2020). From this study, they found that the combination of biological agents and insecticide can significantly eradicate the infected rice plants and vectors

2.3 CBD models

Most of the reviews presented on coffee berry disease provide qualitative studies that describe the current status and the existing strategies to manage the spread and actions of the new epidemic (see, for example, McDonald (1926), Masaba and Van Der Vossen (1982), Silva (2010), Mouen *et al.* (2010), etc.).

Researchers have started to formulate mathematical models for CBD. For example, Melese *et al.* (2022) developed a nonlinear deterministic mathematical model to analyze the transmission dynamics of Coffee Berry Disease (CBD) on coffee farms. Using a compartmental approach, it identified disease-free and endemic equilibrium points, with stability con-

firmed through mathematical techniques. Sensitivity analysis highlighted key parameters influencing disease spread, particularly the role of climate variability in increasing infection rates. The research emphasized that favorable climatic conditions enhance pathogen and vector production, making adaptation strategies essential. Numerical simulations suggested effective chemical, cultural, and biological control measures can help manage CBD. The findings conclude that the disease persists if the basic reproduction number (R_0) is greater than one, underscoring the need for optimized intervention strategies.

2.4 CLR models

Several CLR models have been considered in recent years. The factors that affect CLR intensity in several plots in Honduras were investigated by (Avelino *et al.*, 2006). Their study established that the number of leaves on the coffee plants and their production were positively related to the spread of the pandemic. The growth of epidemics was adversely correlated with soil pH and fertilization.

By modeling the evolution of the fraction of infected bushes and farms, (Vandermeer and Rohani, 2014) investigates the connection between the local and regional dynamics of the CLR model. The study results showed that including a blue sky bifurcation in the model's basic structure can induce tipping point behavior, implying that the emergence of disease epizootics may be unforeseen.

A study on the germination and infection risk in Colombia and neighboring countries based on the climate was carried out by (Bebber *et al.*, 2016). According to their findings, an increase in canopy moisture increases the risk of infection.

Research by Vandermeer *et al.* (2018) used an SI epidemiological model of the host to represent the CLR dynamics on a coffee farm in Chiapas. They discovered that infection rates between components are less homogeneous than infection rates within connected components, implying that the disease's early stages have a pattern that may be detected using basic network theory concepts.

Djuikem *et al.* (2021a) constructed and analyzed a PDE model to describe CLR transmission in a coffee farm during wet and dry seasons and its behavior over time. They used a biocontrol based on a mycoparasite like *Lecanicillium lecanii* always to prevent CLR reproduction in their model. According to the findings, a biocontrol efficacy of 75% is sufficient to maintain berry production in the plantation while resulting in minimal yield loss. Furthermore, higher efficiency leads to the eradication of disease.

Djuikem *et al.* (2021b) proposed a model of the coffee leaf rust (CLR) With optimal control. Their study found that coffee growers should maximize the amount of mycoparasitic fungi (within prescribed boundaries) just during the first year and stop treating in subsequent seasons.

2.5 Co-infection of CBD and CLR

The co-infection concept has been captured in several mathematical models of infectious diseases. For instance, Nthiiri *et al.* (2015), performed mathematical modelling of tuberculosis as an opportunistic respiratory co-infection in HIV/AIDS in the presence of protection. According to the numerical simulations of this study, reduced disease prevalence rates result from improved protection against a disease, which reduces the number of new cases of the illness. Thus, efforts to raise public knowledge of preventative measures should be strengthened.

The phenomenon of co-infection, like human diseases, is expected to alter the course of infection in co-infected plants (Anco, 2018). However, co-infection in plants such as coffee is a topic that hasn't gotten much attention. Thus, this research seeks to study the co-infection of CBD and CLR.

Chapter 3: Method of Solution

3.1 Formulation of the model

The coffee plants in the plantation are divided into eight groups at any time t, namely: the susceptible coffee plants S(t), coffee plants exposed to *Colletotrichum kahawae* (the infected coffee plants which have not shown symptoms) $E_k(t)$, plants exposed to *Hemileia vastatrix* $E_v(t)$, co-exposed coffee plants $E_{kv}(t)$, the CBD infected coffee plants $I_k(t)$, the CLR infected coffee plants $I_v(t)$, the co-infected coffee plants $I_{kv}(t)$ and recovered coffee plants $R(t)$. Let N(t) the total number of coffee plants, then $N(t) = S(t) + E_k(t) + I_k(t) + E_v(t) + I_v(t) + E_{kv}(t) + I_{kv}(t) + R(t)$.

The number of *Colletotrichum kahawae* and *Hemileia vastatrix* pathogens in the plantation at any time t is $P_k(t)$ and $P_v(t)$ respectively.

3.1.1 Flow Among the Classes

The susceptible coffee trees are recruited at a rate Λ. Some coffee trees will vacate all classes due to natural death at a constant rate μ. Susceptible coffee trees are exposed to the disease through contact with the pathogen. Thus, Coffee trees are exposed to the coffee berry disease through contact with *Colletotrichum kahawae* at a rate ϖ_k . Also, Coffee trees are exposed to coffee leaf rust through contact with *Hemileia vastatrix* at the rate ϖ_v. By these rates, coffee trees in $S(t)$ class will move to $E_k(t)$ class at the rate ϖ_k and $E_v(t)$ class at the rate ϖ_v.

Some coffee trees in $E_k(t)$ are exposed to coffee leaf rust and move to $E_{kv}(t)$ and $I_{kv}(t)$ at the rates $(1 - q_v)\varpi_v$ and $q_v\varpi_v (0 < q_v < 1)$ respectively, others progress to $I_k(t)$ at the rate η_k and others progress to $R(t)$ at the rate α_k. Similarly, some coffee trees in $E_v(t)$ are exposed to coffee berry disease and move to $E_{kv}(t)$ and $I_{kv}(t)$ at the rates $(1 - q_k)\varpi_k$ and $q_k\varpi_k (0 < q_k < 1)$ respectively, while others progress to I_v at the rate η_v and others

progress to $R(t)$ at the rate α_v.

A fraction of coffee trees in $E_{kv}(t)$ class progress to $I_{kv}(t)$ at the rate η_{kv}. Other coffee trees in $E_{kv}(t)$ recover from CLR and move to $E_k(t)$ and $I_k(t)$ at the rate $(1-\xi_v)\omega_v$ and $\xi_v\omega_v(0<\xi_v<1)$ respectively. In addition, other coffee trees in $E_{kv}(t)$ recover from CBD and move to $E_v(t)$ and $I_v(t)$ at the rates $(1-\xi_k)\omega_k$ and $\xi_k\omega_k$ $(0<\xi_k<1)$ respectively, and both CBD and CLR at the rate α_{kv}.

Some coffee trees in $I_k(t)$ are infected by CLR at the rate ϖ_v, and move to $I_{kv}(t)$ and others recover and progress to $R(t)$ at the rate ρ_k. Similarly, some coffee trees in $I_v(t)$ are infected by CBD at the rate ϖ_k and move to $I_{kv}(t)$ and others recover and progress to $R(t)$ at the rate ρ_v. Coffee trees in $I_{kv}(t)$ class recover from CLR at the rate π_v and move to $I_k(t)$, CBD at the rate π_k and move to $I_v(t)$, and both CLR and CBD at the rate ρ_{kv} and progress to $R(t)$.

A proportion of coffee trees in $I_k(t)$ and $I_{kv}(t)$ classes will die from CBD-induced deaths at the rate δ_k, and another proportion in $I_v(t)$ and $I_{kv}(t)$ classes will die from CLR-induced deaths at the rate δ_v. In addition, coffee trees $E_k(t)$, $I_k(t)$, $E_{kv}(t)$ and $I_{kv}(t)$ contribute to the increase of P_k pathogen in the environment at the rates γ_1, γ_2, γ_3 and γ_4 respectively. Also, coffee trees $E_v(t)$, $I_v(t)$, $E_{kv}(t)$ and $I_{kv}(t)$ contribute to the increase of P_v pathogen in the environment at the rates τ_1, τ_2, τ_3 and τ_4 respectively. Finally, pathogens in P_k and P_v classes decay at the rate δ_1 and δ_2 respectively.

3.1.2 Model Assumptions

The following are the assumptions of the model:

i) The fungus multiplies only on the coffee plant.

ii) There is permanent immunity upon recovery.

iii) There is a disease-related death of coffee plants.

iv) There is on planting once coffee plants die(dry).

v) Infection can only occur one after the other.

3.1.3 Model Flow Chart

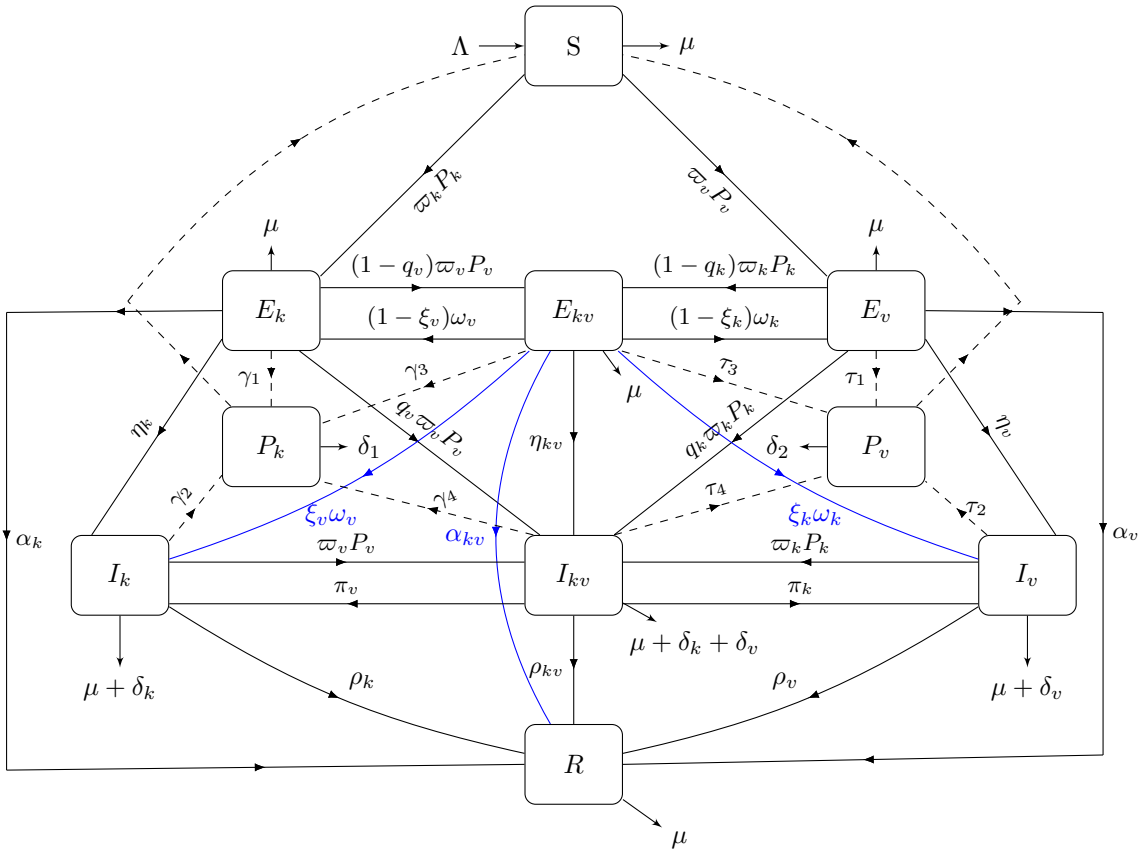

Figure 3.1: Flow chart

3.1.4 Model Flow Equations

From the flow chart, we derive the following equations:

$$\begin{aligned}
\frac{dS}{dt} &= \Lambda - (\varpi_k P_k + \varpi_v P_v + \mu)S \\
\frac{dE_k}{dt} &= \varpi_k P_k S + (1-\xi_v)\omega_v E_{kv} - (\alpha_k + \varpi_v P_v + \mu + \eta_k)E_k \\
\frac{dE_v}{dt} &= \varpi_v P_v S + (1-\xi_k)\omega_k E_{kv} - (\alpha_v + \varpi_k P_k + \mu + \eta_v)E_v \\
\frac{dE_{kv}}{dt} &= (1-q_v)\varpi_v P_v E_k + (1-q_k)\varpi_k P_k E_v - (\alpha_{kv} + \omega_k + \omega_v + \mu + \eta_{kv})E_{kv} \\
\frac{dI_k}{dt} &= \eta_k E_k + \xi_v\omega_v E_{kv} + \pi_v I_{kv} - (\varpi_v P_v + \rho_k + \mu + \delta_k)I_k
\end{aligned}$$

$$\begin{aligned}
\frac{dI_v}{dt} &= \eta_v E_v + \xi_k \omega_k E_{kv} + \pi_k I_{kv} - (\varpi_k P_k + \rho_v + \mu + \delta_v) I_v \\
\frac{dI_{kv}}{dt} &= q_v \varpi_v P_v E_k + q_k \varpi_k P_k E_v + \varpi_k P_k I_v + \varpi_v P_v I_k + \eta_{kv} E_{kv} - (\pi_v + \pi_k + \rho_{kv} + \mu + \delta_k + \delta_v) I_{kv} \\
\frac{dP_k}{dt} &= \gamma_1 E_k + \gamma_2 I_k + \gamma_3 E_{kv} + \gamma_4 I_{kv} - \delta_1 P_k \\
\frac{dP_v}{dt} &= \tau_1 E_v + \tau_2 I_v + \tau_3 E_{kv} + \tau_4 I_{kv} - \delta_2 P_v \\
\frac{dR}{dt} &= \alpha_k E_k + \alpha_v E_v + \alpha_{kv} E_{kv} + \rho_k I_k + \rho_v I_v + \rho_{kv} I_{kv} - \mu R
\end{aligned} \tag{3.1}$$

3.2 Co-infection model analysis

3.2.1 Basic Properties of the co-infection model

We discuss the Positivity and Boundedness of the solutions of the model.

3.2.1.1 Positivity of the solutions of the co-infection model

Lemma 1. *Let* $S_0 > 0$, $E_{k0} \geq 0$,$E_{v0} \geq 0$, $E_{kv0} \geq 0$,$I_{k0} \geq 0$, $I_{v0} \geq 0$, $I_{kv0} \geq 0$, $P_{k0} \geq 0$, $P_{v0} \geq 0$, *and* $R_0 \geq 0$ *be the initial conditions of the system (3.1) then the solutions* S, E_k,E_v, E_{kv},I_k, I_v, I_{kv}, P_k, P_v, *and* R *are non-negative* $\forall\, t > 0$

Proof. From system (3.1), we define T as the maximum endemic time, and it is given by $T = \sup\{t > 0 \mid S(\tau) > 0,\ E_k(\tau) \geq 0,\ E_v(\tau) \geq 0,\ E_{kv}(\tau) \geq 0,\ I_k(\tau) \geq 0,\ I_v(\tau) \geq 0,\ I_{kv} \geq 0,\ P_k(\tau) \geq 0,\ P_v \geq 0,\ R(\tau) \geq 0\ \forall \tau \in [0,\ t]\}$.

Consider $S_0 > 0$, $E_{k0} \geq 0$,$E_{v0} \geq 0$, $E_{kv0} \geq 0$,$I_{k0} \geq 0$, $I_{v0} \geq 0$, $I_{kv0} \geq 0$, $P_{k0} \geq 0$, $P_{v0} \geq 0$, $R_0 \geq 0$. Also, let us consider the first equation of system (3.1)

$$\frac{dS}{dt} = \Lambda - (\varpi_k P_k + \varpi_v P_v + \mu) S \tag{3.2}$$

Equation (3.2) can be written as

$$\frac{dS}{dt} + (\varpi_k P_k + \varpi_v P_v + \mu) S = \Lambda \tag{3.3}$$

upon multiplication of both sides of equation (3.3) by the integrating factor, we get

$$\frac{d}{dt}\left(S(t) \exp\left[\int_0^T (\varpi_k P_k + \varpi_v P_v + \mu)(s) ds \right] \right) = \Lambda \exp\left(\int_0^T (\varpi_k P_k + \varpi_v P_v + \mu)(s) ds \right) \tag{3.4}$$

Integrating both sides of equation (3.4) from 0 to T, we get

$$S(T) = \exp\left[-\int_0^T (\varpi_k P_k + \varpi_v P_v + \mu)(s)ds\right]\left\{S_0 + \int_0^T \Lambda \exp\left[\int_0^{\tilde{T}} (\varpi_k P_k + \varpi_v P_v + \mu)(\tau)d\tau\right] d\tilde{T}\right\} \tag{3.5}$$

Thus $S(t) > 0 \; \forall \; t > 0$.

For the second equation of system (3.1), we have

$$\begin{aligned}\frac{dE_k}{dt} =& \varpi_k P_k S + (1-\xi_v)\omega_v E_{kv} - (\alpha_k + \varpi_v P_v + \mu + \eta_k)E_k \\ \geq& -(\alpha_k + \varpi_v P_v + \mu + \eta_k)E_k\end{aligned}$$

$$\begin{aligned}\Rightarrow E_k \geq& E_{k0}\exp\left[-\int_0^T (\alpha_k + \varpi_v P_v + \mu + \eta_k)(s)ds\right] \\ \geq& E_{k0}\exp\left\{-\left[(\alpha_k + \mu + \eta_k)T + \int_0^T \varpi_v P_v(s)ds\right]\right\} \geq 0\end{aligned} \tag{3.6}$$

Proving the remaining eight equations in the same manner, we obtain

$E_v(t) \geq 0$, $E_{kv}(t) \geq 0$,$I_k(t) \geq 0$, $I_v(t) \geq 0$, $I_{kv}(t) \geq 0$, $P_k(t) \geq 0$, $P_v(t) \geq 0$ $R(t) \geq 0$.

Thus all the solutions are non-negative $\forall \; t > 0$. □

3.2.1.2 Boundedness of the solutions of the co-infection model

We demonstrate that every feasible solution is uniformly bounded in a proper subset $\mathscr{D} = \mathscr{D}_N \cup \mathscr{D}_{P_k} \cup \mathscr{D}_{P_v} \subset \mathbb{R}_+^8 \times \mathbb{R}_+^1 \times \mathbb{R}_+^1$.

Lemma 2. *Let the initial conditions of system (3.1) be non-negative in* $\mathbb{R}_+^{10}$,
$\mathscr{D}_N = \left\{(S,\ E_k,\ E_v,\ E_{kv},\ I_k,\ I_v,\ I_{kv},\ R) \in \mathbb{R}_+^8 : N(t) \leq \frac{\Lambda}{\mu}\right\}$,
$\mathscr{D}_{P_k} = \left\{P_k \in \mathbb{R}_+^1 : P_k(t) \leq \frac{\Lambda(\gamma_1+\gamma_2+\gamma_3+\gamma_4)}{\mu\delta_1}\right\}$ *and* $\mathscr{D}_{P_v} = \left\{P_v \in \mathbb{R}_+^1 : P_v(t) \leq \frac{\Lambda(\tau_1+\tau_2+\tau_3+\tau_4)}{\mu\delta_2}\right\}$
then the set $\mathscr{D} = \mathscr{D}_N \cup \mathscr{D}_{P_k} \cup \mathscr{D}_{P_v} \subset \mathbb{R}_+^8 \times \mathbb{R}_+^1 \times \mathbb{R}_+^1$ *is positively invariant*

Proof. In this lemma, we are required to show that $\mathscr{D}_N$, $\mathscr{D}_{P_k}$ and $\mathscr{D}_{P_v}$ are positively invariant. To start, We sum the first seven equations and the last equation of the system

(3.1) to get

$$\frac{dN}{dt} = \Lambda - \mu N - (\delta_k I_k + \delta_v I_v + \delta_k I_{kv} + \delta_v I_{kv}). \tag{3.7}$$

In the absence of the CBD and CLR, we have

$$\frac{dN}{dt} \leq \Lambda - \mu N. \tag{3.8}$$

Upon solving equation (3.8) for N, we get

$$N(t) \leq \frac{\Lambda}{\mu} + \left\{ N_0 - \frac{\Lambda}{\mu} \right\} e^{-\mu t}. \tag{3.9}$$

Thus

$$N(t) \leq \frac{\Lambda}{\mu} \text{ as } t \to \infty.$$

It follows that the feasible region for the coffee plant population in the system (3.1) is defined by

$$\mathscr{D}_N = \left\{ (S,\ E_k,\ E_v,\ E_{kv},\ I_k,\ I_v,\ I_{kv},\ R) \in \mathbb{R}_+^8 : N(t) \leq \frac{\Lambda}{\mu} \right\}$$

Considering the eighth equation of system (3.1), the equation for *Colletotrichum kahawae* pathogens

$\frac{dP_k}{dt} = \gamma_1 E_k + \gamma_2 I_k + \gamma_3 E_{kv} + \gamma_4 I_{kv} - \delta_1 P_k.$

We rewrite it as

$$\frac{dP_k}{dt} \leq \frac{\Lambda(\gamma_1 + \gamma_2 + \gamma_3 + \gamma_4)}{\mu} - \delta_1 P_k. \tag{3.10}$$

Solving equation (3.10) we get

$$P_k(t) \leq \frac{\Lambda(\gamma_1 + \gamma_2 + \gamma_3 + \gamma_4}{\mu\delta_1} + \left(P_{k0} - \frac{\Lambda(\gamma_1 + \gamma_2 + \gamma_3 + \gamma_4)}{\mu\delta_1} \right) e^{-\delta_1 t} \tag{3.11}$$

Hence

$$P_k(t) \leq \frac{\Lambda(\gamma_1 + \gamma_2 + \gamma_3 + \gamma_4)}{\mu\delta_1} \text{ as } t \to \infty.$$

$$\mathscr{D}_{P_k} = \left\{ P_k \in \mathbb{R}_+^1 : P_k(t) \leq \frac{\Lambda(\gamma_1 + \gamma_2 + \gamma_3 + \gamma_4)}{\mu\delta_1} \right\}$$

From the ninth equation of system (3.1), the equation for *Hemileia vastatrix* pathogens

$\frac{dP_v}{dt} = \tau_1 E_v + \tau_2 I_v + \tau_3 E_{kv} + \tau_4 I_{kv} - \delta_2 P_v,$

we have

$$\frac{dP_v}{dt} \leq \frac{\Lambda(\tau_1 + \tau_2 + \tau_3 + \tau_4)}{\mu} - \delta_2 P_v. \tag{3.12}$$

Upon solving equation (3.12) for $P_v(t)$, we obtain

$$P_v(t) \leq \frac{\Lambda(\tau_1 + \tau_2 + \tau_3 + \tau_4)}{\mu\delta_1} + \left(P_{v0} - \frac{\Lambda(\tau_1 + \tau_2 + \tau_3 + \tau_4)}{\mu\delta_2}\right) e^{-\delta_2 t}. \tag{3.13}$$

Therefore

$$P_v(t) \leq \frac{\Lambda(\tau_1 + \tau_2 + \tau_3 + \tau_4)}{\mu\delta_2} \text{ as } t \to \infty.$$

Hence, the feasible region for *Hemileia vastatrix* pathogens is given by

$$\mathscr{D}_{P_v} = \left\{ P_v \in \mathbb{R}^1_+ : P_v(t) \leq \frac{\Lambda(\tau_1 + \tau_2 + \tau_3 + \tau_4)}{\mu\delta_2} \right\}$$

Consequently, the feasible region defined by the set $\mathscr{D} = \mathscr{D}_N \cup \mathscr{D}_{P_k} \cup \mathscr{D}_{P_k} \subset \mathbb{R}^8_+ \times \mathbb{R}^1_+ \times \mathbb{R}^1_+$ is positively invariant □

It follows that every feasible solution of system (3.1) is uniformly bounded in $\mathscr{D}$, thus the system is appropriate for The study of the dynamics of CBD-CLR co-infection.

3.2.2 Equilibrium points of the Co-infection model

This section computes the disease-free equilibrium and Endemic Equilibrium points.

3.2.2.1 Disease Free Equilibrium point (DFE)

The DFE for the CBD-CLR co-infection model is a situation in which there is no infection in the plant population. The DFE of the CBD-CLR co-infection system (3.1) is calculated by equating the right-hand side of the equations of the system to zero and substituting $S = S^0$, $E_k = E_k^0 = 0$, $E_v = E_v^0 = 0$, $E_{kv} = E_{kv}^0 = 0$,$I_k = I_k^0 = 0$, $I_v = I_v^0 = 0$, $I_{kv} = I_{kv}^0 = 0$,$P_k = P_k^0 = 0$, $P_v = P_v^0 = 0$, $R = R^0 = 0$ then solving the resulting system of equations. Thus, we get

$DFE = \mathscr{E}_{kv}^0 = (S^0, E_k^0, E_v^0, E_{kv}^0, I_k^0, I_v^0, I_{kv}^0, P_k^0, P_v^0, R^0) = (\frac{\Lambda}{\mu}, 0, 0, 0, 0, 0, 0, 0, 0, 0)$

3.2.2.2 Endemic Equilibrium point ($\mathscr{E}^*_{kv}$)

The endemic equilibrium for the CBD-CLR co-infection model is a situation in which the infection persists in the plant population We denote the endemic equilibrium by $\mathscr{E}^*_{kv} = \{S^*, E^*_k, E^*_v, E^*_{kv}, I^*_k, I^*_v, I^*_{kv}, P^*_k, P^*_v, R^*\}$. Equating the right hand side of system (3.1) to zero and substituting $S = S^*$, $E_k = E^*_k$, $E_v = E^*_v$, $E_{kv} = E^*_{kv}$,$I_k = I^*_k$, $I_v = I^*_v$, $I_{kv} = I^*_{kv}$, $R = R^*$, $P_k = P^*_k$, $P_v = P^*_v$, $\varpi_k P_k = \varpi_k P^*_k = \beta^*_k$, $\varpi_v P_v = \varpi_v P^*_v = \beta^*_v$, we get

$$\left.\begin{aligned}
0 &= \Lambda - d_1 S^* \\
0 &= \beta^*_k S^* + (1-\xi_v)\omega_v E^*_{kv} - d_2 E^*_k \\
0 &= \beta^*_v S^* + (1-\xi_k)\omega_k E^*_{kv} - d_3 E^*_v \\
0 &= (1-q_v)\beta^*_v E^*_k + (1-q_k)\beta^*_k E^*_v - d_4 E^*_{kv} \\
0 &= \eta_k E^*_k + \xi_v \omega_v E^*_{kv} + \pi_v I^*_{kv} - d_5 I^*_k \\
0 &= \eta_v E^*_v + \xi_k \omega_k E^*_{kv} + \pi_k I^*_{kv} - d_6 I^*_v \\
0 &= q_v \beta^*_v E^*_k + q_k \beta^*_k E^*_v + \beta^*_k I^*_v + \beta^*_v I^*_k + \eta_{kv} E^*_{kv} - d_7 I^*_{kv} \\
0 &= \gamma_1 E^*_k + \gamma_2 I^*_k + \gamma_3 E^*_{kv} + \gamma_4 I^*_{kv} - \delta_1 P^*_k \\
0 &= \tau_1 E^*_v + \tau_2 I^*_v + \tau_3 E^*_{kv} + \tau_4 I^*_{kv} - \delta_2 P^*_v \\
0 &= \alpha_k E^*_k + \alpha_v E^*_v + \alpha_{kv} E^*_{kv} + \rho_k I^*_k + \rho_v I^*_v + \rho_{kv} I^*_{kv} - \mu R^*
\end{aligned}\right\} \tag{3.14}$$

where

$d_1 = \beta^*_k + \beta^*_v + \mu$

$d_2 = \beta^*_v + \alpha_k + \mu + \eta_k$

$d_3 = \beta^*_k + \alpha_v + \mu + \eta_v$

$d_4 = \alpha_{kv} + \omega_k + \omega_v + \mu + \eta_{kv}$

$d_5 = \beta^*_v + \rho_k + \mu + \delta_k$

$d_6 = \beta^*_k + \rho_v + \mu + \delta_v$

$d_7 = \pi_v + \pi_k + \rho_{kv} + \mu + \delta_k + \delta_v$

From the system of equations (3.14), we solve for S^*, E^*_k, E^*_v, E^*_{kv}, I^*_k, I^*_v, I^*_{kv}, P^*_k, P^*_v and R^*

to get

$$
\begin{aligned}
S^* &= \frac{\Lambda}{d_1} \\
E_k^* &= \frac{j_1\beta_k^*\Lambda + d_1(1-\xi_v)\omega_v j_2}{d_1 d_2 j_1} \\
E_v^* &= \frac{j_1\beta_v^*\Lambda + d_1(1-\xi_k)\omega_k j_2}{d_1 d_3 j_1} \\
E_{kv}^* &= \frac{j_2}{j_1} \\
I_k^* &= \frac{j_5}{d_1 d_2 d_5 j_1 j_4} \\
I_v^* &= \frac{j_6}{d_1 d_3 d_6 j_1 j_4} \\
I_{kv}^* &= \frac{j_3}{j_4} \\
P_k^* &= \frac{d_5 j_4\gamma_1(j_1\beta_k^*\Lambda + d_1(1-\xi_v)\omega_v j_2) + \gamma_2 j_5 + d_1 d_2 d_5\gamma_3 j_2 j_4 + d_1 d_2 d_5\gamma_4 j_1 j_3}{d_1 d_2 d_5 j_1 j_4\delta_1} \\
P_v^* &= \frac{d_6 j_4\tau_1(j_1\beta_v^*\Lambda + d_1(1-\xi_k)\omega_k j_2) + \tau_2 j_6 + d_1 d_3 d_6\tau_3 j_2 j_4 + d_1 d_3 d_6\tau_4 j_1 j_3}{d_1 d_3 d_6 j_1 j_4\delta_2} \\
R^* &= \frac{d_3\alpha_k(j_1\beta_k^*\Lambda + d_1(1-\xi_v)\omega_v j_2) + d_2\alpha_v(j_1\beta_v^*\Lambda + d_1(1-\xi_k)\omega_k j_2)}{d_1 d_2 d_3 d_5 j_1 j_5\mu} \\
&\quad + \frac{d_1 d_2 d_5\alpha_{kv} j_2 j_4 + \rho_k j_5}{d_1 d_2 d_5 j_1 j_4\mu} + \frac{\rho_v j_6}{d_1 d_3 d_6 j_1 j_4\mu} + \frac{\rho_{kv} j_3}{j_4\mu}
\end{aligned}
$$

where

$$j_1 = d_1[d_2(1-q_k)\beta_k^*(\alpha_{kv}+\xi_k\omega_k+(1-\xi_v)\omega_v+\xi_v\omega_v+\mu+\eta_{kv})+d_2(q_k\beta_k^*+\alpha_v+\mu+\eta_v)(\alpha_{kv}+(1-\xi_k)\omega_k+\xi_k\omega_k+(1-\xi_v)\omega_v+\xi_v\omega_v+\mu+\eta_{kv})+d_3(1-q_v)\beta_v^*(\alpha_{kv}+(1-\xi_k)\omega_k+\xi_k\omega_k+\xi_v\omega_v+\mu+\eta_{kv})+d_3(q_v\beta_v^*+\alpha_k+\mu+\eta_k)(\alpha_{kv}+(1-\xi_k)\omega_k+\xi_k\omega_k+(1-\xi_v)\omega_v+\xi_v\omega_v+\mu+\eta_{kv})]$$

$$j_2 = \beta_v^*\beta_k^*\Lambda(d_3(1-q_v)+d_2(1-q_k))$$

$$j_3 = d_5 d_6[d_3 q_v\beta_v^*(j_1\beta_k^*\Lambda+d_1(1-\xi_v)\omega_v j_2)+d_2 q_k\beta_k^*(j_1\beta_v^*\Lambda+d_1(1-\xi_k)\omega_k j_2)+\eta_{kv} j_2 d_1 d_2 d_3]+d_2 d_5[\beta_k^*(\eta_v(j_1\beta_v^*\Lambda+d_1(1-\xi_k)\omega_k j_2)+d_1 d_3\xi_k\omega_k j_2)]+d_3 d_6[\beta_v^*(\eta_k(j_1\beta_k^*\Lambda+d_1(1-\xi_v)\omega_v j_2)+d_1 d_2\xi_v\omega_v j_2)]$$

$$j_4 = d_1 d_2 d_3 j_1((\rho_{kv}+\mu+\delta_k+\delta_v)d_5 d_6+\pi_k d_5(\rho_v+\mu+\delta_v)+\pi_v(\rho_k+\mu+\delta_k)d_6)$$

$$j_5 = j_4[\eta_k(j_1\beta_k^*\Lambda+d_1(1-\xi_v)\omega_v j_2)+d_1 d_2\xi_v\omega_v j_2]+d_1 d_2 j_1 j_3\pi_v$$

$$j_6 = j_4[\eta_v(j_1\beta_v^*\Lambda+d_1(1-\xi_k)\omega_k j_2)+d_1 d_3\xi_k\omega_k j_2]+d_1 d_3 j_1 j_3\pi_k$$

3.2.3 Reproduction number ($\mathscr{R}_{kv0}$) due co-infection Model

In this section we use the next generation method and notations in Van den Driessche and Watmough (2002) to compute $\mathscr{R}_{kv0}$. Given the system (3.1), we consider the following infected compartments.

$$\begin{aligned}
\frac{dE_k}{dt} &= \varpi_k P_k S + (1-\xi_v)\omega_v E_{kv} - (\alpha_k + \varpi_v P_v + \mu + \eta_k)E_k \\
\frac{dE_v}{dt} &= \varpi_v P_v S + (1-\xi_k)\omega_k E_{kv} - (\alpha_v + \varpi_k P_k + \mu + \eta_v)E_v \\
\frac{dE_{kv}}{dt} &= (1-q_v)\varpi_v P_v E_k + (1-q_k)\varpi_k P_k E_v - (\alpha_{kv} + \omega_k + \omega_v + \mu + \eta_{kv})E_{kv} \\
\frac{dI_k}{dt} &= \eta_k E_k + \xi_v \omega_v E_{kv} + \pi_v I_{kv} - (\varpi_v P_v + \rho_k + \mu + \delta_k)I_k \\
\frac{dI_v}{dt} &= \eta_v E_v + \xi_k \omega_k E_{kv} + \pi_k I_{kv} - (\varpi_k P_k + \rho_v + \mu + \delta_v)I_v \\
\frac{dI_{kv}}{dt} &= q_v \varpi_v P_v E_k + q_k \varpi_k P_k E_v + \varpi_k P_k I_v + \varpi_v P_v I_k + \eta_{kv} E_{kv} - (\pi_v + \pi_k + \rho_{kv} + \mu + \delta_k + \delta_v)I_{kv} \\
\frac{dP_k}{dt} &= \gamma_1 E_k + \gamma_2 I_k + \gamma_3 E_{kv} + \gamma_4 I_{kv} - \delta_1 P_k \\
\frac{dP_v}{dt} &= \tau_1 E_v + \tau_2 I_v + \tau_3 E_{kv} + \tau_4 I_{kv} - \delta_2 P_v
\end{aligned} \tag{3.15}$$

Letting $G = [E_k, E_v, E_{kv}, I_k, I_v, I_{kv}, P_k, P_v]^T$, system (3.15) can be rewritten as

$$\frac{dG}{dt} = \mathscr{F}(G) - \mathscr{V}(G)$$

where matrices $\mathscr{F}$ and $\mathscr{V}$ represent, respectively, the rates at which new infections arise and how often infections are transferred into and out of any compartment.

Matrices $\mathscr{F}$ and $\mathscr{V}$ are given as follows:

$$\mathscr{F} = \begin{bmatrix}
\varpi_k P_k S \\
\varpi_v P_v S \\
(1-q_v)\varpi_v P_v E_k + (1-q_k)\varpi_k P_k E_v \\
0 \\
0 \\
q_v \varpi_v P_v E_k + q_k \varpi_k P_k E_v + \varpi_k P_k I_v + \varpi_v P_v I_k \\
0 \\
0
\end{bmatrix} \text{ and}$$

$$\mathscr{V} = \begin{bmatrix} -(1-\xi_v)\omega_v E_{kv} + (\alpha_k + \varpi_v P_v + \mu + \eta_k)E_k \\ -(1-\xi_k)\omega_k E_{kv} + (\alpha_v + \varpi_k P_k + \mu + \eta_v)E_v \\ (\alpha_{kv} + \omega_k + \omega_v + \mu + \eta_{kv})E_{kv} \\ -\eta_k E_k - \xi_v\omega_v E_{kv} - \pi_v I_{kv} + (\varpi_v P_v + \rho_k + \mu + \delta_k)I_k \\ -\eta_v E_v - \xi_k\omega_k E_{kv} - \pi_k I_{kv} + (\varpi_k P_k + \rho_v + \mu + \delta_v)I_v \\ -\eta_{kv} E_{kv} + (\pi_v + \pi_k + \rho_{kv} + \mu + \delta_k + \delta_v)I_{kv} \\ -\gamma_1 E_k - \gamma_2 I_k - \gamma_3 E_{kv} - \gamma_4 I_{kv} + \delta_1 P_k \\ -\tau_1 E_v - \tau_2 I_v - \tau_3 E_{kv} - \tau_4 I_{kv} + \delta_2 P_v \end{bmatrix}$$

By partial differentiation of the components of matrices $\mathscr{F}$ and $\mathscr{V}$ at the disease free equilibrium, we obtain

$$F = \begin{bmatrix} 0 & 0 & 0 & 0 & 0 & 0 & \frac{\varpi_k \Lambda}{\mu} & 0 \\ 0 & 0 & 0 & 0 & 0 & 0 & 0 & \frac{\varpi_v \Lambda}{\mu} \\ 0 & 0 & 0 & 0 & 0 & 0 & 0 & 0 \\ 0 & 0 & 0 & 0 & 0 & 0 & 0 & 0 \\ 0 & 0 & 0 & 0 & 0 & 0 & 0 & 0 \\ 0 & 0 & 0 & 0 & 0 & 0 & 0 & 0 \\ 0 & 0 & 0 & 0 & 0 & 0 & 0 & 0 \\ 0 & 0 & 0 & 0 & 0 & 0 & 0 & 0 \end{bmatrix} \text{ and}$$

$$V = \begin{bmatrix} a_1 & 0 & -(1-\xi_v)\omega_v & 0 & 0 & 0 & 0 & 0 \\ 0 & a_2 & -(1-\xi_k)\omega_k & 0 & 0 & 0 & 0 & 0 \\ 0 & 0 & a_3 & 0 & 0 & 0 & 0 & 0 \\ -\eta_k & 0 & -\xi_v\omega_v & a_4 & 0 & -\pi_v & 0 & 0 \\ 0 & -\eta_v & -\xi_k\omega_k & 0 & a_5 & -\pi_k & 0 & 0 \\ 0 & 0 & -\eta_{kv} & 0 & 0 & a_6 & 0 & 0 \\ -\gamma_1 & 0 & -\gamma_3 & -\gamma_2 & 0 & -\gamma_4 & \delta_1 & 0 \\ 0 & -\tau_1 & -\tau_3 & 0 & -\tau_2 & -\tau_4 & 0 & \delta_2 \end{bmatrix}$$

where

$a_1 = \alpha_k + \mu + \eta_k,$

$a_2 = \alpha_v + \mu + \eta_v,$

$a_3 = \alpha_{kv} + \omega_k + \omega_v + \mu + \eta_{kv},$

$a_4 = \rho_k + \mu + \delta_k,$

$a_5 = \rho_v + \mu + \delta_v$ and

$a_6 = \pi_v + \pi_k + \rho_{kv} + \mu + \delta_k + \delta_v$

The inverse of V is given by

$$V^{-1} = \begin{bmatrix} \frac{1}{a_1} & 0 & \frac{(1-\xi_v)\omega_v}{a_1 a_3} & 0 & 0 & 0 & 0 & 0 \\ 0 & \frac{1}{a_2} & \frac{(1-\xi_k)\omega_k}{a_2 a_3} & 0 & 0 & 0 & 0 & 0 \\ 0 & 0 & \frac{1}{a_3} & 0 & 0 & 0 & 0 & 0 \\ \frac{\eta_k}{a_1 a_4} & 0 & \frac{a_1\pi_v\eta_{kv}+(1-\xi_v)\omega_v\eta_k a_6+a_1 a_6\xi_v\omega_v}{a_1 a_3 a_4 a_6} & \frac{1}{a_4} & 0 & \frac{\pi_v}{a_4 a_6} & 0 & 0 \\ 0 & \frac{\eta_v}{a_2 a_5} & \frac{a_2\pi_k\eta_{kv}+(1-\xi_k)\omega_k\eta_k a_6+a_2 a_6\xi_k\omega_k}{a_2 a_3 a_5 a_6} & 0 & \frac{1}{a_5} & \frac{\pi_k}{a_5 a_6} & 0 & 0 \\ 0 & 0 & \frac{\eta_{kv}}{a_3 a_6} & 0 & 0 & \frac{1}{a_6} & 0 & 0 \\ \frac{a_4\gamma_1+\eta_k\gamma_2}{a_1 a_4\delta_1} & 0 & \frac{N1}{a_1 a_3 a_4 a_6\delta_1} & \frac{\gamma_2}{a_4\delta_1} & 0 & \frac{\pi_v\gamma_2+a_6\gamma_4}{a_4 a_6\delta_1} & \frac{1}{\delta_1} & 0 \\ 0 & \frac{a_5\tau_1+\eta_v\tau_2}{a_2 a_5\delta_2} & \frac{N2}{a_2 a_3 a_5 a_6\delta_2} & 0 & \frac{\tau_2}{a_5\delta_2} & \frac{\pi_k\tau_2+a_5\tau_4}{a_5 a_6\delta_2} & 0 & \frac{1}{\delta_2} \end{bmatrix}$$

where

$a_1 = \alpha_k + \mu + \eta_k,$

$a_2 = \alpha_v + \mu + \eta_v,$

$a_3 = \alpha_{kv} + \omega_k + \omega_v + \mu + \eta_{kv},$

$a_4 = \rho_k + \mu + \delta_k,$

$a_5 = \rho_v + \mu + \delta_v,$

$a_6 = \pi_v + \pi_k + \rho_{kv} + \mu + \delta_k + \delta_v,$

$N1 = (1-\xi_v)\omega_v a_4 a_6\gamma_1 + a_1 a_4 a_6\gamma_3 + a_1\pi_v\eta_{kv}\gamma_2 + (1-\xi_v)\omega_v\eta_k a_6\gamma_2 + a_1 a_2\eta_{kv}\gamma_4 - a_1 a_6\xi_v\omega_v\gamma_2$

and

$N2 = (1-\xi_k)\omega_k a_5 a_6\tau_1 + a_2 a_5 a_6\tau_3 + a_2\pi_k\eta_{kv}\tau_2 + (1-\xi_k)\omega_k\eta_v a_6\tau_2 + a_2 a_5\eta_{kv}\tau_4 + a_2 a_6\xi_k\omega_k\tau_2$

Computing the product of F and V^{-1}, we get

$$FV^{-1} = \begin{bmatrix} \frac{\varpi_k\Lambda(a_4\gamma_1+\eta_k\gamma_2)}{a_1a_4\mu\delta_1} & 0 & \frac{\varpi_k\Lambda N1}{a_1a_3a_4a_6\mu\delta_1} & \frac{\varpi_k\Lambda\gamma_2}{a_4\mu\delta_1} & 0 & \frac{\varpi_k\Lambda(\pi_v\gamma_2+a_6\gamma_4)}{a_4a_6\mu\delta_1} & \frac{\varpi_k\Lambda}{\mu\delta_1} & 0 \\ 0 & \frac{\varpi_v\Lambda(a_5\tau_1+\eta_v\tau_2)}{a_2a_5\mu\delta_2} & \frac{\varpi_v\Lambda N2}{a_2a_3a_5a_6\mu\delta_2} & 0 & \frac{\varpi_v\Lambda\tau_2}{a_5\mu\delta_2} & \frac{\varpi_v\Lambda(\pi_k\tau_2+a_5\tau_4)}{a_5a_6\mu\delta_2} & 0 & \frac{\varpi_v\Lambda}{\mu\delta_2} \\ 0 & 0 & 0 & 0 & 0 & 0 & 0 & 0 \\ 0 & 0 & 0 & 0 & 0 & 0 & 0 & 0 \\ 0 & 0 & 0 & 0 & 0 & 0 & 0 & 0 \\ 0 & 0 & 0 & 0 & 0 & 0 & 0 & 0 \\ 0 & 0 & 0 & 0 & 0 & 0 & 0 & 0 \\ 0 & 0 & 0 & 0 & 0 & 0 & 0 & 0 \end{bmatrix}$$

Clearly, $\{\frac{\varpi_k\Lambda(a_4\gamma_1+\eta_k\gamma_2)}{a_1a_4\mu\delta_1}, \frac{\varpi_v\Lambda(a_5\tau_1+\eta_v\tau_2)}{a_2a_5\mu\delta_2}, 0, 0, 0, 0, 0, 0\}$ are the eigenvalues of FV^{-1}. Thus dominant eigenvalues of FV^{-1} are:

$\frac{\varpi_k\Lambda(a_4\gamma_1+\eta_k\gamma_2)}{a_1a_4\mu\delta_1} = \frac{\varpi_k\Lambda((\rho_k+\mu+\delta_k)\gamma_1+\eta_k\gamma_2)}{(\alpha_k+\mu+\eta_k)(\rho_k+\mu+\delta_k)\mu\delta_1}$ and

$\frac{\varpi_v\Lambda(a_5\tau_1+\eta_v\tau_2)}{a_2a_5\mu\delta_2} = \frac{\varpi_v\Lambda((\rho_v+\mu+\delta_v)\tau_1+\eta_v\tau_2)}{(\alpha_v+\mu+\eta_v)(\rho_v+\mu+\delta_v)\mu\delta_2}$

Therefore, the reproduction number ($\mathscr{R}_{kv0}$) is given by

$$\mathscr{R}_{kv0} = \max(\mathscr{R}_{k0}, \mathscr{R}_{v0}) \tag{3.16}$$

where

$$\mathscr{R}_{k0} = \frac{\varpi_k\Lambda((\rho_k+\mu+\delta_k)\gamma_1+\eta_k\gamma_2)}{(\alpha_k+\mu+\eta_k)(\rho_k+\mu+\delta_k)\mu\delta_1} \tag{3.17}$$

$$\mathscr{R}_{v0} = \frac{\varpi_v\Lambda((\rho_v+\mu+\delta_v)\tau_1+\eta_v\tau_2)}{(\alpha_v+\mu+\eta_v)(\rho_v+\mu+\delta_v)\mu\delta_2} \tag{3.18}$$

3.2.4 The Impact of CBD on CLR

We investigate the impact of CBD on CLR and vice versa. First, we rewrite $\mathscr{R}_{k0}$ in terms of $\mathscr{R}_{v0}$. Since,

$$\mathscr{R}_{v0} = \frac{\varpi_v\Lambda((\rho_v+\mu+\delta_v)\tau_1+\eta_v\tau_2)}{(\alpha_v+\mu+\eta_v)(\rho_v+\mu+\delta_v)\mu\delta_2}$$

$$\Rightarrow \Lambda = \frac{(\alpha_v+\mu+\eta_v)(\rho_v+\mu+\delta_v)\mu\delta_2\mathscr{R}_{v0}}{\varpi_v((\rho_v+\mu+\delta_v)\tau_1+\eta_v\tau_2)}$$

By substitution of Λ in $\mathscr{R}_{k0}$, we get

$$\mathscr{R}_{k0} = \frac{\varpi_k((\rho_k+\mu+\delta_k)\gamma_1+\eta_k\gamma_2)(\alpha_v+\mu+\eta_v)(\rho_v+\mu+\delta_v)\delta_2\mathscr{R}_{v0}}{(\alpha_k+\mu+\eta_k)(\rho_k+\mu+\delta_k)\delta_1\varpi_v((\rho_v+\mu+\delta_v)\tau_1+\eta_v\tau_2)} \tag{3.19}$$

To investigate the impact of CLR on CBD, we differentiate (3.19) with respect to $\mathscr{R}_{v0}$. Thus

$$\frac{\partial \mathscr{R}_{k0}}{\partial \mathscr{R}_{v0}} = \frac{\varpi_k((\rho_k+\mu+\delta_k)\gamma_1+\eta_k\gamma_2)(\alpha_v+\mu+\eta_v)(\rho_v+\mu+\delta_v)\delta_2}{(\alpha_k+\mu+\eta_k)(\rho_k+\mu+\delta_k)\delta_1\varpi_v((\rho_v+\mu+\delta_v)\tau_1+\eta_v\tau_2)} > 0 \tag{3.20}$$

Equation (3.20) demonstrates that CLR cases increase the number of CBD cases.

To rewrite $\mathscr{R}_{v0}$ in terms of $\mathscr{R}_{k0}$, we solve for Λ in equation (3.17) to obtain

$$\Lambda = \frac{(\alpha_k+\mu+\eta_k)(\rho_k+\mu+\delta_k)\mu\delta_1\mathscr{R}_{k0}}{\varpi_k((\rho_k+\mu+\delta_k)\gamma_1+\eta_k\gamma_2)}$$

Hence,

$$\mathscr{R}_{v0} = \frac{\varpi_v((\rho_v+\mu+\delta_v)\tau_1+\eta_v\tau_2)(\alpha_k+\mu+\eta_k)(\rho_k+\mu+\delta_k)\delta_1\mathscr{R}_{k0}}{(\alpha_v+\mu+\eta_v)(\rho_v+\mu+\delta_v)\delta_2\varpi_k((\rho_k+\mu+\delta_k)\gamma_1+\eta_k\gamma_2)}. \tag{3.21}$$

Thus,

$$\frac{\partial \mathscr{R}_{v0}}{\partial \mathscr{R}_{k0}} = \frac{\varpi_v((\rho_v+\mu+\delta_v)\tau_1+\eta_v\tau_2)(\alpha_k+\mu+\eta_k)(\rho_k+\mu+\delta_k)\delta_1}{(\alpha_v+\mu+\eta_v)(\rho_v+\mu+\delta_v)\delta_2\varpi_k((\rho_k+\mu+\delta_k)\gamma_1+\eta_k\gamma_2)} > 0. \tag{3.22}$$

Equation (3.22) implies that CBD cases increase the number of CLR cases.

3.2.5 Local stability of the Disease Free equilibrium (DFE)

The following is a statement of the stability of the disease-free equilibrium (DFE) for CBD and CLR co-infection, a situation in which there is no disease infection in the plant population.

Theorem 1. *The disease-free equilibrium $\mathscr{E}^0_{kv}$ is locally asymptotically stable when $\mathscr{R}_{kv0} < 1$ (that is; $\mathscr{R}_{k0} < 1$ and $\mathscr{R}_{v0} < 1$) and unstable when $\mathscr{R}_{kv0} > 1$ (that is; $\mathscr{R}_{k0} > 1$ and $\mathscr{R}_{v0} > 1$).*

3.2.6 Bifurcation Analysis

Bifurcation is the qualitative change in behavior under a variation or change of some system parameters. Using the center manifold theory described in (Castillo-Chavez and

Song, 2004), we examine the nature of the bifurcation. The coefficients of the normal form representing the system's dynamics on the central manifold, say a and b, are two significant numbers. These coefficients determine the bifurcation. Specifically, the bifurcation is forward if $a < 0$ and $b > 0$ and backward if $a > 0$ and $b > 0$. This method could lead to the following outcome:

Theorem 2. *If $m > n$, $a > 0$ then the system (3.1) has a backward bifurcation at $\mathscr{R}_{kv0} = 1$, otherwise the system has a forward bifurcation*

Proof. we first examine transmission rates ϖ_k and ϖ_v as bifurcation parameters such that $\mathscr{R}_{k0} = 1$ and $\mathscr{R}_{v0} = 1$ when

$$\varpi_k = \varpi_k^* = \frac{(\alpha_k + \mu + \eta_k)(\rho_k + \mu + \delta_k)\mu\delta_1}{\Lambda((\rho_k + \mu + \delta_k)\gamma_1 + \eta_k\gamma_2)}$$

and

$$\varpi_v = \varpi_v^* = \frac{(\alpha_v + \mu + \eta_v)(\rho_v + \mu + \delta_v)\delta_2\varpi_k((\rho_k + \mu + \delta_k)\gamma_1 + \eta_k\gamma_2)}{((\rho_v + \mu + \delta_v)\tau_1 + \eta_v\tau_2)(\alpha_k + \mu + \eta_k)(\rho_k + \mu + \delta_k)\delta_1\mathscr{R}_{k0}}$$

substituting $S = x_1$, $E_k = x_2$, $E_v = x_3$, $E_{kv} = x_4$,$I_k = x_5$, $I_v = x_6$, $I_{kv} = x_7$, $P_k = x_8$, $P_v = x_9$, $R = x_{10}$ in system (3.1), we obtain the transformed system $\frac{dx}{dt} = F(x)$ where $x = (x_1,\ x_2,\ x_3,\ x_4,\ x_5,\ x_6,\ x_7,\ x_8,\ x_9,\ x_{10})^T$ and $F = (f_1,\ f_2,\ f_3,\ f_4,\ f_5,\ f_6,\ f_7,\ f_8,\ f_9,\ f_{10})^T$

as shown below

$$\left.\begin{aligned}
\frac{dx_1}{dt} &= \Lambda - (\varpi_k x_8 + \varpi_v x_9 + \mu)x_1 \\
\frac{dx_2}{dt} &= \varpi_k x_8 x_1 + (1-\xi_v)\omega_v x_4 - (\alpha_k + \varpi_v x_9 + \mu + \eta_k)x_2 \\
\frac{dx_3}{dt} &= \varpi_v x_9 x_1 + (1-\xi_k)\omega_k x_4 - (\alpha_v + \varpi_k x_8 + \mu + \eta_v)x_3 \\
\frac{dx_4}{dt} &= (1-q_v)\varpi_v x_9 x_2 + (1-q_k)\varpi_k x_8 x_3 - (\alpha_{kv} + \omega_k + \omega_v + \mu + \eta_{kv})x_4 \\
\frac{dx_5}{dt} &= \eta_k x_2 + \xi_v\omega_v x_4 + \pi_v x_7 - (\varpi_v x_9 + \rho_k + \mu + \delta_k)x_5 \\
\frac{dx_6}{dt} &= \eta_v x_3 + \xi_k\omega_k x_4 + \pi_k x_7 - (\varpi_k x_8 + \rho_v + \mu + \delta_v)x_6 \\
\frac{dx_7}{dt} &= q_v\varpi_v x_9 x_2 + q_k\varpi_k x_8 x_3 + \varpi_k x_8 x_6 + \varpi_v x_9 x_5 + \eta_{kv}x_4 - (\pi_v + \pi_k + \rho_{kv} + \mu + \delta_k + \delta_v)x_7 \\
\frac{dx_8}{dt} &= \gamma_1 x_2 + \gamma_2 x_5 + \gamma_3 x_4 + \gamma_4 x_7 - \delta_1 x_8 \\
\frac{dx_9}{dt} &= \tau_1 x_3 + \tau_2 x_6 + \tau_3 x_4 + \tau_4 x_7 - \delta_2 x_9 \\
\frac{dx_{10}}{dt} &= \alpha_k x_2 + \alpha_v x_3 + \alpha_{kv} x_4 + \rho_k x_5 + \rho_v x_6 + \rho_{kv} x_7 - \mu x_{10}
\end{aligned}\right\} \quad (3.23)$$

The Jacobian matrix of system (3.23) at $\mathscr{E}^0_{kv}$ is given by

$$J(\mathscr{E}^0_{kv}) = \begin{bmatrix}
-\mu & 0 & 0 & 0 & 0 & 0 & 0 & \frac{-\varpi_k\Lambda}{\mu} & \frac{-\varpi_v\Lambda}{\mu} & 0 \\
0 & -a_1 & 0 & (1-\xi_v)\omega_v & 0 & 0 & 0 & \frac{\varpi_k\Lambda}{\mu} & 0 & 0 \\
0 & 0 & -a_2 & (1-\xi_k)\omega_k & 0 & 0 & 0 & 0 & \frac{\varpi_v\Lambda}{\mu} & 0 \\
0 & 0 & 0 & -a_3 & 0 & 0 & 0 & 0 & 0 & 0 \\
0 & \eta_k & 0 & \xi_v\omega_v & -a_4 & 0 & \pi_v & 0 & 0 & 0 \\
0 & 0 & \eta_v & \xi_k\omega_k & 0 & -a_5 & \pi_k & 0 & 0 & 0 \\
0 & 0 & 0 & \eta_{kv} & 0 & 0 & -a_6 & 0 & 0 & 0 \\
0 & \gamma_1 & 0 & \gamma_3 & \gamma_2 & 0 & \gamma_4 & -\delta_1 & 0 & 0 \\
0 & 0 & \tau_1 & \tau_3 & 0 & \tau_2 & \tau_4 & 0 & -\delta_2 & 0 \\
0 & \alpha_k & \alpha_v & \alpha_{kv} & \rho_k & \rho_v & \rho_{kv} & 0 & 0 & -\mu
\end{bmatrix} \quad (3.24)$$

where

$a_1 = \alpha_k + \mu + \eta_k$

$a_2 = \alpha_v + \mu + \eta_v$

$a_3 = \alpha_{kv} + \omega_k + \omega_v + \mu + \eta_{kv}$

$a_4 = \rho_k + \mu + \delta_k$

$a_5 = \rho_v + \mu + \delta_v$

$a_6 = \pi_v + \pi_k + \rho_{kv} + \mu + \delta_k + \delta_v$

We begin by computing the right eigenvector of $J(\mathscr{E}^0_{kv})$, which is represented by $w = (w_1,\ w_2,\ w_3,\ w_4,\ w_5,\ w_6,\ w_7,\ w_8,\ w_9,\ w_{10})^T$

$$\begin{bmatrix} -\mu & 0 & 0 & 0 & 0 & 0 & 0 & \frac{-\varpi_k\Lambda}{\mu} & \frac{-\varpi_v\Lambda}{\mu} & 0 \\ 0 & -a_1 & 0 & (1-\xi_v)\omega_v & 0 & 0 & 0 & \frac{\varpi_k\Lambda}{\mu} & 0 & 0 \\ 0 & 0 & -a_2 & (1-\xi_k)\omega_k & 0 & 0 & 0 & 0 & \frac{\varpi_v\Lambda}{\mu} & 0 \\ 0 & 0 & 0 & -a_3 & 0 & 0 & 0 & 0 & 0 & 0 \\ 0 & \eta_k & 0 & \xi_v\omega_v & -a_4 & 0 & \pi_v & 0 & 0 & 0 \\ 0 & 0 & \eta_v & \xi_k\omega_k & 0 & -a_5 & \pi_k & 0 & 0 & 0 \\ 0 & 0 & 0 & \eta_{kv} & 0 & 0 & -a_6 & 0 & 0 & 0 \\ 0 & \gamma_1 & 0 & \gamma_3 & \gamma_2 & 0 & \gamma_4 & -\delta_1 & 0 & 0 \\ 0 & 0 & \tau_1 & \tau_3 & 0 & \tau_2 & \tau_4 & 0 & -\delta_2 & 0 \\ 0 & \alpha_k & \alpha_v & \alpha_{kv} & \rho_k & \rho_v & \rho_{kv} & 0 & 0 & -\mu \end{bmatrix} \begin{pmatrix} w_1 \\ w_2 \\ w_3 \\ w_4 \\ w_5 \\ w_6 \\ w_7 \\ w_8 \\ w_9 \\ w_{10} \end{pmatrix} = \begin{pmatrix} 0 \\ 0 \\ 0 \\ 0 \\ 0 \\ 0 \\ 0 \\ 0 \\ 0 \\ 0 \end{pmatrix} \tag{3.25}$$

We can rewrite equation (3.25) as

$$\begin{cases} -\mu w_1 - \dfrac{\varpi_k\Lambda}{\mu} w_8 - \dfrac{\varpi_v\Lambda}{\mu} w_9 = 0 \\ -a_1 w_2 + (1-\xi_v)\omega_v w_4 + \dfrac{\varpi_k\Lambda}{\mu} w_8 = 0 \\ -a_2 w_3 + (1-\xi_k)\omega_k w_4 + \dfrac{\varpi_v\Lambda}{\mu} w_9 = 0 \\ -a_3 w_4 = 0 \\ \eta_k w_2 + \xi_v\omega_v w_4 - a_4 w_5 + \pi_v w_7 = 0 \\ \eta_v w_3 + \xi_k\omega_k w_4 - a_5 w_6 + \pi_k w_7 = 0 \\ \eta_{kv} w_4 - a_6 w_7 = 0 \\ \gamma_1 w_2 + \gamma_3 w_4 + \gamma_2 w_5 + \gamma_4 w_7 - \delta_1 w_8 = 0 \\ \tau_1 w_3 + \tau_3 w_4 + \tau_2 w_6 + \tau_4 w_7 - \tau_2 w_9 = 0 \\ \alpha_k w_2 + \alpha_v w_3 + \alpha_{kv} w_4 + \rho_k w_5 + \rho_v w_6 + \rho_{kv} w_7 - \mu w_{10} = 0 \end{cases} \tag{3.26}$$

Upon solving equation (3.26), we

$$\begin{cases} w_1 = -\dfrac{\varpi_k\Lambda(a_4\gamma_1+\gamma_2\eta_k)}{\mu^2\delta_1 a_4}w_2 - \dfrac{\varpi_v\Lambda(a_5\tau_1+\tau_2\eta_v)}{\mu^2\tau_2 a_5}w_3 \\ w_2 = w_2 > 0 \\ w_3 = w_3 > 0 \\ w_4 = 0 \\ w_5 = \dfrac{\eta_k}{a_4}w_2 \\ w_6 = \dfrac{\eta_v}{a_5}w_3 \\ w_7 = 0 \\ w_8 = \dfrac{a_4\gamma_1+\gamma_2\eta_k}{\delta_1 a_4}w_2 \\ w_9 = \dfrac{a_5\tau_1+\tau_2\eta_v}{\tau_2 a_5}w_3 \\ w_{10} = \dfrac{a_4\alpha_k+\rho_k\eta_k}{\mu a_4}w_2 + \dfrac{a_5\alpha_v+\rho_v\eta_v}{\mu a_5}w_3 \end{cases} \tag{3.27}$$

Also, by computing the left eigenvector of $J(\mathscr{E}^0_{kv})$, which is represented by

$v = (v_1,\ v_2,\ v_3,\ v_4,\ v_5,\ v_6,\ v_7,\ v_8,\ v_9,\ v_{10})^T$, it follows that

$$\begin{bmatrix} -\mu & 0 & 0 & 0 & 0 & 0 & 0 & 0 & 0 & 0 \\ 0 & -a_1 & 0 & 0 & \eta_k & 0 & 0 & \gamma_1 & 0 & \alpha_k \\ 0 & 0 & -a_2 & 0 & 0 & \eta_v & 0 & 0 & \tau_1 & \alpha_v \\ 0 & (1-\xi_v)\omega_v & (1-\xi_k)\omega_k & -a_3 & \xi_v\omega_v & \xi_k\omega_k & \eta_{kv} & \gamma_3 & \tau_3 & \alpha_{kv} \\ 0 & 0 & 0 & 0 & -a_4 & 0 & 0 & \gamma_2 & 0 & \rho_k \\ 0 & 0 & 0 & 0 & 0 & -a_5 & 0 & 0 & \tau_2 & \rho_v \\ 0 & 0 & 0 & 0 & \pi_v & \pi_k & -a_6 & \gamma_4 & \tau_4 & \rho_{kv} \\ -\frac{\varpi_k\Lambda}{\mu} & \frac{\varpi_k\Lambda}{\mu} & 0 & 0 & 0 & 0 & 0 & -\delta_1 & 0 & 0 \\ -\frac{\varpi_v\Lambda}{\mu} & 0 & \frac{\varpi_v\Lambda}{\mu} & 0 & 0 & 0 & 0 & 0 & -\delta_2 & 0 \\ 0 & 0 & 0 & 0 & 0 & 0 & 0 & 0 & 0 & -\mu \end{bmatrix} \begin{pmatrix} v_1 \\ v_2 \\ v_3 \\ v_4 \\ v_5 \\ v_6 \\ v_7 \\ v_8 \\ v_9 \\ v_{10} \end{pmatrix} = \begin{pmatrix} 0 \\ 0 \\ 0 \\ 0 \\ 0 \\ 0 \\ 0 \\ 0 \\ 0 \\ 0 \end{pmatrix} \tag{3.28}$$

We express equation (3.28) as

$$\begin{cases} -\mu v_1 = 0 \\ -a_1 v_2 + \eta_k v_5 + \gamma_1 v_8 + \alpha_k v_{10} = 0 \\ -a_2 v_3 + \eta_v v_6 + \tau_1 v_9 + \alpha_v v_{10} = 0 \\ (1-\xi_v)\omega_v v_2 + (1-\xi_k)\omega_k v_3 - a_3 v_4 + \xi_v \omega_v v_5 + \xi_k \omega_k v_6 + \eta_{kv} v_7 + \gamma_3 v_8 + \tau_3 v_9 + \alpha_{kv} v_{10} = 0 \\ -a_4 v_5 + \gamma_2 v_8 + \rho_k v_{10} = 0 \\ -a_5 v_6 + \tau_2 v_9 + \rho_v v_{10} = 0 \\ \pi_v v_5 + \pi_k v_6 - a_6 v_7 + \gamma_4 v_8 + \tau_4 v_9 + \rho_{kv} v_{10} = 0 \\ -\dfrac{\varpi_k \Lambda}{\mu} v_1 + \dfrac{\varpi_k \Lambda}{\mu} v_2 - \delta_1 v_8 = 0 \\ -\dfrac{\varpi_v \Lambda}{\mu} v_1 + \dfrac{\varpi_v \Lambda}{\mu} v_3 - \delta_2 v_9 = 0 \\ -\mu v_{10} = 0 \end{cases} \tag{3.29}$$

Upon solving equation (3.29) by substitution, we obtain

$$\begin{cases} v_1 = 0 \\ v_2 = v_2 > 0 \\ v_3 = v_3 > 0 \\ v_4 = \dfrac{a_4 a_6 \delta_1 \mu (1-\xi_v)\omega_v + \eta_{kv}(\pi_v \gamma_2 \varpi_k \Lambda + a_4 \gamma_4 \varpi_k \Lambda) + a_6 \xi_v \omega_v \gamma_2 \varpi_k \Lambda + a_4 a_6 \gamma_3 \varpi_k \Lambda}{a_3 a_4 a_6 \delta_1 \mu} v_2 \\ \qquad + \dfrac{a_5 a_6 \delta_2 \mu (1-\xi_k)\omega_k + \eta_{kv}(\pi_k \tau_2 \varpi_v \Lambda + a_5 \tau_4 \varpi_v \Lambda) + a_6 \xi_k \omega_k \tau_2 \varpi_v \Lambda + a_5 a_6 \tau_3 \varpi_v \Lambda}{a_3 a_5 a_6 \delta_2 \mu} v_3 \\ v_5 = \dfrac{\gamma_2 \varpi_k \Lambda}{a_4 \delta_1 \mu} v_2 \\ v_6 = \dfrac{\tau_2 \varpi_v \Lambda}{a_5 \delta_2 \mu} v_3 \\ v_7 = \dfrac{\pi_v \gamma_2 \varpi_k \Lambda + a_4 \gamma_4 \varpi_k \Lambda}{a_4 a_6 \delta_1 \mu} v_2 + \dfrac{\pi_k \tau_2 \varpi_v \Lambda + a_5 \tau_4 \varpi_v \Lambda}{a_5 a_6 \delta_2 \mu} v_3 \\ v_8 = \dfrac{\varpi_k \Lambda}{\delta_1 \mu} v_2 \\ v_9 = \dfrac{\varpi_v \Lambda}{\delta_2 \mu} v_3 \\ v_{10} = 0 \end{cases} \tag{3.30}$$

According to (Castillo-Chavez and Song, 2004), equations (3.31) and (3.32) below define the coefficients a and b;

$$a = \sum_{k,i,j=1}^{n} v_k w_i w_j \frac{\partial^2 f_k}{\partial x_i \partial x_j}(\mathscr{E}^0_{kv}) \tag{3.31}$$

$$b = \sum_{k,i=1}^{n} v_k w_i \frac{\partial^2 f_k}{\partial x_i \partial \varpi_v}(\mathscr{E}^0_{kv}) \tag{3.32}$$

Considering only the non-zero elements of the left eigenvector v and system (3.23), it follows that

$$\begin{aligned} a =& v_2 w_1 w_8 \frac{\partial^2 f_2}{\partial x_1 \partial x_8}(\mathscr{E}^0_{kv}) + v_2 w_2 w_9 \frac{\partial^2 f_2}{\partial x_2 \partial x_9}(\mathscr{E}^0_{kv}) + v_3 w_1 w_9 \frac{\partial^2 f_3}{\partial x_1 \partial x_9}(\mathscr{E}^0_{kv}) \\ &+ v_3 w_3 w_8 \frac{\partial^2 f_3}{\partial x_3 \partial x_8}(\mathscr{E}^0_{kv}) + v_4 w_3 w_8 \frac{\partial^2 f_4}{\partial x_3 \partial x_8}(\mathscr{E}^0_{kv}) + v_4 w_2 w_9 \frac{\partial^2 f_4}{\partial x_2 \partial x_9}(\mathscr{E}^0_{kv}) \\ &+ v_5 w_5 w_9 \frac{\partial^2 f_5}{\partial x_5 \partial x_9}(\mathscr{E}^0_{kv}) + v_6 w_6 w_8 \frac{\partial^2 f_6}{\partial x_6 \partial x_8}(\mathscr{E}^0_{kv}) + v_7 w_5 w_9 \frac{\partial^2 f_7}{\partial x_5 \partial x_9}(\mathscr{E}^0_{kv}) \\ &+ v_7 w_6 w_8 \frac{\partial^2 f_7}{\partial x_6 \partial x_8}(\mathscr{E}^0_{kv}) + v_7 w_3 w_8 \frac{\partial^2 f_7}{\partial x_3 \partial x_8}(\mathscr{E}^0_{kv}) + v_7 w_2 w_9 \frac{\partial^2 f_7}{\partial x_2 \partial x_9}(\mathscr{E}^0_{kv}) \end{aligned}$$

and

$$b = v_3 w_9 \frac{\partial^2 f_3}{\partial x_9 \partial \varpi_v}(\mathscr{E}^0_{kv})$$

where the f_is represent the right hand side of the system (3.23). By partial differentiation, we have:

$$\begin{gathered} \frac{\partial^2 f_2}{\partial x_1 \partial x_8}(\mathscr{E}^0_{kv}) = \varpi_k, \ \frac{\partial^2 f_2}{\partial x_2 \partial x_9}(\mathscr{E}^0_{kv}) = -\varpi_v \\ \frac{\partial^2 f_3}{\partial x_1 \partial x_9}(\mathscr{E}^0_{kv}) = \varpi_v, \ \frac{\partial^2 f_3}{\partial x_3 \partial x_8}(\mathscr{E}^0_{kv}) = -\varpi_k \\ \frac{\partial^2 f_4}{\partial x_3 \partial x_8}(\mathscr{E}^0_{kv}) = (1-q_k)\varpi_k, \ \frac{\partial^2 f_4}{\partial x_2 \partial x_9}(\mathscr{E}^0_{kv}) = (1-q_v)\varpi_v \\ \frac{\partial^2 f_5}{\partial x_5 \partial x_9}(\mathscr{E}^0_{kv}) = -\varpi_v, \ \frac{\partial^2 f_6}{\partial x_6 \partial x_8}(\mathscr{E}^0_{kv}) = -\varpi_k \\ \frac{\partial^2 f_7}{\partial x_5 \partial x_9}(\mathscr{E}^0_{kv}) = \varpi_v, \ \frac{\partial^2 f_7}{\partial x_6 \partial x_8}(\mathscr{E}^0_{kv}) = \varpi_k \\ \frac{\partial^2 f_7}{\partial x_3 \partial x_8}(\mathscr{E}^0_{kv}) = q_k\varpi_k, \ \frac{\partial^2 f_7}{\partial x_2 \partial x_9}(\mathscr{E}^0_{kv}) = q_v\varpi_v \\ \frac{\partial^2 f_3}{\partial x_9 \partial \varpi_v}(\mathscr{E}^0_{kv}) = \frac{\Lambda}{\mu} \end{gathered}$$

It follows that

$$b = v_3 w_3 \frac{\Lambda(a_5\tau_1 + \tau_2\eta_v)}{\mu\tau_2 a_5} \ \text{ and } \ a = m - n$$

where

$$
\begin{aligned}
m =& v_2w_2w_3\frac{(1-q_k)\varpi_k(a_4\gamma_1+\gamma_2\eta_k)(a_4a_6\delta_1\mu(1-\xi_v)\omega_v+\eta_{kv}(\pi_v\gamma_2\varpi_k\Lambda+a_4\gamma_4\varpi_k\Lambda)+a_6\xi_v\omega_v\gamma_2\varpi_k\Lambda+a_4a_6\gamma_3\varpi_k\Lambda)}{a_3a_4^2a_6\delta_1^2\mu}\\
&+v_3w_2w_3\frac{(1-q_k)\varpi_k(a_4\gamma_1+\gamma_2\eta_k)(a_5a_6\delta_2\mu(1-\xi_k)\omega_k+\eta_{kv}(\pi_k\tau_2\varpi_v\Lambda+a_5\tau_4\varpi_v\Lambda)+a_6\xi_k\omega_k\tau_2\varpi_v\Lambda+a_5a_6\tau_3\varpi_v\Lambda)}{a_3a_4a_5a_6\delta_1\delta_2\mu}\\
&+v_2w_2w_3\frac{(1-q_v)\varpi_v(a_5\tau_1+\tau_2\eta_v)(a_4a_6\delta_1\mu(1-\xi_v)\omega_v+\eta_{kv}(\pi_v\gamma_2\varpi_k\Lambda+a_4\gamma_4\varpi_k\Lambda)+a_6\xi_v\omega_v\gamma_2\varpi_k\Lambda+a_4a_6\gamma_3\varpi_k\Lambda)}{a_3a_4a_5a_6\tau_2\delta_1\mu}\\
&+v_3w_2w_3\frac{(1-q_v)\varpi_v(a_5\tau_1+\tau_2\eta_v)(a_5^2a_6\tau_2\delta_2\mu(1-\xi_k)\omega_k+\eta_{kv}(\pi_k\tau_2\varpi_v\Lambda+a_5\tau_4\varpi_v\Lambda)+a_6\xi_k\omega_k\tau_2\varpi_v\Lambda+a_5a_6\tau_3\varpi_v\Lambda}{a_3a_5a_6\delta_2\mu}\\
&+v_2w_2w_3\frac{\varpi_v\eta_k(a_5\tau_1+\tau_2\eta_v)(\pi_v\gamma_2\varpi_k\Lambda+a_4\gamma_4\varpi_k\Lambda)}{a_4^2a_5a_6\tau_2\delta_1\mu}+v_3w_2w_3\frac{\varpi_v\eta_k(a_5\tau_1+\tau_2\eta_v)(\pi_k\tau_2\varpi_v\Lambda+a_5\tau_4\varpi_v\Lambda)}{\tau_2a_4a_5^2a_6\delta_2\mu}\\
&+v_2w_2w_3\frac{\varpi_k\eta_v(a_4\gamma_1+\gamma_2\eta_k)(\pi_v\gamma_2\varpi_k\Lambda+a_4\gamma_4\varpi_k\Lambda)}{a_4^2a_5a_6\delta_1^2\mu}+v_3w_2w_3\frac{\varpi_k\eta_v(a_4\gamma_1+\gamma_2\eta_k)(\pi_k\tau_2\varpi_v\Lambda+a_5\tau_4\varpi_v\Lambda)}{\delta_1a_4a_5^2a_6\delta_2\mu}\\
&+v_2w_2w_3\frac{q_k\varpi_k(a_4\gamma_1+\gamma_2\eta_k)(\pi_v\gamma_2\varpi_k\Lambda+a_4\gamma_4\varpi_k\Lambda)}{a_4^2a_6\delta_1^2\mu}+v_3w_2w_3\frac{q_k\varpi_k(a_4\gamma_1+\gamma_2\eta_k)(\pi_k\tau_2\varpi_v\Lambda+a_5\tau_4\varpi_v\Lambda)}{\delta_1a_4a_5a_6\delta_2\mu}\\
&+v_2w_2w_3\frac{q_v\varpi_v(a_5\tau_1+\tau_2\eta_v)(\pi_v\gamma_2\varpi_k\Lambda+a_4\gamma_4\varpi_k\Lambda)}{a_4a_5a_6\delta_1\tau_2\mu}+v_3w_2w_3\frac{q_v\varpi_v(a_5\tau_1+\tau_2\eta_v)(\pi_k\tau_2\varpi_v\Lambda+a_5\tau_4\varpi_v\Lambda)}{a_5^2a_6\delta_2\tau_2\mu}
\end{aligned}
$$

$$
\begin{aligned}
n =& v_2w_2^2\frac{\varpi_k^2\Lambda(a_4\gamma_1+\gamma_2\eta_k)^2}{\mu^2\delta_1^2a_4^2}+v_2w_2w_3\frac{\varpi_k\varpi_v\Lambda(a_4\gamma_1+\gamma_2\eta_k)(a_5\tau_1+\tau_2\eta_v)}{\mu^2\tau_2\delta_1a_4a_5}+v_2w_2w_3\frac{\varpi_v(a_5\tau_1+\tau_2\eta_v)}{\tau_2a_5}\\
&+v_3w_2w_3\frac{\varpi_v\varpi_k\Lambda(a_4\gamma_1+\gamma_2\eta_k)(a_5\tau_1+\tau_2\eta_v)}{\mu^2\delta_1a_4\tau_2a_5}+v_3w_3^2\frac{\varpi_v^2\Lambda(a_5\tau_1+\tau_2\eta_v)^2}{\mu^2\tau_2^2a_5^2}+v_3w_3\frac{a_4\gamma_1+\gamma_2\eta_k}{\delta_1a_4}w_2\varpi_k\\
&+v_2w_2w_3\frac{\varpi_v\varpi_k\Lambda\gamma_2\eta_k(a_5\tau_1+\tau_2\eta_v)}{\delta_1\mu\tau_2a_4^2a_5}+v_3w_2w_3\frac{\varpi_k\varpi_v\Lambda\tau_2\eta_v(a_4\gamma_1+\gamma_2\eta_k)}{\delta_1a_4a_5^2\delta_2\mu}
\end{aligned}
$$

Therefore, the system (3.1) has a backward bifurcation at $\mathscr{R}_{kv0}=1$ if $m>n$, otherwise the system has a forward bifurcation □

We thoroughly analyze the equilibrium points of the various sub-models formed from the co-infection model since the endemic equilibrium of the co-infection model could not be found explicitly. Without loss of generality, we assume that the co-infection model and its sub-models have similar features since the reproduction numbers of the sub-models are the same as those found from the co-infection model. In the following section, we get started by analyzing the CBD model.

3.3 CBD Model

This section studies the dynamics of the first sub-model, the CBD Model. Using the variables, parameters, and presumptions given in the model system (3.1), we derive the

CBD model by letting $E_v = 0$, $E_{kv} = 0$,$I_v = 0$, $I_{kv} = 0$,$P_v = 0$. Hence, the CBD model is given by

$$\left.\begin{aligned}
\frac{dS}{dt} &= \Lambda - (\varpi_k P_k + \mu)S \\
\frac{dE_k}{dt} &= \varpi_k P_k S - (\alpha_k + \mu + \eta_k)E_k \\
\frac{dI_k}{dt} &= \eta_k E_k - (\rho_k + \mu + \delta_k)I_k \\
\frac{dP_k}{dt} &= \gamma_1 E_k + \gamma_2 I_k - \delta_1 P_k \\
\frac{dR}{dt} &= \alpha_k E_k + \rho_k I_k - \mu R
\end{aligned}\right\} \tag{3.33}$$

3.3.1 CBD Disease Free Equilibrium point (DFE)

The DFE for CBD is a situation in which there is no CBD infection in the plant population. Therefore DFE for CBD model (3.33) is given by

$$\mathscr{E}_k^0 = (S^0, E_k^0, I_k^0, P_k^0, R^0) = \left(\frac{\Lambda}{\mu}, 0, 0, 0, 0\right)$$

3.3.2 Reproduction number ($\mathscr{R}_{k0}$) due to the CBD Model

According to Diekmann *et al.* (1990) $\mathscr{R}_{k0}$ is the average number of secondary infections produced by a 'typical' infected plant in a completely susceptible plant population. Using the next generation method and notations in (Van den Driessche and Watmough, 2002), we compute $\mathscr{R}_{k0}$. From System (3.33), the infected compartments are given by the following system

$$\left.\begin{aligned}
\frac{dE_k}{dt} &= \varpi_k P_k S - (\alpha_k + \mu + \eta_k)E_k \\
\frac{dI_k}{dt} &= \eta_k E_k - (\rho_k + \mu + \delta_k)I_k \\
\frac{dP_k}{dt} &= \gamma_1 E_k + \gamma_2 I_k - \delta_1 P_k
\end{aligned}\right\} \tag{3.34}$$

In view of the descriptions in (Van den Driessche and Watmough, 2002) and system (3.34), we derive

$$\mathscr{F} = \begin{bmatrix} \varpi_k P_k S \\ 0 \\ 0 \end{bmatrix} \text{ and}$$

$$\mathscr{V} = \begin{bmatrix} (\alpha_k + \mu + \eta_k)E_k \\ -\eta_k E_k + (\rho_k + \mu + \delta_k)I_k \\ -\gamma_1 E_k - \gamma_2 I_k + \delta_1 P_k \end{bmatrix}.$$

And it follows that

$$F = \begin{bmatrix} 0 & 0 & \frac{\varpi_k \Lambda}{\mu} \\ 0 & 0 & 0 \\ 0 & 0 & 0 \end{bmatrix} \text{ and}$$

$$V = \begin{bmatrix} (\alpha_k + \mu + \eta_k) & 0 & 0 \\ -\eta_k & (\rho_k + \mu + \delta_k) & 0 \\ -\gamma_1 & -\gamma_2 & \delta_1 \end{bmatrix}$$

The inverse of V is given by

$$V^{-1} = \begin{bmatrix} \frac{1}{(\alpha_k+\mu+\eta_k)} & 0 & 0 \\ \frac{\eta_k}{(\alpha_k+\mu+\eta_k)(\rho_k+\mu+\delta_k)} & \frac{1}{(\rho_k+\mu+\delta_k)} & 0 \\ \frac{(\rho_k+\mu+\delta_k)\gamma_1+\eta_k\gamma_2}{(\alpha_k+\mu+\eta_k)(\rho_k+\mu+\delta_k)\delta_1} & \frac{\gamma_2}{(\rho_k+\mu+\delta_k)\delta_1} & \frac{1}{\delta_1} \end{bmatrix}$$

Computing the product of F and V^{-1}, obtain

$$FV^{-1} = \begin{bmatrix} \frac{\varpi_k\Lambda((\rho_k+\mu+\delta_k)\gamma_1+\eta_k\gamma_2)}{(\alpha_k+\mu+\eta_k)(\rho_k+\mu+\delta_k)\mu\delta_1} & \frac{\varpi_k\Lambda\gamma_2}{(\rho_k+\mu+\delta_k)\mu\delta_1} & \frac{\varpi_k\Lambda}{\mu\delta_1} \\ 0 & 0 & 0 \\ 0 & 0 & 0 \end{bmatrix}$$

Clearly, the dominant eigenvalue of FV^{-1} is $\frac{\varpi_k\Lambda((\rho_k+\mu+\delta_k)\gamma_1+\eta_k\gamma_2)}{(\alpha_k+\mu+\eta_k)(\rho_k+\mu+\delta_k)\mu\delta_1}$. Hence

$$\mathscr{R}_{k0} = \frac{\varpi_k\Lambda((\rho_k + \mu + \delta_k)\gamma_1 + \eta_k\gamma_2)}{(\alpha_k + \mu + \eta_k)(\rho_k + \mu + \delta_k)\mu\delta_1}$$

3.3.3 Local Stability of the DFE

Theorem 3. *The DFE of Coffee Berry Disease, $\mathscr{E}_k^0$ is locally asymptotically stable if $\mathscr{R}_{k0} < 1$ and unstable if $\mathscr{R}_{k0} > 1$.*

Proof. If the Jacobian matrix's eigenvalues at $\mathscr{E}_k^0$ have negative real parts, $\mathscr{E}_k^0$ is considered to be locally asymptotically stable. Evaluating the Jacobian matrix of System (3.33) at

$\mathscr{E}_k^0$, we get

$$J(\mathscr{E}_k^0) = \begin{bmatrix} -\mu & 0 & 0 & \frac{-\varpi_k \Lambda}{\mu} & 0 \\ 0 & -(\alpha_k + \mu + \eta_k) & 0 & \frac{\varpi_k \Lambda}{\mu} & 0 \\ 0 & \eta_k & -(\rho_k + \mu + \delta_k) & 0 & 0 \\ 0 & \gamma_1 & \gamma_2 & -\delta_1 & 0 \\ 0 & \alpha_k & \rho_k & 0 & -\mu \end{bmatrix} \tag{3.35}$$

It is clear that $\lambda_1 = -\mu$ and $\lambda_2 = -\mu$ are the eigenvalues of matrix (3.35). Thus, we reduce the matrix to get

$$J_1(\mathscr{E}_k^0) = \begin{bmatrix} -(\alpha_k + \mu + \eta_k) & 0 & \frac{\varpi_k \Lambda}{\mu} \\ \eta_k & -(\rho_k + \mu + \delta_k) & 0 \\ \gamma_1 & \gamma_2 & -\delta_1 \end{bmatrix} \tag{3.36}$$

The characteristic equation of matrix (3.36) is given by

$$\lambda^3 + p_1\lambda^2 + p_2\lambda + p_3 = 0 \tag{3.37}$$

where

$p_1 = (\alpha_k + \mu + \eta_k) + (\rho_k + \mu + \delta_k) + \delta_1$

$p_2 = \delta_1(\rho_k + \mu + \delta_k) + (\alpha_k + \mu + \eta_k)((\rho_k + \mu + \delta_k) + \delta_1) - \frac{\varpi_k \Lambda \gamma_1}{\mu}$

$p_3 = (\alpha_k + \mu + \eta_k)(\rho_k + \mu + \delta_k)\delta_1 - \frac{\varpi_k \Lambda((\rho_k + \mu + \delta_k)\gamma_1 + \eta_k \gamma_2)}{\mu}$

According to Routh-Hurwitz criterion (Beards, 1995), equation (3.37) has roots with negative real parts if

$$p_1,\ p_2,\ p_3 > 0 \tag{3.38}$$

and

$$p_1 p_2 > p_3 \tag{3.39}$$

Considering the coefficients p_1, p_2 and p_3, it is clear that $p_1 > 0$. In order to show that $p_2,\ p_3 > 0$, we first express p_2 in terms of $\mathscr{R}_{k0}$. Thus we rewrite $\mathscr{R}_{k0}$ as

$$\mathscr{R}_{k0}(\alpha_k + \mu + \eta_k)\delta_1 - \frac{\varpi_k \Lambda \eta_k \gamma_2}{\mu(\rho_k + \mu + \delta_k)} = \frac{\varpi_k \Lambda \gamma_1}{\mu} \tag{3.40}$$

Substituting the equation (3.76) in p_2 we get

$$p_2 = \delta_1(\rho_k+\mu+\delta_k)+(\alpha_k+\mu+\eta_k)(\rho_k+\mu+\delta_k)+\frac{\varpi_k\Lambda\eta_k\gamma_2}{\mu(\rho_k+\mu+\delta_k)}+(\alpha_k+\mu+\eta_k)\delta_1(1-\mathscr{R}_{k0})$$

Therefore, $p_2,\ p_3 > 0$ when $\mathscr{R}_{k0} < 1$. Also it is clear that $p_2,\ p_3 < 0$ when $\mathscr{R}_{k0} > 1$. Hence, $\mathscr{E}_k^0$ is locally asymptotically stable if $\mathscr{R}_{k0} < 1$ and unstable if $\mathscr{R}_{k0} > 1$.

□

3.3.4 Global stability of disease-free equilibrium

Theorem 4. *$\mathscr{E}_k^0$ is globally asymptotically stable if $\mathscr{R}_{k0} < 1$ and unstable if $\mathscr{R}_{k0} > 1$.*

Proof. Consider the Lyapunov function

$$\mathscr{L} = \frac{(\rho_k+\mu+\delta_k)\gamma_1+\eta_k\gamma_2)}{(\alpha_k+\mu+\eta_k)}E_k+\gamma_2 I_k+(\rho_k+\mu+\delta_k)P_k \tag{3.41}$$

Taking derivative of $\mathscr{L}$, we get

$$\frac{d\mathscr{L}}{dt} = \frac{(\rho_k+\mu+\delta_k)\gamma_1+\eta_k\gamma_2)}{(\alpha_k+\mu+\eta_k)}\frac{dE_k}{dt}+\gamma_2\frac{dI_k}{dt}+(\rho_k+\mu+\delta_k)\frac{dP_k}{dt} \tag{3.42}$$

substituting the values of $\frac{dE_k}{dt}$, $\frac{dI_k}{dt}$ and $\frac{dP_k}{dt}$ in equation (3.42), we get

$$\begin{aligned}\frac{d\mathscr{L}}{dt} &= \frac{(\rho_k+\mu+\delta_k)\gamma_1+\eta_k\gamma_2)}{(\alpha_k+\mu+\eta_k)}[\varpi_k P_k S-(\alpha_k+\mu+\eta_k)E_k]+\gamma_2[\eta_k E_k-(\rho_k+\mu+\delta_k)I_k]\\ &+(\rho_k+\mu+\delta_k)[\gamma_1 E_k+\gamma_2 I_k-\delta_1 P_k]\end{aligned} \tag{3.43}$$

Upon simplifying equation (3.43), we obtain

$$\frac{d\mathscr{L}}{dt} = \left(\frac{\varpi_k(\rho_k+\mu+\delta_k)\gamma_1+\eta_k\gamma_2)}{(\alpha_k+\mu+\eta_k)}S-(\rho_k+\mu+\delta_k)\delta_1\right)P_k \tag{3.44}$$

Since $S \le S^0 = \frac{\Lambda}{\mu}$, equation (3.44) can be rewritten as

$$\frac{d\mathscr{L}}{dt} \le \left(\frac{\varpi_k\Lambda(\rho_k+\mu+\delta_k)\gamma_1+\eta_k\gamma_2)}{(\alpha_k+\mu+\eta_k)\mu}-(\rho_k+\mu+\delta_k)\delta_1\right)P_k \tag{3.45}$$

Clearly $\frac{d\mathscr{L}}{dt} \le 0$ when $\mathscr{R}_{k0} < 1$ and $\frac{d\mathscr{L}}{dt} = 0$ when $P_k = 0$. Therefore, if $P_k \to 0$ as $t \to \infty$, then $(S,\ E_k,\ I_k,\ P_k,\ R) \to (S^0,\ 0,\ 0,\ 0,\ 0) = (\frac{\Lambda}{\mu},\ 0,\ 0,\ 0,\ 0)$ as $t \to \infty$. Hence, $\mathscr{E}_k^0$ is the largest invariant set of $\{\mathscr{D} = \mathscr{D}_N \cup \mathscr{D}_{P_k} \subset \mathbb{R}_+^4 \times \mathbb{R}_+^1 : \frac{d\mathscr{L}}{dt} = 0\}$ According to LaSalle's invariance principle (Lasalle, 1976), $\mathscr{E}_k^0$ is globally asymptotically stable in $\mathscr{D}$ provided that $\mathscr{R}_{k0} < 1$. □

3.3.5 Existence of Endemic Equilibrium ($\mathscr{E}_k^*$) of Coffee Berry Disease

Equating the right hand side of system (3.33) to zero and substituting $S = S^*$, $E_k = E_k^*$, $I_k = I_k^*$, $P_k = P_k^*$, $R = R^*$, we obtain

$$\begin{aligned} 0 &= \Lambda - (\varpi_k P_k^* + \mu) S^* \\ 0 &= \varpi_k P_k^* S^* - (\alpha_k + \mu + \eta_k) E_k^* \\ 0 &= \eta_k E_k^* - (\rho_k + \mu + \delta_k) I_k^* \\ 0 &= \gamma_1 E_k^* + \gamma_2 I_k^* - \delta_1 P_k^* \\ 0 &= \alpha_k E_k^* + \rho_k I_k^* - \mu R^* \end{aligned} \tag{3.46}$$

From system (3.46), we solve for S^*, E_k^*, I_k^*, P_k^* and R^* to get

$$\begin{aligned} S^* &= \frac{\Lambda}{\mu \mathscr{R}_{k0}} \\ E_k^* &= \frac{\mu \delta_1 (\rho_k + \mu + \delta_k)\,(\mathscr{R}_{k0} - 1)}{\varpi_k (\gamma_1 (\rho_k + \mu + \delta_k) + \gamma_2 \eta_k)} \\ I_k^* &= \frac{\eta_k}{(\rho_k + \mu + \delta_k)} E_k^* \\ P_k^* &= \frac{\mu\,(\mathscr{R}_{k0} - 1)}{\varpi_k} \\ R^* &= \frac{\alpha_k (\rho_k + \mu + \delta_k) + \rho_k \eta_k}{(\rho_k + \mu + \delta_k)\mu} E_k^* \end{aligned} \tag{3.47}$$

Thus, the following theorem holds.

Theorem 5. *There exist a unique positive* $\mathscr{E}_k^* = (S^*,\ E_k^*,\ I_k^*,\ P_k^*,\ R^*)$ *if* $\mathscr{R}_{k0} > 1$

3.3.6 Local Stability of Endemic Equilibrium

Theorem 6. *The Endemic Equilibrium Point of Coffee Berry Disease,* $\mathscr{E}_k^*$ *is locally asymptotically stable if* $\mathscr{R}_{k0} > 1$.

Proof. The Jacobian of system (3.33) at $\mathscr{E}_k^* = (S^*,\ E_k^*,\ I_k^*,\ P_k^*,\ R^*))$ is given by

$$J(\mathscr{E}_k^*) = \begin{bmatrix} -(\mu+\varpi_k P_k^*) & 0 & 0 & -\varpi_k S^* & 0 \\ \varpi_k P_k^* & -(\alpha_k+\mu+\eta_k) & 0 & \varpi_k S^* & 0 \\ 0 & \eta_k & -(\rho_k+\mu+\delta_k) & 0 & 0 \\ 0 & \gamma_1 & \gamma_2 & -\delta_1 & 0 \\ 0 & \alpha_k & \rho_k & 0 & -\mu \end{bmatrix} \tag{3.48}$$

Clearly, from matrix (3.48), $\lambda_1 = -\mu$ is one of the eigenvalues. Thus, we consider the reduced matrix

$$J_1(\mathscr{E}_k^*) = \begin{bmatrix} -(\mu+\varpi_k P_k^*) & 0 & 0 & -\varpi_k S^* \\ \varpi_k P_k^* & -(\alpha_k+\mu+\eta_k) & 0 & \varpi_k S^* \\ 0 & \eta_k & -(\rho_k+\mu+\delta_k) & 0 \\ 0 & \gamma_1 & \gamma_2 & -\delta_1 \end{bmatrix} \tag{3.49}$$

The trace of matrix (3.49) is given by

$$tr(J_1(\mathscr{E}_k^*)) = -\{(\mu+\varpi_k P_k^*) + (\alpha_k+\mu+\eta_k) + (\rho_k+\mu+\delta_k) + \delta_1\} < 0 \tag{3.50}$$

and the determinant is given by

$$det(J_1(\mathscr{E}_k^*)) = \mu(\alpha_k+\mu+\eta_k)(\rho_k+\mu+\delta_k)\delta_1\,(\mathscr{R}_{k0}-1)\,. \tag{3.51}$$

In view of equation (3.51), $det(J_1(\mathscr{E}_k^*)) > 0$ when $\mathscr{R}_{k0} > 1$. Thus, by Routh-Hurwitz criterion (Beards, 1995), since matrix (3.49) has a positive determinant when $\mathscr{R}_{k0} > 1$ and negative trace, it follows that all the eigenvalues of the matrix (3.49) have negative real parts. Therefore, $\mathscr{E}_k^*$ is locally asymptotically stable if $\mathscr{R}_{k0} > 1$ □

3.3.7 Global Stability of the Endemic Equilibrium Point

Theorem 7. *The Endemic Equilibrium Point $\mathscr{E}_k^*$ of the system (3.33) is globally asymptotically stable if $\mathscr{R}_{k0} > 1$.*

Proof. Consider the following Lyapunov function

$$\begin{aligned} \mathscr{L}(S, E_k, I_k, P_k, R) = &\left(S - S^* \ln \frac{S}{S^*}\right) + \left(E_k - E_k^* \ln \frac{E_k}{E_k^*}\right) + \left(I_k - I_k^* \ln \frac{I_k}{I_k^*}\right) \\ &+ \left(P_k - P_k^* \ln \frac{P_k}{P_k^*}\right) + \left(R - R^* \ln \frac{R}{R^*}\right). \end{aligned} \tag{3.52}$$

Differentiating L with respect to t, we get

$$\frac{d\mathscr{L}}{dt} = \left(1 - \frac{S^*}{S}\right)\frac{dS}{dt} + \left(1 - \frac{E_k^*}{E_k}\right)\frac{dE_k}{dt} + \left(1 - \frac{I_k^*}{I_k}\right)\frac{dI_k}{dt} + \left(1 - \frac{P_k^*}{P_k}\right)\frac{dP_k}{dt} + \left(1 - \frac{R^*}{R}\right)\frac{dR}{dt}. \tag{3.53}$$

Using system (3.33), we express equation (3.53) as

$$\begin{aligned} \tfrac{d\mathscr{L}}{dt} = \; & \left(1 - \tfrac{S^*}{S}\right)(\Lambda - (\varpi_k P_k + \mu)S) + \left(1 - \tfrac{E_k^*}{E_k}\right)(\varpi_k P_k S - (\alpha_k + \mu + \eta_k)E_k) \\ & + \left(1 - \tfrac{I_k^*}{I_k}\right)(\eta_k E_k - (\rho_k + \mu + \delta_k)I_k) + \left(1 - \tfrac{P_k^*}{P_k}\right)(\gamma_1 E_k + \gamma_2 I_k - \delta_1 P_k) \\ & + \left(1 - \tfrac{R^*}{R}\right)(\alpha_k E_k + \rho_k I_k - \mu R). \end{aligned} \tag{3.54}$$

Rearranging system (3.46), we obtain

$$\begin{aligned} \Lambda &= (\varpi_k P_k^* + \mu)S^* \\ (\alpha_k + \mu + \eta_k) &= \frac{\varpi_k P_k^* S^*}{E_k^*} \\ (\rho_k + \mu + \delta_k) &= \frac{\eta_k E_k^*}{I_k^*} \\ \delta_1 &= \frac{\gamma_1 E_k^* + \gamma_2 I_k^*}{P_k^*} \\ \mu &= \frac{\alpha_k E_k^* + \rho_k I_k^*}{R^*} \end{aligned} \tag{3.55}$$

Substituting equation (3.55) in (3.54), we get

$$\begin{aligned} \frac{d\mathscr{L}}{dt} = & \left(1 - \frac{S^*}{S}\right)((\varpi_k P_k^* + \mu)S^* - (\varpi_k P_k + \mu)S) + \left(1 - \frac{E_k^*}{E_k}\right)\left(\varpi_k P_k S - \frac{\varpi_k P_k^* S^*}{E_k^*}E_k\right) \\ & + \left(1 - \frac{I_k^*}{I_k}\right)\left(\eta_k E_k - \frac{\eta_k E_k^*}{I_k^*}I_k\right) + \left(1 - \frac{P_k^*}{P_k}\right)\left(\gamma_1 E_k + \gamma_2 I_k - \frac{\gamma_1 E_k^* + \gamma_2 I_k^*}{P_k^*}P_k\right) \\ & + \left(1 - \frac{R^*}{R}\right)\left(\alpha_k E_k + \rho_k I_k - \frac{\alpha_k E_k^* + \rho_k I_k^*}{R^*}R\right) \end{aligned} \tag{3.56}$$

Equation (3.56) can be written as

$$\begin{aligned} \frac{d\mathscr{L}}{dt} = & -\mu\frac{(S - S^*)^2}{S} + \varpi_k P_k^* S^*\left(1 - \frac{1}{w}\right) - \varpi_k P_k^* S^*(xw - x) + \varpi_k P_k^* S^*\left(wz - x - \frac{wz}{x} + 1\right) \\ & + \eta_k E_k^*\left(x - y - \frac{x}{y} + 1\right) + \gamma_1 E_k^*\left(x - z - \frac{x}{z} + 1\right) + \gamma_2 I_k^*\left(y - z - \frac{y}{z} + 1\right) \\ & + \alpha_k E_k^*\left(x - q - \frac{x}{q} + 1\right) + \rho_k I_k^*\left(y - q - \frac{y}{q} + 1\right) \end{aligned} \tag{3.57}$$

where $w = \frac{S}{S^*}$, $x = \frac{E_k}{E_k^*}$, $y = \frac{I_k}{I_k^*}$, $z = \frac{P_k}{P_k^*}$ and $q = \frac{R}{R^*}$

Upon simplifying equation (3.57), we get

$\frac{d\mathscr{L}}{dt} = -\mu\frac{(S-S^*)^2}{S} + f(q,w,x,y,z)$

Where

$$f(q,w,x,y,z) = \left.\begin{array}{l} \varpi_k P_k^* S^* \left(2 - \frac{1}{w} - wx + wz - \frac{wz}{x}\right) + \eta_k E_k^*(x - y - \frac{x}{y} + 1) \\ +\gamma_1 E_k^*(x - z - \frac{x}{z} + 1) + \gamma_2 I_k^*(y - z - \frac{y}{z} + 1) \\ +\alpha_k E_k^* \left(x - q - \frac{x}{q} + 1\right) + \rho_k I_k^* \left(y - q - \frac{y}{q} + 1\right) \end{array}\right\} \quad (3.58)$$

Using geometric mean inequality (Hoffman, 1981), we obtain

$2 - \frac{1}{w} - wx + wz - \frac{wz}{x} \leq 0$

$x - y - \frac{x}{y} + 1 \leq 0$

$x - z - \frac{x}{z} + 1 \leq 0$

$y - z - \frac{y}{z} + 1 \leq 0$

$x - q - \frac{x}{q} + 1 \leq 0$

$y - q - \frac{y}{q} + 1 \leq 0$

Therefore, $f(q,w,x,y,z) \leq 0$ and it follows that $\frac{d\mathscr{L}}{dt} \leq 0$ in $\mathscr{D}$. The equality $\frac{d\mathscr{L}}{dt} = 0$ if $q = w = x = y = z = 1$ and $S = S^*$. Hence, according to LaSalle's invariance principle Lasalle (1976), $\mathscr{E}_k^0$ is globally asymptotically stable in $\mathscr{D}$

□

3.3.8 Bifurcation Analysis

Using the center manifold theory described in (Castillo-Chavez and Song, 2004), we examine the nature of the bifurcation. The coefficients of the normal form representing the system's dynamics on the central manifold, let's say a and b, are two significant numbers. These coefficients determine the bifurcation. Specifically, the bifurcation is forward if $a < 0$ and $b > 0$ and backward if $a > 0$ and $b > 0$. This method could lead to the following outcome:

Theorem 8. *If $\mathscr{R}_{k0} < 1$ and $a < 0$ then system (3.33) exhibits a forward bifurcation at*

$\mathscr{R}_{k0} = 1$. *If* $a > 0$, *then the system exhibits a backward bifurcation at* $\mathscr{R}_{k0} = 1$

Proof. we first examine transmission rate ϖ_k as a bifurcation parameter such that $\mathscr{R}_{k0} = 1$ when

$$\varpi_k = \varpi_k^* = \frac{(\alpha_k + \mu + \eta_k)(\rho_k + \mu + \delta_k)\mu\delta_1}{\Lambda((\rho_k + \mu + \delta_k)\gamma_1 + \eta_k\gamma_2)}$$

Substituting $S = x_1$, $E_k = x_2$, $I_k = x_3$, $P_k = x_4$ and $R = x_5$ in system (3.33), we obtain the transformed system $\frac{dx}{dt} = F(x)$ where $x = (x_1,\ x_2,\ x_3,\ x_4,\ x_5)^T$ and $F = (f_1,\ f_2,\ f_3,\ f_4,\ f_5)^T$ as shown below

$$\left.\begin{aligned}
\frac{dx_1}{dt} &= \Lambda - (\varpi_k x_4 + \mu)x_1 \\
\frac{dx_2}{dt} &= \varpi_k x_4 x_1 - (\alpha_k + \mu + \eta_k)x_2 \\
\frac{dx_3}{dt} &= \eta_k x_2 - (\rho_k + \mu + \delta_k)x_3 \\
\frac{dx_4}{dt} &= \gamma_1 x_2 + \gamma_2 x_3 - \delta_1 x_4 \\
\frac{dx_5}{dt} &= \alpha_k x_2 + \rho_k x_3 - \mu x_5
\end{aligned}\right\} \tag{3.59}$$

The Jacobian matrix of system (3.59) at $\mathscr{E}_k^0$ is given by

$$J(\mathscr{E}_k^0) = \begin{bmatrix}
-\mu & 0 & 0 & \frac{-\varpi_k\Lambda}{\mu} & 0 \\
0 & -(\alpha_k + \mu + \eta_k) & 0 & \frac{\varpi_k\Lambda}{\mu} & 0 \\
0 & \eta_k & -(\rho_k + \mu + \delta_k) & 0 & 0 \\
0 & \gamma_1 & \gamma_2 & -\delta_1 & 0 \\
0 & \alpha_k & \rho_k & 0 & -\mu
\end{bmatrix} \tag{3.60}$$

We begin by computing the right eigenvector of $J(\mathscr{E}_k^0)$, which is represented by $w = (w_1,\ w_2,\ w_3,\ w_4,\ w_5)^T$

$$\begin{bmatrix}
-\mu & 0 & 0 & \frac{-\varpi_k\Lambda}{\mu} & 0 \\
0 & -(\alpha_k + \mu + \eta_k) & 0 & \frac{\varpi_k\Lambda}{\mu} & 0 \\
0 & \eta_k & -(\rho_k + \mu + \delta_k) & 0 & 0 \\
0 & \gamma_1 & \gamma_2 & -\delta_1 & 0 \\
0 & \alpha_k & \rho_k & 0 & -\mu
\end{bmatrix}
\begin{pmatrix} w_1 \\ w_2 \\ w_3 \\ w_4 \\ w_5 \end{pmatrix} =
\begin{pmatrix} 0 \\ 0 \\ 0 \\ 0 \\ 0 \end{pmatrix} \tag{3.61}$$

We can rewrite equation (3.61) as

$$\begin{cases} -\mu w_1 - \frac{\varpi_k \Lambda}{\mu} w_4 = 0 \\ -(\alpha_k + \mu + \eta_k) w_2 + \frac{\varpi_k \Lambda}{\mu} w_4 = 0 \\ \eta_k w_2 - (\rho_k + \mu + \delta_k) w_3 = 0 \\ \gamma_1 w_2 + \gamma_2 w_3 - \delta_1 w_4 = 0 \\ \alpha_k w_2 + \rho_k w_3 - \mu w_5 = 0 \end{cases} \tag{3.62}$$

Upon solving equation (3.62), we obtain

$$\begin{cases} w_1 = -\dfrac{\varpi_k \Lambda(\gamma_1(\rho_k + \mu + \delta_k) + \gamma_2 \eta_k)}{\mu^2 \delta_1 (\rho_k + \mu + \delta_k)} w_2 \\ w_2 = w_2 > 0 \\ w_3 = \dfrac{\eta_k}{(\rho_k + \mu + \delta_k)} w_2 \\ w_4 = \dfrac{\gamma_1(\rho_k + \mu + \delta_k) + \gamma_2 \eta_k}{\delta_1 (\rho_k + \mu + \delta_k)} w_2 \\ w_5 = \dfrac{\rho_k \eta_k}{\alpha_k(\rho_k + \mu + \delta_k) + (\rho_k + \mu + \delta_k)(\mu + \sigma)} w_2 \end{cases} \tag{3.63}$$

Also, by computing the left eigenvector of $J(\mathscr{E}_k^0)$, which is represented by $v = (v_1,\ v_2,\ v_3,\ v_4,\ v_5)^T$, it follows that

$$\begin{bmatrix} -\eta & 0 & 0 & 0 & 0 \\ 0 & -(\alpha_k + \mu + \eta_k) & \eta_k & \gamma_1 & \alpha_k \\ 0 & 0 & -(\rho_k + \mu + \delta_k) & \gamma_2 & \rho_k \\ -\frac{\varpi_k \Lambda}{\mu} & \frac{\varpi_k \Lambda}{\mu} & 0 & -\delta_1 & 0 \\ 0 & 0 & 0 & 0 & -\mu \end{bmatrix} \begin{pmatrix} v_1 \\ v_2 \\ v_3 \\ v_4 \\ v_5 \end{pmatrix} = \begin{pmatrix} 0 \\ 0 \\ 0 \\ 0 \\ 0 \end{pmatrix} \tag{3.64}$$

We can express equation (3.64) as

$$\begin{cases} -\mu v_1 = 0 \\ -(\alpha_k + \mu + \eta_k) v_2 + \eta_k v_3 + \gamma_1 v_4 + \alpha_k v_5 = 0 \\ -(\rho_k + \mu + \delta_k) v_3 + \gamma_2 v_4 + \rho_k v_5 = 0 \\ -\frac{\varpi_k \Lambda}{\mu} v_1 + \frac{\varpi_k \Lambda}{\mu} v_2 - \delta_1 v_4 = 0 \\ -\mu v_5 = 0 \end{cases} \tag{3.65}$$

Upon solving equation (3.65), we obtain

$$\begin{cases} v_1 = 0 \\ v_2 = v_2 \\ v_3 = \dfrac{\gamma_2 \varpi_k \Lambda}{\delta_1 \mu(\rho_k + \mu + \delta_k)} v_2 \\ v_4 = \dfrac{\varpi_k \Lambda}{\delta_1 \mu} v_2 \\ v_5 = 0 \end{cases} \tag{3.66}$$

Using Theorem 4.1 in (Castillo-Chavez and Song, 2004), we define the coefficients a and b as follows:

$$a = \sum_{k,i,j=1}^{n} v_k w_i w_j \frac{\partial^2 f_k}{\partial x_i \partial x_j}(\mathscr{E}_k^0) \tag{3.67}$$

$$b = \sum_{k,i=1}^{n} v_k w_i \frac{\partial^2 f_k}{\partial x_i \partial \varpi_k}(\mathscr{E}_k^0) \tag{3.68}$$

Considering only the non-zero elements of the left eigenvector v and system (3.59), it follows that:

$$a = v_2 w_1 w_4 \frac{\partial^2 f_2}{\partial x_1 \partial x_4}(\mathscr{E}_k^0)$$

and

$$b = v_2 w_4 \frac{\partial^2 f_2}{\partial x_4 \partial \varpi_k}(\mathscr{E}_k^0)$$

where the f_is represent the right hand side of the system (3.59). By partial differentiation, we obtain:

$$\frac{\partial^2 f_2}{\partial x_1 \partial x_4}(\mathscr{E}_k^0) = \varpi_k$$

$$\frac{\partial^2 f_2}{\partial x_4 \partial \varpi_k}(\mathscr{E}_k^0) = \frac{\Lambda}{\mu}$$

It follows that

$$a = -v_2 w_2^2 \frac{\varpi_k^2 \Lambda(\gamma_1(\rho_k + \mu + \delta_k) + \gamma_2 \eta_k)^2}{\mu^2 \delta_1 (\rho_k + \mu + \delta_k)^2}$$

and

$$b = v_2 w_2 \frac{\Lambda(\gamma_1(\rho_k + \mu + \delta_k) + \gamma_2 \eta_k)}{\delta_1(\rho_k + \mu + \delta_k)\mu}$$

Clearly $a < 0$ and $b > 0$, hence system (3.33) exhibits a forward bifurcation at $\mathscr{R}_{k0} = 1$ $\square$

When the bifurcation is forward, it indicates that the endemic equilibrium is locally asymptotically stable for $\mathscr{R}_{k0} > 1$, the disease-free equilibrium is locally asymptotically stable for $\mathscr{R}_{k0} < 1$, and the population of coffee plants contains no CBD.

3.4 CLR disease model

This section studies the dynamics of the first sub-model, the CLR Model. Using the variables, parameters, and presumptions given in the model system (3.1), we derive the CLR model by letting $E_k = 0$, $E_{kv} = 0$,$I_k = 0$, $I_{kv} = 0$,$P_k = 0$. Hence, the CLR model is given by

$$\left.\begin{aligned}
\frac{dS}{dt} &= \Lambda - (\varpi_v P_v + \mu)S \\
\frac{dE_v}{dt} &= \varpi_v P_v S - (\alpha_v + \mu + \eta_v)E_v \\
\frac{dI_v}{dt} &= \eta_v E_v - (\rho_v + \mu + \delta_v)I_v \\
\frac{dP_v}{dt} &= \tau_1 E_v + \tau_2 I_v - \delta_2 P_v \\
\frac{dR}{dt} &= \alpha_v E_v + \rho_v I_v - \mu R
\end{aligned}\right\} \tag{3.69}$$

3.4.1 CLR Disease Free Equilibrium point (DFE)

The DFE for CLR is a situation with no CLR infection in the plant population. Therefore DFE for CLR model (3.69) is given by

$$\mathscr{E}_v^0 = (S^0, E_v^0, I_v^0, P_v^0, R^0) = \left(\frac{\Lambda}{\mu}, 0, 0, 0, 0\right)$$

3.4.2 Reproduction number ($\mathscr{R}_{v0}$) due to the CLR Model

Using the next generation method and notations in (Van den Driessche and Watmough, 2002), we compute $\mathscr{R}_{v0}$. From System (3.69), the infected compartments are given by the following system

$$\left.\begin{aligned}
\frac{dE_v}{dt} &= \varpi_v P_v S - (\alpha_v + \mu + \eta_v)E_v \\
\frac{dI_v}{dt} &= \eta_v E_v - (\rho_v + \mu + \delta_v)I_v \\
\frac{dP_v}{dt} &= \tau_1 E_v + \tau_2 I_v - \delta_2 P_v
\end{aligned}\right\} \tag{3.70}$$

In view of the descriptions in (Van den Driessche and Watmough, 2002) and system (3.70), we derive

$$\mathscr{F} = \begin{bmatrix} \varpi_v P_v S \\ 0 \\ 0 \end{bmatrix}$$

$$\mathscr{V} = \begin{bmatrix} (\alpha_v + \mu + \eta_v)E_v \\ -\eta_v E_v + (\rho_v + \mu + \delta_v)I_v \\ -\tau_1 E_v - \tau_2 I_v + \delta_2 P_v \end{bmatrix}$$

And it follows that

$$F = \begin{bmatrix} 0 & 0 & \frac{\varpi_v \Lambda}{\mu} \\ 0 & 0 & 0 \\ 0 & 0 & 0 \end{bmatrix}$$

$$V = \begin{bmatrix} (\alpha_v + \mu + \eta_v) & 0 & 0 \\ -\eta_v & (\rho_v + \mu + \delta_v) & 0 \\ -\tau_1 & -\tau_2 & \delta_2 \end{bmatrix}$$

The inverse of V is given by

$$V^{-1} = \begin{bmatrix} \frac{1}{(\alpha_v+\mu+\eta_v)} & 0 & 0 \\ \frac{\eta_v}{(\alpha_v+\mu+\eta_v)(\rho_v+\mu+\delta_v)} & \frac{1}{(\rho_v+\mu+\delta_v)} & 0 \\ \frac{(\rho_v+\mu+\delta_v)\tau_1+\eta_v\tau_2}{(\alpha_v+\mu+\eta_v)(\rho_v+\mu+\delta_v)\delta_2} & \frac{\tau_2}{(\rho_v+\mu+\delta_v)\delta_2} & \frac{1}{\delta_2} \end{bmatrix}$$

Computing the product of F and V^{-1}, we obtain

$$FV^{-1} = \begin{bmatrix} \frac{\varpi_v\Lambda((\rho_v+\mu+\delta_v)\tau_1+\eta_v\tau_2)}{(\alpha_v+\mu+\eta_v)(\rho_v+\mu+\delta_v)\mu\delta_2} & \frac{\varpi_v\Lambda\tau_2}{(\rho_v+\mu+\delta_v)\mu\delta_2} & \frac{\varpi_v\Lambda}{\mu\delta_2} \\ 0 & 0 & 0 \\ 0 & 0 & 0 \end{bmatrix}$$

Clearly, the dominant eigenvalue of FV^{-1} is $\frac{\varpi_v\Lambda((\rho_v+\mu+\delta_v)\tau_1+\eta_v\tau_2)}{(\alpha_v+\mu+\eta_v)(\rho_v+\mu+\delta_v)\mu\delta_2}$. Hence

$$\mathscr{R}_{v0} = \frac{\varpi_v\Lambda((\rho_v + \mu + \delta_v)\tau_1 + \eta_v\tau_2)}{(\alpha_v + \mu + \eta_v)(\rho_v + \mu + \delta_v)\mu\delta_2}$$

3.4.3 Stability analysis of the CLR model

3.4.4 Local Stability of the DFE

Theorem 9. *The DFE of Coffee Leaf Rust, $\mathscr{E}_v^0$ is locally asymptotically stable if $\mathscr{R}_{v0} < 1$ and unstable if $\mathscr{R}_{v0} > 1$.*

Proof. If the Jacobian matrix's eigenvalues at $\mathscr{E}_v^0$ have negative real parts, $\mathscr{E}_v^0$ is considered to be locally asymptotically stable. Evaluating the Jacobian matrix of System (3.69) at $\mathscr{E}_k^0$, we get

$$J(\mathscr{E}_v^0) = \begin{bmatrix} -\mu & 0 & 0 & \frac{-\varpi_v\Lambda}{\mu} & 0 \\ 0 & -(\alpha_v+\mu+\eta_v) & 0 & \frac{\varpi_v\Lambda}{\mu} & 0 \\ 0 & \eta_v & -(\rho_v+\mu+\delta_v) & 0 & 0 \\ 0 & \tau_1 & \tau_2 & -\delta_2 & 0 \\ 0 & \alpha_v & \rho_v & 0 & -\mu \end{bmatrix} \tag{3.71}$$

It is clear that $\lambda_1 = -\mu$ and $\lambda_2 = -\mu$ are the eigenvalues of matrix (3.35). Thus, we reduce the matrix to get

$$J_1(\mathscr{E}_v^0) = \begin{bmatrix} -(\alpha_v+\mu+\eta_v) & 0 & \frac{\varpi_v\Lambda}{\mu} \\ \eta_v & -(\rho_v+\mu+\delta_v) & 0 \\ \tau_1 & \tau_2 & -\delta_2 \end{bmatrix} \tag{3.72}$$

The characteristic equation of matrix (3.72) is given by

$$\lambda^3 + p_1\lambda^2 + p_2\lambda + p_3 = 0 \tag{3.73}$$

where

$p_1 = (\alpha_v+\mu+\eta_v) + (\rho_v+\mu+\delta_v) + \delta_2$

$p_2 = \delta_2(\rho_v+\mu+\delta_v) + (\alpha_v+\mu+\eta_v)((\rho_v+\mu+\delta_v)+\delta_2) - \frac{\varpi_v\Lambda\tau_1}{\mu}$

$p_3 = (\alpha_v+\mu+\eta_v)(\rho_v+\mu+\delta_v)\delta_2 - \frac{\varpi_v\Lambda((\rho_v+\mu+\delta_v)\tau_1+\eta_v\tau_2)}{\mu}$

According to Routh-Hurwitz criterion (Beards, 1995), equation (3.37) has roots with negative real parts if

$$p_1,\ p_2,\ p_3 > 0 \tag{3.74}$$

and

$$p_1p_2 > p_3 \tag{3.75}$$

Considering the coefficients p_1, p_2 and p_3, it is clear that $p_1 > 0$. In order to show that $p_2,\ p_3 > 0$, we first express p_2 in terms of $\mathscr{R}_{v0}$. Thus we rewrite $\mathscr{R}_{v0}$ as

$$\mathscr{R}_{v0}(\alpha_v+\mu+\eta_v)\delta_2 - \frac{\varpi_v\Lambda\eta_v\tau_2}{\mu(\rho_v+\mu+\delta_v)} = \frac{\varpi_v\Lambda\tau_1}{\mu} \tag{3.76}$$

Substituting the equation (3.76) in p_2 we get

$$p_2 = \delta_1(\rho_v+\mu+\delta_v)+(\alpha_v+\mu+\eta_v)(\rho_v+\mu+\delta_v)+\frac{\varpi_v\Lambda\eta_v\tau_2}{\mu(\rho_v+\mu+\delta_v)}+(\alpha_v+\mu+\eta_v)\delta_2(1-\mathscr{R}_{v0})$$

Therefore, $p_2,\ p_3 > 0$ when $\mathscr{R}_{v0} < 1$. Also it is clear that $p_2,\ p_3 < 0$ when $\mathscr{R}_{v0} > 1$. Hence, $\mathscr{E}_v^0$ is locally asymptotically stable if $\mathscr{R}_{v0} < 1$ and unstable if $\mathscr{R}_{v0} > 1$.

□

3.4.5 Global stability of disease-free equilibrium

Theorem 10. *$\mathscr{E}_v^0$ is globally asymptotically stable if $\mathscr{R}_{v0} < 1$ and unstable if $\mathscr{R}_{v0} > 1$.*

Proof. Consider the Lyapunov function

$$\mathscr{L} = \frac{(\rho_v+\mu+\delta_v)\tau_1+\eta_v\tau_2)}{(\alpha_v+\mu+\eta_v)}E_v+\tau_2 I_v+(\rho_v+\mu+\delta_v)P_v \tag{3.77}$$

Taking derivative of $\mathscr{L}$, we get

$$\frac{d\mathscr{L}}{dt} = \frac{(\rho_v+\mu+\delta_v)\tau_1+\eta_v\tau_2)}{(\alpha_v+\mu+\eta_v)}\frac{dE_v}{dt}+\tau_2\frac{dI_v}{dt}+(\rho_v+\mu+\delta_v)\frac{dP_v}{dt} \tag{3.78}$$

substituting the values of $\frac{dE_v}{dt}$, $\frac{dI_v}{dt}$ and $\frac{dP_v}{dt}$ in equation (3.78), we get

$$\begin{aligned}\frac{d\mathscr{L}}{dt} &= \frac{(\rho_v+\mu+\delta_v)\tau_1+\eta_v\tau_2)}{(\alpha_v+\mu+\eta_v)}[\varpi_v P_v S-(\alpha_v+\mu+\eta_v)E_v]+\tau_2[\eta_v E_v-(\rho_v+\mu+\delta_v)I_v]\\ &+(\rho_v+\mu+\delta_v)[\tau_1 E_v+\tau_2 I_v-\delta_2 P_v]\end{aligned} \tag{3.79}$$

Upon simplifying equation (3.79), we obtain

$$\frac{d\mathscr{L}}{dt} = \left(\frac{\varpi_v(\rho_v+\mu+\delta_v)\tau_1+\eta_v\tau_2)}{(\alpha_v+\mu+\eta_v)}S-(\rho_v+\mu+\delta_v)\delta_2\right)P_v \tag{3.80}$$

Since $S \le S^0 = \frac{\Lambda}{\mu}$, equation (3.80) can be rewritten as

$$\frac{d\mathscr{L}}{dt} \le \left(\frac{\varpi_v\Lambda(\rho_v+\mu+\delta_v)\tau_1+\eta_v\tau_2)}{(\alpha_v+\mu+\eta_v)\mu}-(\rho_v+\mu+\delta_v)\delta_2\right)P_v \tag{3.81}$$

Clearly $\frac{d\mathscr{L}}{dt} \le 0$ when $\mathscr{R}_{v0} < 1$ and $\frac{d\mathscr{L}}{dt} = 0$ when $P_v = 0$. Therefore, if $P_v \to 0$ as $t \to \infty$, then $(S,\ E_v,\ I_v,\ P_v,\ R) \to (S^0,\ 0,\ 0,\ 0,\ 0) = (\frac{\Lambda}{\mu},\ 0,\ 0,\ 0,\ 0)$ as $t \to \infty$. Hence, $\mathscr{E}_v^0$ is the largest invariant set of $\{\mathscr{D} = \mathscr{D}_N \cup \mathscr{D}_{P_v} \subset \mathbb{R}_+^4 \times \mathbb{R}_+^1 : \frac{d\mathscr{L}}{dt} = 0\}$. According to LaSalle's invariance principle (Lasalle, 1976), $\mathscr{E}_v^0$ is globally asymptotically stable in $\mathscr{D}$ provided that $\mathscr{R}_{v0} < 1$. □

3.4.6 Existence of Endemic Equilibrium ($\mathscr{E}_v^*$) of Coffee Leaf Rust

Equating the right hand side of system (3.69) to zero and substituting $S = S^*$, $E_v = E_v^*$, $I_v = I_v^*$, $P_v = P_v^*$, $R = R^*$, we obtain

$$\begin{aligned} 0 &= \Lambda - (\varpi_v P_v^* + \mu) S^* \\ 0 &= \varpi_v P_v^* S^* - (\alpha_v + \mu + \eta_v) E_v^* \\ 0 &= \eta_v E_v^* - (\rho_v + \mu + \delta_v) I_v^* \\ 0 &= \tau_1 E_v^* + \tau_2 I_v^* - \delta_2 P_v^* \\ 0 &= \alpha_k E_v^* + \rho_v I_v^* - \mu R^* \end{aligned} \tag{3.82}$$

From system (3.82), we solve for S^*, E_v^*, I_v^*, P_v^* and R^* to get

$$\begin{aligned} S^* &= \frac{\Lambda}{\mu \mathscr{R}_{v0}} \\ E_v^* &= \frac{\mu \delta_2 (\rho_v + \mu + \delta_v)\left(\mathscr{R}_{v0} - 1\right)}{\varpi_v (\tau_1 (\rho_v + \mu + \delta_v) + \tau_2 \eta_v)} \\ I_v^* &= \frac{\eta_v}{(\rho_v + \mu + \delta_v)} E_v^* \\ P_v^* &= \frac{\mu \left(\mathscr{R}_{v0} - 1\right)}{\varpi_v} \\ R^* &= \frac{\alpha_v (\rho_v + \mu + \delta_v) + \rho_v \eta_v}{(\rho_v + \mu + \delta_v)\mu} E_v^* \end{aligned} \tag{3.83}$$

Thus, the following theorem holds.

Theorem 11. *There exist a unique positive* $\mathscr{E}_v^* = (S^*,\ E_v^*,\ I_k^*,\ P_v^*,\ R^*)$ *if* $\mathscr{R}_{v0} > 1$

3.4.7 Local Stability of Endemic Equilibrium

Theorem 12. *The Endemic Equilibrium Point of Coffee Leaf Rust,* $\mathscr{E}_v^*$ *is locally asymptotically stable if* $\mathscr{R}_{v0} > 1$.

Proof. The Jacobian of system (3.69) at $\mathscr{E}_v^* = (S^*,\ E_v^*,\ I_v^*,\ P_v^*,\ R^*))$ is given by

$$J(\mathscr{E}_v^*) = \begin{bmatrix} -(\mu+\varpi_v P_v^*) & 0 & 0 & -\varpi_v S^* & 0 \\ \varpi_v P_v^* & -(\alpha_v+\mu+\eta_v) & 0 & \varpi_v S^* & 0 \\ 0 & \eta_v & -(\rho_v+\mu+\delta_v) & 0 & 0 \\ 0 & \tau_1 & \tau_2 & -\delta_2 & 0 \\ 0 & \alpha_v & \rho_v & 0 & -\mu \end{bmatrix} \tag{3.84}$$

Clearly, from matrix (3.84), $\lambda_1 = -\mu$ is one of the eigenvalues. Thus, we consider the reduced matrix

$$J_1(\mathscr{E}_v^*) = \begin{bmatrix} -(\mu+\varpi_v P_v^*) & 0 & 0 & -\varpi_k S^* \\ \varpi_v P v^* & -(\alpha_v+\mu+\eta_v) & 0 & \varpi_v S^* \\ 0 & \eta_v & -(\rho_v+\mu+\delta_v) & 0 \\ 0 & \tau_1 & \tau_2 & -\delta_2 \end{bmatrix} \tag{3.85}$$

The trace of matrix (3.85) is given by

$$tr(J_1(\mathscr{E}_v^*)) = -\{(\mu+\varpi_v P_v^*) + (\alpha_v+\mu+\eta_v) + (\rho_v+\mu+\delta_v) + \delta_2\} < 0 \tag{3.86}$$

and the determinant is given by

$$det(J_1(\mathscr{E}_v^*)) = \mu(\alpha_v+\mu+\eta_v)(\rho_v+\mu+\delta_v)\delta_2\,(\mathscr{R}_{v0}-1)\,. \tag{3.87}$$

In view of equation (3.87), $det(J_1(\mathscr{E}_v^*)) > 0$ when $\mathscr{R}_{v0} > 1$. Thus, by Routh-Hurwitz criteria, since matrix (3.85) has a positive determinant when $\mathscr{R}_{v0} > 1$ and negative trace, it follows that all the eigenvalues of the matrix (3.85) have negative real parts. Therefore, $\mathscr{E}_v^*$ is locally asymptotically stable if $\mathscr{R}_{v0} > 1$ □

3.4.8 Global Stability of the Endemic Equilibrium Point

Theorem 13. *The Endemic Equilibrium Point $\mathscr{E}_v^*$ of the system (3.69) is globally asymptotically stable if $\mathscr{R}_{v0} > 1$.*

Proof. Consider the following Lyapunov function

$$\begin{aligned} \mathscr{L}(S, E_v, I_v, P_v, R) = &\left(S - S^* \ln\frac{S}{S^*}\right) + \left(E_v - E_v^* \ln\frac{E_v}{E_v^*}\right) + \left(I_v - I_v^* \ln\frac{I_v}{I_v^*}\right) \\ &+ \left(P_v - P_v^* \ln\frac{P_v}{P_v^*}\right) + \left(R - R^* \ln\frac{R}{R^*}\right). \end{aligned} \tag{3.88}$$

Differentiating L with respect to t, we get

$$\frac{d\mathscr{L}}{dt} = \left(1 - \frac{S^*}{S}\right)\frac{dS}{dt} + \left(1 - \frac{E_v^*}{E_v}\right)\frac{dE_v}{dt} + \left(1 - \frac{I_v^*}{I_v}\right)\frac{dI_v}{dt} + \left(1 - \frac{P_v^*}{P_v}\right)\frac{dP_v}{dt} + \left(1 - \frac{R^*}{R}\right)\frac{dR}{dt}. \tag{3.89}$$

Using system (3.69), we express equation (3.89) as

$$\begin{aligned} \tfrac{d\mathscr{L}}{dt} = \; & \left(1 - \tfrac{S^*}{S}\right)(\Lambda - (\varpi_v P_v + \mu)S) + \left(1 - \tfrac{E_v^*}{E_v}\right)(\varpi_v P_v S - (\alpha_v + \mu + \eta_v)E_v) \\ & + \left(1 - \tfrac{I_v^*}{I_v}\right)(\eta_v E_v - (\rho_v + \mu + \delta_v)I_v) + \left(1 - \tfrac{P_v^*}{P_v}\right)(\tau_1 E_v + \tau_2 I_v - \delta_2 P_v) \\ & + \left(1 - \tfrac{R^*}{R}\right)(\alpha_v E_v + \rho_v I_v - \mu R). \end{aligned} \tag{3.90}$$

Rearranging system (3.82), we obtain

$$\begin{aligned} \Lambda &= (\varpi_v P_v^* + \mu)S^* \\ (\alpha_v + \mu + \eta_v) &= \frac{\varpi_v P_v^* S^*}{E_v^*} \\ (\rho_v + \mu + \delta_v) &= \frac{\eta_v E_v^*}{I_v^*} \\ \delta_2 &= \frac{\tau_1 E_k^* + \tau_2 I_v^*}{P_v^*} \\ \mu &= \frac{\alpha_v E_v^* + \rho_v I_v^*}{R^*} \end{aligned} \tag{3.91}$$

Substituting equation (3.91) in (3.90), we get

$$\begin{aligned} \frac{d\mathscr{L}}{dt} = & \left(1 - \frac{S^*}{S}\right)((\varpi_v P_v^* + \mu)S^* - (\varpi_v P_v + \mu)S) + \left(1 - \frac{E_v^*}{E_v}\right)\left(\varpi_v P_v S - \frac{\varpi_v P_v^* S^*}{E_v^*}E_v\right) \\ & + \left(1 - \frac{I_v^*}{I_v}\right)\left(\eta_v E_v - \frac{\eta_v E_v^*}{I_v^*}I_v\right) + \left(1 - \frac{P_v^*}{P_v}\right)\left(\tau_1 E_k + \tau_2 I_v - \frac{\tau_1 E_v^* + \tau_2 I_v^*}{P_v^*}P_v\right) \\ & + \left(1 - \frac{R^*}{R}\right)\left(\alpha_v E_v + \rho_v I_v - \frac{\alpha_v E_v^* + \rho_v I_v^*}{R^*}R\right) \end{aligned} \tag{3.92}$$

Equation (3.92) can be written as

$$\begin{aligned} \frac{d\mathscr{L}}{dt} = & -\mu\frac{(S - S^*)^2}{S} + \varpi_v P_v^* S^*\left(1 - \frac{1}{w}\right) - \varpi_v P_v^* S^*(xw - x) + \varpi_v P_v^* S^*\left(wz - x - \frac{wz}{x} + 1\right) \\ & + \eta_v E_v^*\left(x - y - \frac{x}{y} + 1\right) + \tau_1 E_v^*\left(x - z - \frac{x}{z} + 1\right) + \tau_2 I_v^*\left(y - z - \frac{y}{z} + 1\right) \\ & + \alpha_v E_v^*\left(x - q - \frac{x}{q} + 1\right) + \rho_v I_v^*\left(y - q - \frac{y}{q} + 1\right) \end{aligned} \tag{3.93}$$

where $w = \frac{S}{S^*}$, $x = \frac{E_v}{E_v^*}$, $y = \frac{I_v}{I_v^*}$, $z = \frac{P_v}{P_v^*}$ and $q = \frac{R}{R^*}$

Upon simplifying equation (3.93), we get

$\frac{d\mathscr{L}}{dt} = -\mu\frac{(S-S^*)^2}{S} + f(q,w,x,y,z)$

Where

$$f(q,w,x,y,z) = \left.\begin{array}{l} \varpi_v P_v^* S^* \left(2 - \frac{1}{w} - wx + wz - \frac{wz}{x}\right) + \eta_v E_v^*(x - y - \frac{x}{y} + 1) \\ +\tau_1 E_v^*(x - z - \frac{x}{z} + 1) + \tau_2 I_v^*(y - z - \frac{y}{z} + 1) \\ +\alpha_v E_v^* \left(x - q - \frac{x}{q} + 1\right) + \rho_v I_v^* \left(y - q - \frac{y}{q} + 1\right) \end{array}\right\} \tag{3.94}$$

Using geometric mean inequality (Hoffman, 1981), we obtain

$2 - \frac{1}{w} - wx + wz - \frac{wz}{x} \leq 0$

$x - y - \frac{x}{y} + 1 \leq 0$

$x - z - \frac{x}{z} + 1 \leq 0$

$y - z - \frac{y}{z} + 1 \leq 0$

$x - q - \frac{x}{q} + 1 \leq 0$

$y - q - \frac{y}{q} + 1 \leq 0$

Therefore, $f(q,w,x,y,z) \leq 0$ and it follows that $\frac{d\mathscr{L}}{dt} \leq 0$ in $\mathscr{D}$. The equality $\frac{d\mathscr{L}}{dt} = 0$ if $q = w = x = y = z = 1$ and $S = S^*$. Hence, according to LaSalle's invariance principle Lasalle (1976), $\mathscr{E}_k^0$ is globally asymptotically stable in $\mathscr{D}$

□

3.5 Numerical Simulation

In this section, we investigate the dynamics of the system model (3.1) when $\mathscr{R}_{kv0} < 1$ and $\mathscr{R}_{kv0} > 1$ by use of Matlab. We utilize realistic estimates of the simulation parameter values, consistent with those found in the literature. The set of parameter values is shown in Table 3.1 and the results are shown in Figures 3.2 and 3.3.

Table 3.1: Parameter values

Parameter	Value ($months^{-1}$)	Source
Λ	0.00133	Muhumuza (2018)
ϖ_k	0.0007954551	Assumed
ϖ_v	0.000209819	Assumed
μ	0.00056	Muhumuza (2018)
δ_k	0.0001	Assumed
δ_v	0.01	Assumed
δ_1	0.0900982	Estimate
δ_2	0.19009821	Estimate
q_k	0.3	Assumed
q_v	0.3	Assumed
ξ_k	0.00911	Assumed
ξ_v	0.009	Assumed
ω_k	0.09	Assumed
ω_v	0.08	Assumed
π_k	0.004	Assumed
π_v	0.0039	Assumed
η_k	0.01	Estimate
η_v	0.05	Estimate
η_{kv}	0.01	Estimate
ρ_k	0.005	Assumed
ρ_v	0.0433	Assumed
ρ_{kv}	0.0052	Assumed
α_k	0.001	Assumed
α_v	0.001	Assumed
α_{kv}	0.013	Assumed
γ_1	0.0587365	Estimate
γ_2	0.0487364	Estimate
γ_3	0.0091	Estimate
γ_4	0.00921	Estimate
τ_1	0.1	Assumed
τ_2	0.1	Assumed
τ_3	0.191	Assumed
τ_4	0.12	Assumed

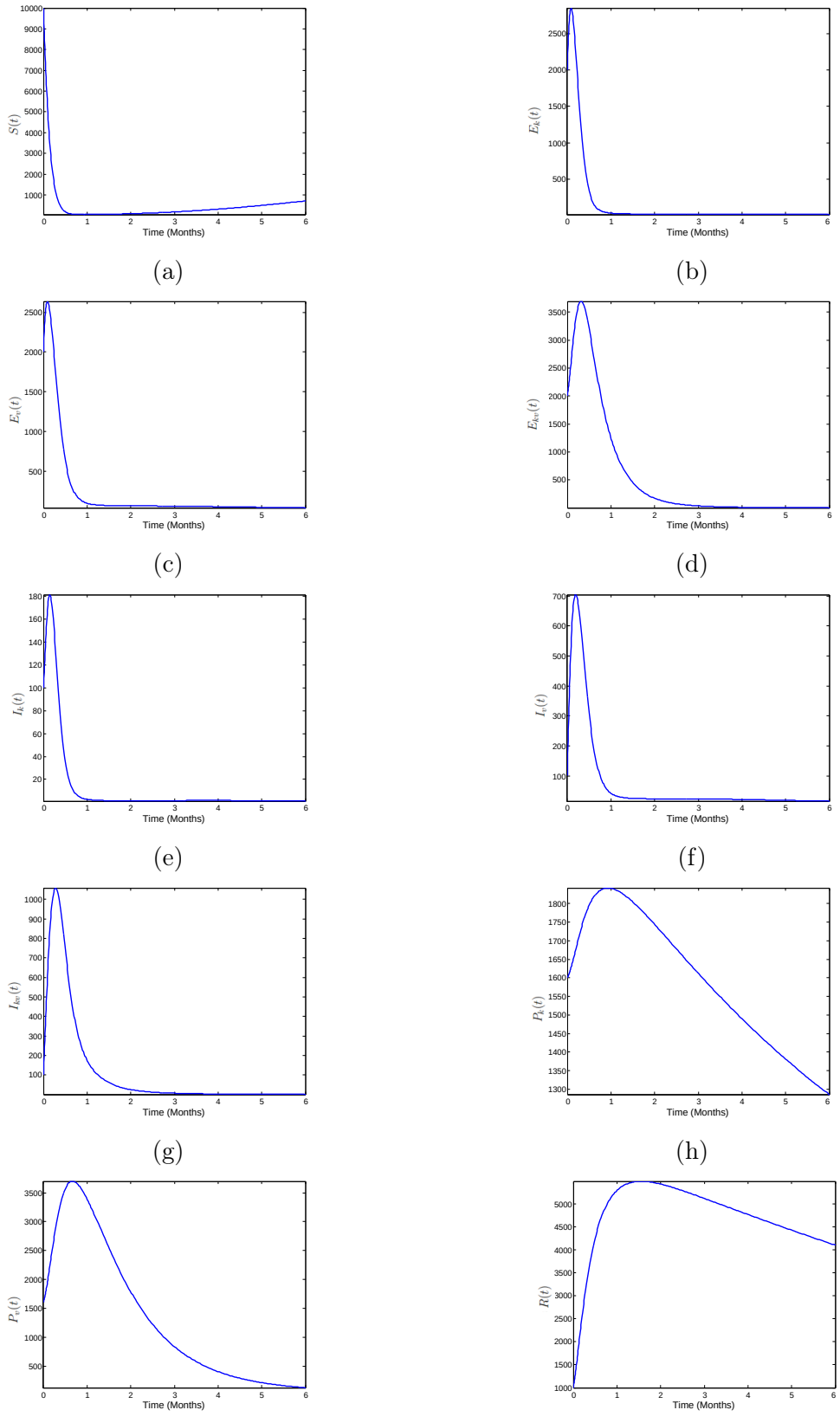

(a) (b) (c) (d) (e) (f) (g) (h) (i) (j)

Figure 3.2: Graphs showing the dynamics of model system (3.1) when $\mathscr{R}_{kv0} < 1$

The set of graphs in Figure 3.2 illustrates the dynamics of different model variables over time when the basic reproduction number, $\mathscr{R}_{kv0} = \max\{\mathscr{R}_{k0}, \mathscr{R}_{v0}\}$, is less than 1. This scenario suggests that the disease cannot sustain itself within the coffee plantation, leading to its eventual eradication. The graphs show the evolution of different compartments in the model, representing various states of coffee plants and environmental pathogen levels. Figure 3.2 (a) represents susceptible coffee plants $S(t)$, over time $\mathscr{R}_{kv0} = \max\{\mathscr{R}_{k0}, \mathscr{R}_{v0}\} < 1$. The curve shows a gradual decline, indicating that some susceptible plants are transitioning into exposed compartments due to interacting with pathogens. Since $\mathscr{R}_{kv0} < 1$ implies that the disease will eventually die out, the number of susceptible plants does not experience a drastic depletion. Instead, it stabilizes after an initial decline. The presence of a non-zero susceptible population at the end of the period suggests that the infection did not spread aggressively enough to convert all susceptible plants into exposed states. In Figure 3.2(b), the population of coffee plants exposed to coffee berry disease (CBD) $(E_k(t))$ declines sharply, suggesting that these plants either progress to the infected stage or recover, preventing the disease from sustaining itself. Similarly, Figure 3.2(c) displays the coffee plants exposed to coffee leaf rust (CLR) ($(E_v(t))$, which also exhibits a decreasing trend, further reinforces the inability of the disease to spread under the given conditions. Figure 3.2 (d), which tracks co-exposed coffee plants $(E_{kv}(t))$, follows a similar pattern of decline, indicating that dual exposure does not significantly prolong disease persistence.

Figures 3.2 (e) and (f) depict the number of coffee plants infected with CBD ($(I_k(t))$ and CLR ($(I_k(t))$, respectively. Both graphs show an initial rise, followed by a gradual decline, signifying that although the diseases may initially infect a portion of the population, they eventually die out as infected plants recover or die. In Figure 3.2 (g), coffee plants co-infected with both diseases$(I_{kv}(t))$ exhibit a peak before experiencing a sharp decline, indicating that plants with dual infections either recover or succumb to the disease, preventing further transmission. The recovery process is evident in Figure 3.2(h), where the

number of recovered coffee plants ($R(t)$) steadily increases, confirming that most infected plants eventually recover rather than dying.

Additionally, Figures 3.2 (i) and (j) illustrate the environmental pathogen levels of coffee berry disease ($P_k(t)$) and coffee leaf rust ($P_v(t)$), both of which decrease over time. This suggests that without sustained infections, the environmental reservoirs of these pathogens diminish, further supporting the conclusion that the diseases are being eradicated. Overall, these graphs confirm that when $\mathscr{R}_{kv0} < 1$, the disease naturally declines and eventually disappears from the system. The decreasing trends in infected plant populations and pathogen levels suggest that the plantation will return to a disease-free equilibrium. Figure 3.3 illustrates the dynamics of the model system (3.1) when $\mathscr{R}_{kv0} > 1$, indicating that the infection is spreading and sustained within the coffee plantation. Unlike the previous case where $\mathscr{R}_{kv0} < 1$, here the disease persists and significantly impacts different plant groups.

Figure 3.3 (a) shows the dynamics of susceptible plants, $S(t)$, which decrease rapidly over time. This suggests that a large portion of the population is transitioning into exposed states due to the high infection rate associated with $\mathscr{R}_{kv0} < 1$. The continuous decline in susceptible plants highlights the significant impact of the disease. Figure 3.3 (b) represents the dynamics of coffee plants exposed to *Colletotrichum kahawae*, $E_k(t)$. The curve initially rises, indicating an increasing number of plants entering this exposed category. However, it eventually declines, suggesting that many exposed plants transition into the infected category.

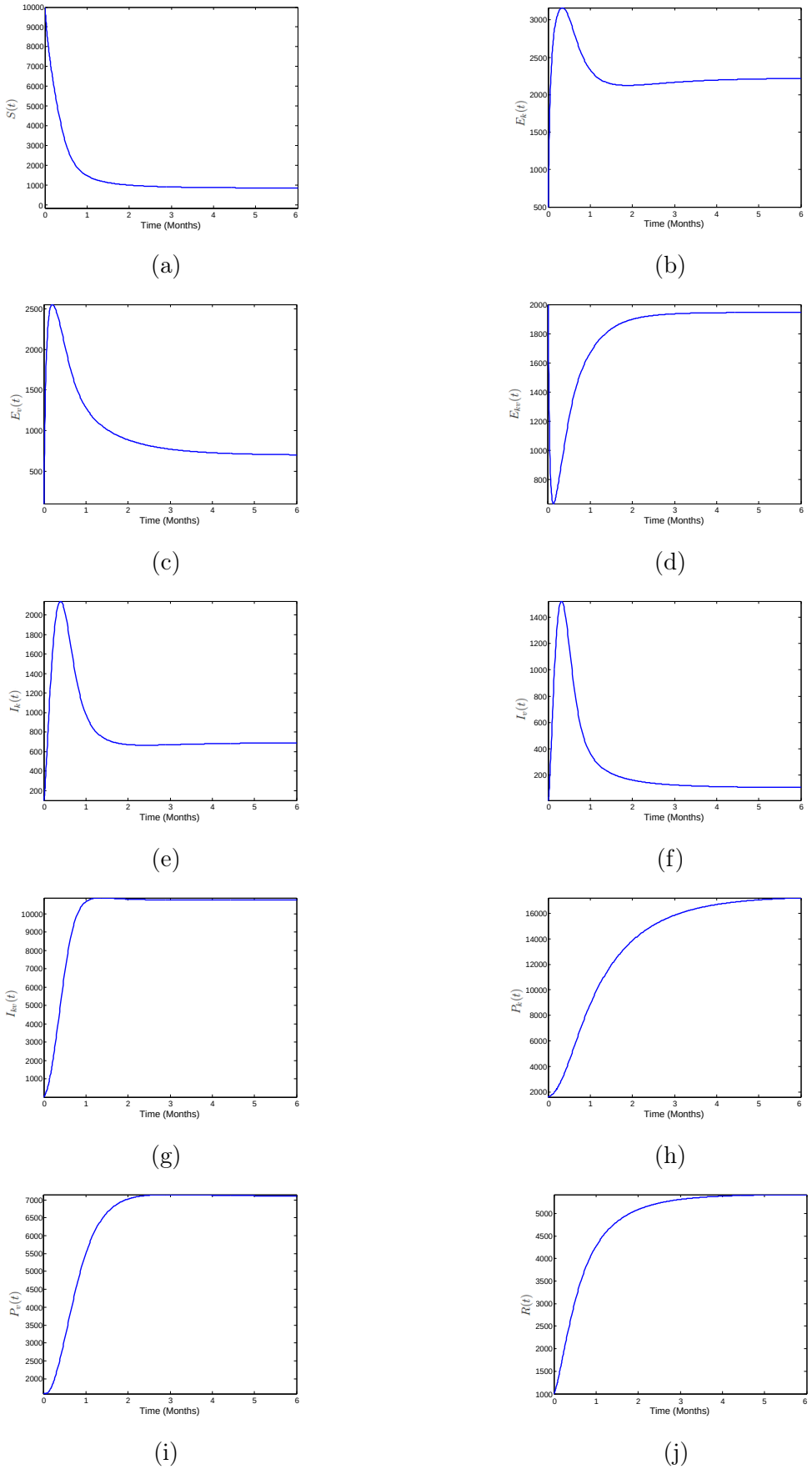

Figure 3.3: Graphs showing the dynamics of model system (3.1) when $\mathscr{R}_{kv0} > 1$

Figure 3.3 (c) depicts the dynamics of plants exposed to *Hemileiavastatrix*, $E_v(t)$, following a similar trend to $E_k(t)$. The initial increase in exposed plants confirms active disease transmission, while the eventual decrease suggests that plants are progressing into later stages of infection. Figure 3.3 (d) corresponds to the co-exposed coffee plants, $E_{kv}(t)$, showing a sharp increase before reaching a steady state. This suggests that co-exposure to both pathogens is occurring at a high rate, and many plants remain in this category. Figure 3.3 (e) and (f) illustrate the dynamics of coffee berry disease (CBD)-infected plants, $I_k(t)$, and coffee leaf rust (CLR)-infected plants, $I_v(t)$, respectively. Both show an initial increase followed by a decline, indicating that infection spreads rapidly but later stabilizes or diminishes as plants either recover or move into more advanced stages of disease. Figure 3.3 (g) shows the dynamics of co-infected plants, $I_{kv}(t)$, which steadily increase before reaching a plateau. This implies that plants infected by both pathogens accumulate over time, contributing to a high disease burden in the plantation. Figure 3.3 (h) represents recovered plants, $R(t)$, displaying a continuous rise. This suggests that over time, a portion of the infected population recovers, potentially gaining immunity. Figure 3.3 (i) and (j) show the dynamics of the pathogen populations, $P_k(t)$ for *Colletotrichumkahawae* and $P_v(t)$ for *Hemileiavastatrix*, respectively. Both pathogen populations increase over time, indicating sustained transmission and persistence of the disease within the plantation. Overall, Figure 3.3 demonstrates that when $\mathscr{R}_{kv0} > 1$, the infection persists, and multiple plant groups are continuously affected. Unlike the case where $\mathscr{R}_{kv0} < 1$, here the pathogens establish themselves within the plantation, leading to an ongoing epidemic. The steady increase in infected and co-infected plants and the growing pathogen populations highlight the need for interventions to control the disease spread.

Chapter 4: Optimal Control and cost effectiveness analysis of the co-infection model

4.1 Optimal Control Analysis

4.1.1 Introduction

Any epidemiological study's goal is to enhance current control measures and eventually get rid of the epidemic in the population it is affecting. The use of optimal control is essential for making decisions regarding workable control techniques to implement to end the epidemic (Kar and Jana, 2013). The comprehension of CBD-CLR co-infection is consequently greatly aided by the inclusion of optimal control in epidemic modeling. An optimal control problem is established and numerically analyzed to determine optimal control policies that reduce the number of infected coffee plants at a relatively low cost. The CBD-CLR Co-infection Model (3.1) is expanded to incorporate control measures in this chapter. We aim to evaluate how controls affect recruitment and CBD-CLR Co-infection in the dynamics of an epidemic.

4.1.2 Co-infection model with controls

We developed a strategy to reduce CBD and CLR infections. This is accomplished by incorporating seven time-dependent control measures ($u_i(t),\ i = 1, 2, \cdots, 7$) that reduce the rate of CBD and CLR infection. The control measures are defined as:

(i) u_1- prevention of CBD infection by use of cultural measures (pruning and weeding) and planting resistant coffee varieties such as K7 (k gene), Hibrido de Timor (Ck-1 or T gene) and Rume Sudan (R and K genes)

(ii) u_2- prevention of CLR infection by spraying copper oxychloride, use of resistant/tolerant plant cultivars from suggested nurseries, as well as cultural measures including appropriate pruning and weeding.

(iii) u_3- Treatment of CBD-infected coffee plants by applying copper-based fungicides such as Nordox 75% EC

(iv) u_4- Treatment of CLR-infected coffee plants by spraying For the management of coffee leaf rust, a tank mixture of copper (5 kg of 50% weightable powder copper oxychloride) and a half-rate organic fungicide (for example, 2 kg of 75% weightable powder chlorothalonil) is also effective.

(v) u_5- Treatment of CBD-CLR Co-infected coffee plants by spraying Tebuconazole

(vi) u_6- Elimination of *Colletotrichum kahawae* pathogens by using bio-control agents such as *Pseudomonas spinosa* ECk-17, *B. mycoides* ECk-06 and *Bacillus megaterium* ECk-05

(vii) u_7- Elimination of *Hemileia vastatrix* pathogens by use of suspensions of *Bacillus* species as a biocontrol

In the presence of controls, the expanded model system of equations for the transmission dynamics of CBD-CLR Co-infection is given by

$$
\begin{aligned}
\frac{dS}{dt} &= \Lambda - (1-u_1)\varpi_k P_k S - (1-u_2)\varpi_v P_v S - \mu S \\
\frac{dE_k}{dt} &= (1-u_1)\varpi_k P_k S + (1-\xi_v)(\omega_v + u_4)E_{kv} - (\alpha_k + u_3)E_k - ((1-u_2)\varpi_v P_v + \mu + \eta_k)E_k \\
\frac{dE_v}{dt} &= (1-u_2)\varpi_v P_v S + (1-\xi_k)(\omega_k + u_3)E_{kv} - (\alpha_v + u_4)E_v - ((1-u_1)\varpi_k P_k + \mu + \eta_v)E_v \\
\frac{dE_{kv}}{dt} &= (1-u_2)(1-q_v)\varpi_v P_v E_k + (1-u_1)(1-q_k)\varpi_k P_k E_v - (\omega_k + u_3)E_{kv} - (\omega_v + u_4)E_{kv} \\
&\quad -(\alpha_{kv} + u_5)E_{kv} - (\mu + \eta_{kv})E_{kv} \\
\frac{dI_k}{dt} &= \eta_k E_k + \xi_v(\omega_v + u_4)E_{kv} + (\pi_v + u_4)I_{kv} - (1-u_2)\varpi_v P_v I_k - (\rho_k + u_3)I_k - (\mu + \delta_k)I_k \\
\frac{dI_v}{dt} &= \eta_v E_v + \xi_k(\omega_k + u_3)E_{kv} + (\pi_k + u_3)I_{kv} - (1-u_1)\varpi_k P_k I_v - (\rho_v + u_4)I_v - (\mu + \delta_v)I_v \\
\frac{dI_{kv}}{dt} &= (1-u_2)q_v\varpi_v P_v E_k + (1-u_1)q_k\varpi_k P_k E_v + (1-u_1)\varpi_k P_k I_v + (1-u_2)\varpi_v P_v I_k + \eta_{kv}E_{kv} \\
&\quad -(\pi_k + u_3)I_{kv} - (\pi_v + u_4)I_{kv} - (\rho_{kv} + u_5)I_{kv} - (\mu + \delta_k + \delta_v)I_{kv}
\end{aligned}
$$

$$\begin{aligned}
\frac{dP_k}{dt} &= \gamma_1 E_k + \gamma_2 I_k + \gamma_3 E_{kv} + \gamma_4 I_{kv} - (\delta_1 + u_6)P_k \\
\frac{dP_v}{dt} &= \tau_1 E_v + \tau_2 I_v + \tau_3 E_{kv} + \tau_4 I_{kv} - (\delta_2 + u_7)P_v \\
\frac{dR}{dt} &= (\alpha_k + u_3)E_k + (\alpha_v + u_4)E_v + (\alpha_{kv} + u_5)E_{kv} + (\rho_k + u_3)I_k + (\rho_v + u_4)I_v + (\rho_{kv} + u_5)I_{kv} \\
&\quad -\mu R
\end{aligned} \tag{4.1}$$

The control set U is Lebesgue measurable (Lebesgue, 1902) and is defined as follows to explore the optimal levels of the controls: $U = \{(u_1(t), u_2(t), u_3(t), u_4(t), u_5(t), u_6(t), u_7(t)) \mid 0 \leq u_i \leq 1,\ i = 1, 2, \cdots, 7;\ t \in [0, T]\}$. The objective function is given by

$$\left.\begin{aligned}
\mathcal{J} = \min_{u_1,u_2,u_3,u_4,u_5,u_6,u_7} \int_0^T & [b_1 E_k(t) + b_2 E_v(t) + b_3 E_{kv}(t) + b_4 I_k(t) + b_5 I_v(t) \\
& + b_6 I_{kv}(t) + b_7 P_k(t) + b_8 P_v(t) + \frac{1}{2}\sum_{i=1}^{7} v_i u_i^2] dt
\end{aligned}\right\} \tag{4.2}$$

T is the intervention time period. The coefficients b_1, b_2, b_3, b_4, b_5, b_6, b_7, and b_8 are the costs associated with minimizing plants exposed to *Colletotrichum Kahawae* (the infected coffee plants which have not showed symptoms) $E_k(t)$, plants exposed to *Hemileia vastatrix* $E_v(t)$, co-exposed plants E_{kv}, the CBD infected coffee plants $I_k(t)$, the CLR infected coffee plants $I_v(t)$, the co-infected plants $I_{kv}(t)$ *Colletotrichum Kahawae* pathogens $P_k(t)$ and *Hemileia vastatrix* pathogens $P_v(t)$ respectively. On the other hand, the parameters v_1, v_2, v_3, v_4, v_5, v_6 and v_7 are the costs weights associated with the controls u_1, u_2, u_3, u_4, u_5, u_6, u_7 respectively. Our goal is to minimize the number of infections and control costs. Consequently, we want to find optimal controls $(u_1^*, u_2^*, u_3^*, u_4^*, u_5^*, u_6^*, u_7^*)$ such that

$$\mathcal{J}(u_1^*, u_2^*, u_3^*, u_4^*, u_5^*, u_6^*, u_7^*) = \min\{\mathcal{J}(u_1, u_2, u_3, u_4, u_5, u_6, u_7) | u_1, u_2, u_3, u_4, u_5, u_6, u_7 \in U\}$$

4.1.3 The Hamiltonian and Optimality System

We use Pontryagin's Maximum Principle (Pontryagin *et al.*, 1962) to define the Hamiltonian ($\mathcal{H}$) as:

$$\left.\begin{aligned}\mathcal{H} =& b_1E_k(t) + b_2E_v(t) + b_3E_{kv}(t) + b_4I_k(t) + b_5I_v(t) + b_6I_{kv}(t) + b_7P_k(t)\\ &+ b_8P_v(t) + \frac{1}{2}v_1u_1^2 + \frac{1}{2}v_2u_2^2 + \frac{1}{2}v_3u_3^2 + \frac{1}{2}v_4u_4^2 + \frac{1}{2}v_5u_5^2 + \frac{1}{2}v_6u_6^2 + \frac{1}{2}v_7u_7^2\\ &+ M_1\frac{dS}{dt} + M_2\frac{dE_k}{dt} + M_3\frac{dE_v}{dt} + M_4\frac{dE_{kv}}{dt} + M_5\frac{dI_k}{dt} + M_6\frac{dI_k}{dt} + M_7\frac{dI_{kv}}{dt}\\ &+ M_8\frac{dP_k}{dt} + M_9\frac{dP_v}{dt} + M_{10}\frac{dR}{dt}\end{aligned}\right\} \tag{4.3}$$

Where M_1, M_2, M_3, M_4, M_5, M_6, M_7, M_8, M_9 and M_{10} are adjoint or co-state variables corresponding to the state variables S, E_k, E_v, E_{kv}, I_k, I_v, I_{kv}, P_k, P_v and R, respectively. Using system (4.1), we can rewrite equation (4.3) as

$$\begin{aligned}\mathcal{H} =& b_1E_k(t) + b_2E_v(t) + b_3E_{kv}(t) + b_4I_k(t) + b_5I_v(t) + b_6I_{kv}(t) + b_7P_k(t) + b_8P_v(t)\\ &+ \frac{1}{2}v_1u_1^2 + \frac{1}{2}v_2u_2^2 + \frac{1}{2}v_3u_3^2 + \frac{1}{2}v_4u_4^2 + \frac{1}{2}v_5u_5^2 + \frac{1}{2}v_6u_6^2 + \frac{1}{2}v_7u_7^2\\ &+ M_1\{\Lambda - (1-u_1)\varpi_kP_kS - (1-u_2)\varpi_vP_vS - \mu S\}\\ &+ M_2\{(1-u_1)\varpi_kP_kS + (1-\xi_v)(\omega_v+u_4)E_{kv} - (\alpha_k+u_3)E_k - ((1-u_2)\varpi_vP_v + \mu + \eta_k)E_k\}\\ &+ M_3\{(1-u_2)\varpi_vP_vS + (1-\xi_k)(\omega_k+u_3)E_{kv} - (\alpha_v+u_4)E_v - ((1-u_1)\varpi_kP_k + \mu + \eta_v)E_v\}\\ &+ M_4\{(1-u_2)(1-q_v)\varpi_vP_vE_k + (1-u_1)(1-q_k)\varpi_kP_kE_v - (\omega_k+u_3)E_{kv} - (\omega_v+u_4)E_{kv}\\ &- (\alpha_{kv}+u_5)E_{kv} - (\mu+\eta_{kv})E_{kv}\}\\ &+ M_5\{\eta_kE_k + \xi_v(\omega_v+u_4)E_{kv} + (\pi_v+u_4)I_{kv} - (1-u_2)\varpi_vP_vI_k - (\rho_k+u_3)I_k - (\mu+\delta_k)I_k\}\\ &+ M_6\{\eta_vE_v + \xi_k(\omega_k+u_3)E_{kv} + (\pi_k+u_3)I_{kv} - (1-u_1)\varpi_kP_kI_v - (\rho_v+u_4)I_v - (\mu+\delta_v)I_v\}\\ &+ M_7\{(1-u_2)q_v\varpi_vP_vE_k + (1-u_1)q_k\varpi_kP_kE_v + (1-u_1)\varpi_kP_kI_v + (1-u_2)\varpi_vP_vI_k + \eta_{kv}E_{kv}\\ &- (\pi_k+u_3)I_{kv} - (\pi_v+u_4)I_{kv} - (\rho_{kv}+u_5)I_{kv} - (\mu+\delta_k+\delta_v)I_{kv}\}\end{aligned}$$

$$+ M_8\{\gamma_1 E_k + \gamma_2 I_k + \gamma_3 E_{kv} + \gamma_4 I_{kv} - (\delta_1 + u_6)P_k\}$$

$$+ M_9\{tau_1 E_v + \tau_2 I_v + \tau_3 E_{kv} + \tau_4 I_{kv} - (\delta_2 + u_7)P_v\}$$

$$+ M_{10}\{(\alpha_k + u_3)E_k + (\alpha_v + u_4)E_v + (\alpha_{kv} + u_5)E_{kv} + (\rho_k + u_3)I_k + (\rho_v + u_4)I_v$$

$$+ (\rho_{kv} + u_5)I_{kv} - \mu R\}. \tag{4.4}$$

Theorem 14. *There exist an optimal control set* $\{u_1^*,\ u_2^*,\ u_3^*,\ u_4^*,\ u_5^*,\ u_6^*,\ u_7^*\}$ *that minimizes* $\mathcal{J}$ *over* U *defined by the equations*

$$u_1^* = \max\{0, \min\{1, \bar{u}_1\}\}$$

$$u_2^* = \max\{0, \min\{1, \bar{u}_2\}\}$$

$$u_3^* = \max\{0, \min\{1, \bar{u}_3\}\}$$

$$u_4^* = \max\{0, \min\{1, \bar{u}_4\}\}$$

$$u_5^* = \max\{0, \min\{1, \bar{u}_5\}\}$$

$$u_6^* = \max\{0, \min\{1, \bar{u}_6\}\}$$

$$u_7^* = \max\{0, \min\{1, \bar{u}_7\}\}$$

where

$$\bar{u}_1 = \frac{\varpi_k P_k(-SM_1 + SM_2 - E_v M_3 + (1-q_k)E_v M_4 - I_v M_6 + q_k E_v M_7 + I_v M_7)}{v_1}$$

$$\bar{u}_2 = \frac{\varpi_v P_v(-SM_1 + SM_3 - E_k M_2 + (1-q_v)E_k M_4 - I_k M_5 + q_v E_k M_7 + I_k M_7)}{v_2}$$

$$\bar{u}_3 = \frac{E_k M_2 - (1-\xi_k)E_{kv} M_3 + E_{kv} M_4 + I_k M_5 - \xi_k E_{kv} M_6 - I_{kv} M_6 + I_{kv} M_7 - E_k M_{10} - I_k M_{10}}{v_3}$$

$$\bar{u}_4 = \frac{E_v M_3 - (1-\xi_v)E_{kv} M_2 + E_{kv} M_4 - \xi_v E_{kv} M_5 + I_v M_6 - I_{kv} M_5 + I_{kv} M_7 - E_v M_{10} - I_v M_{10}}{v_4}$$

$$\bar{u}_5 = \frac{E_{kv} M_4 - E_{kv} M_{10} + I_{kv} M_7 - I_{kv} M_{10}}{v_5}$$

$$\bar{u}_6 = \frac{P_k M_8}{v_6}$$

$$\bar{u}_7 = \frac{P_v M_9}{v_7}$$

and the adjoint variables $M_1,\ M_2, \cdots,\ M_{10}$ *satisfying:*

$$\begin{aligned}
\frac{dM_1}{dt} &= (1-u_1)\varpi_k P_k M_1 + (1-u_2)\varpi_v P_v M_1 + \mu M_1 - (1-u_1)\varpi_k P_k M_2 - (1-u_2)\varpi_v P_v M_3 \\
\frac{dM_2}{dt} &= -b_1 + (\alpha_k + u_3)M_2 + ((1-u_2)\varpi_v P_v + \mu + \eta_k)M_2 - (1-u_2)(1-q_v)\varpi_v P_v M_4 - \eta_k M_5 \\
&\quad -(1-u_2)q_v\varpi_v P_v M_7 - \gamma_1 M_8 - (\alpha_k + u_3)M_{10} \\
\frac{dM_3}{dt} &= -b_2 + (\alpha_v + u_4)M_3 + ((1-u_1)\varpi_k P_k + \mu + \eta_v)M_3 - (1-u_1)(1-q_k)\varpi_k P_k M_4 - \eta_v M_6 \\
&\quad -(1-u_1)q_k\varpi_k P_k M_7 - \tau_1 M_9 - (\alpha_v + u_4)M_{10} \\
\frac{dM_4}{dt} &= -b_3 - (1-\xi_v)(\omega_v + u_4)M_2 - (1-\xi_k)(\omega_k + u_3)M_3 + (\omega_k + u_3)M_4 + (\omega_v + u_4)M_4 \\
&\quad +(\alpha_{kv} + u_5)M_4 + (\mu + \eta_{kv})M_4 - \xi_v(\omega_v + u_4)M_5 - \xi_k(\omega_k + u_3)M_6 - \eta_{kv}M_7 - \gamma_3 M_8 \\
&\quad -\tau_3 M_9 - (\alpha_{kv} + u_5)M_{10} \\
\frac{dM_5}{dt} &= -b_4 + (1-u_2)\varpi_v P_v M_5 + (\rho_k + u_3)M_5 + (\mu + \delta_k)M_5 - (1-u_2)\varpi_v P_v M_7 - \gamma_2 M_8 \\
&\quad -(\rho_k + u_3)M_{10} \\
\frac{dM_6}{dt} &= -b_5 + (1-u_1)\varpi_k P_k M_6 + (\rho_v + u_4)M_6 + (\mu + \delta_v)M_6 - (1-u_1)\varpi_k P_k M_7 - \tau_2 M_9 \\
&\quad -(\rho_v + u_4)M_{10} \\
\frac{dM_7}{dt} &= -b_6 - (\pi_v + u_4)M_5 - (\pi_k + u_3)M_6 + (\pi_k + u_3)M_7 + (\pi_v + u_4)M_7 + (\rho_{kv} + u_5)M_7 \\
&\quad +(\mu + \delta_k + \delta_v)M_7 - \gamma_4 M_8 - \tau_4 M_9 - (\rho_{kv} + u_5)M_{10} \\
\frac{dM_8}{dt} &= -b_7 + (1-u_1)\varpi_k S M_1 - (1-u_1)\varpi_k S M_2 + (1-u_1)\varpi_k E_v M_3 \\
&\quad -(1-u_1)(1-q_k)\varpi_k E_v M_4 + (1-u_1)\varpi_k I_v M_6 - (1-u_1)q_k\varpi_k E_v M_7 \\
&\quad -(1-u_1)\varpi_k I_v M_7 + (\delta_1 + u_6)M_8 \\
\frac{dM_9}{dt} &= -b_8 + (1-u_2)\varpi_v S M_1 + (1-u_2)\varpi_v E_k M_2 - (1-u_2)\varpi_v S M_3 \\
&\quad -(1-u_2)(1-q_v)\varpi_v E_k M_4 + (1-u_2)\varpi_v I_k M_5 - (1-u_2)q_v\varpi_v E_k M_7 \\
&\quad -(1-u_2)\varpi_v I_k M_7 + (\delta_2 + u_7)M_9 \\
\frac{dM_{10}}{dt} &= \mu M_{10}
\end{aligned}$$

(4.5)

Proof. By the Pontryagin's maximum principle (Pontryagin *et al.*, 1962) and the Hamiltonian function (4.4), the adjoint system is computed by

$$\begin{aligned}
\frac{\partial \mathcal{H}}{\partial S} &= -\frac{dM_1}{dt} \\
\frac{\partial \mathcal{H}}{\partial E_k} &= -\frac{dM_2}{dt} \\
\frac{\partial \mathcal{H}}{\partial E_v} &= -\frac{dM_3}{dt} \\
\frac{\partial \mathcal{H}}{\partial E_{kv}} &= -\frac{dM_4}{dt} \\
\frac{\partial \mathcal{H}}{\partial I_k} &= -\frac{dM_5}{dt} \\
\frac{\partial \mathcal{H}}{\partial I_v} &= -\frac{dM_6}{dt} \\
\frac{\partial \mathcal{H}}{\partial I_{kv}} &= -\frac{dM_7}{dt} \\
\frac{\partial \mathcal{H}}{\partial P_k} &= -\frac{dM_8}{dt} \\
\frac{\partial \mathcal{H}}{\partial P_v} &= -\frac{dM_9}{dt} \\
\frac{\partial \mathcal{H}}{\partial R} &= -\frac{dM_{10}}{dt}
\end{aligned} \tag{4.6}$$

Therefore, the adjoint system is given by

$$\begin{aligned}
\frac{dM_1}{dt} &= (1-u_1)\varpi_k P_k M_1 + (1-u_2)\varpi_v P_v M_1 + \mu M_1 - (1-u_1)\varpi_k P_k M_2 - (1-u_2)\varpi_v P_v M_3 \\
\frac{dM_2}{dt} &= -b_1 + (\alpha_k + u_3)M_2 + ((1-u_2)\varpi_v P_v + \mu + \eta_k)M_2 - (1-u_2)(1-q_v)\varpi_v P_v M_4 - \eta_k M_5 \\
&\quad -(1-u_2)q_v\varpi_v P_v M_7 - \gamma_1 M_8 - (\alpha_k + u_3)M_{10} \\
\frac{dM_3}{dt} &= -b_2 + (\alpha_v + u_4)M_3 + ((1-u_1)\varpi_k P_k + \mu + \eta_v)M_3 - (1-u_1)(1-q_k)\varpi_k P_k M_4 - \eta_v M_6 \\
&\quad -(1-u_1)q_k\varpi_k P_k M_7 - \tau_1 M_9 - (\alpha_v + u_4)M_{10} \\
\frac{dM_4}{dt} &= -b_3 - (1-\xi_v)(\omega_v + u_4)M_2 - (1-\xi_k)(\omega_k + u_3)M_3 + (\omega_k + u_3)M_4 + (\omega_v + u_4)M_4 \\
&\quad +(\alpha_{kv} + u_5)M_4 + (\mu + \eta_{kv})M_4 - \xi_v(\omega_v + u_4)M_5 - \xi_k(\omega_k + u_3)M_6 - \eta_{kv}M_7 - \gamma_3 M_8
\end{aligned}$$

$$
\begin{aligned}
& -\tau_3 M_9 - (\alpha_{kv} + u_5) M_{10} \\
\frac{dM_5}{dt} &= -b_4 + (1-u_2)\varpi_v P_v M_5 + (\rho_k + u_3) M_5 + (\mu + \delta_k) M_5 - (1-u_2)\varpi_v P_v M_7 - \gamma_2 M_8 \\
& -(\rho_k + u_3) M_{10} \\
\frac{dM_6}{dt} &= -b_5 + (1-u_1)\varpi_k P_k M_6 + (\rho_v + u_4) M_6 + (\mu + \delta_v) M_6 - (1-u_1)\varpi_k P_k M_7 - \tau_2 M_9 \\
& -(\rho_v + u_4) M_{10} \\
\frac{dM_7}{dt} &= -b_6 - (\pi_v + u_4) M_5 - (\pi_k + u_3) M_6 + (\pi_k + u_3) M_7 + (\pi_v + u_4) M_7 + (\rho_{kv} + u_5) M_7 \\
& +(\mu + \delta_k + \delta_v) M_7 - \gamma_4 M_8 - \tau_4 M_9 - (\rho_{kv} + u_5) M_{10} \\
\frac{dM_8}{dt} &= -b_7 + (1-u_1)\varpi_k S M_1 - (1-u_1)\varpi_k S M_2 + (1-u_1)\varpi_k E_v M_3 \\
& -(1-u_1)(1-q_k)\varpi_k E_v M_4 + (1-u_1)\varpi_k I_v M_6 - (1-u_1) q_k \varpi_k E_v M_7 \\
& -(1-u_1)\varpi_k I_v M_7 + (\delta_1 + u_6) M_8 \\
\frac{dM_9}{dt} &= -b_8 + (1-u_2)\varpi_v S M_1 + (1-u_2)\varpi_v E_k M_2 - (1-u_2)\varpi_v S M_3 \\
& -(1-u_2)(1-q_v)\varpi_v E_k M_4 + (1-u_2)\varpi_v I_k M_5 - (1-u_2) q_v \varpi_v E_k M_7 \\
& -(1-u_2)\varpi_v I_k M_7 + (\delta_2 + u_7) M_9 \\
\frac{dM_{10}}{dt} &= \mu M_{10}
\end{aligned}
\tag{4.7}
$$

Finding the partial derivatives of the Hamiltonian function (4.4) with respect to each control variable yields the optimality equations.

$$
\begin{aligned}
\frac{\partial \mathcal{H}}{\partial u_1} =& \varpi_k P_k S M_1 - \varpi_k P_k S M_2 + \varpi_k P_k E_v M_3 - (1-q_k)\varpi_k P_k E_v M_4 + \varpi_k P_k I_v M_6 \\
& - q_k \varpi_k P_k E_v M_7 - \varpi_k P_k I v M_7 + v_1 u_1 \\
\frac{\partial \mathcal{H}}{\partial u_2} =& \varpi_v P_v S M_1 - \varpi_v P_v S M_3 + \varpi_v P_v E_k M_2 - (1-q_v)\varpi_v P_v E_k M_4 + \varpi_v P_v I_k M_5 \\
& - q_v \varpi_v P_v E_k M_7 - \varpi_v P_v I k M_7 + v_2 u_2 \\
\frac{\partial \mathcal{H}}{\partial u_3} =& - E_k M_2 + (1-\xi_k) E_{kv} M_3 - E_{kv} M_4 - I_k M_5 + \xi_k E_{kv} M_6 + I_{kv} M_6 - I_{kv} M_7 + E_k M_{10} \\
& + I_k M_{10} + v_3 u_3 \\
\frac{\partial \mathcal{H}}{\partial u_4} =& - E_v M_3 + (1-\xi_v) E_{kv} M_2 - E_{kv} M_4 + \xi_v E_{kv} M_5 - I_v M_6 + I_{kv} M_5 - I_{kv} M_7 + E_v M_{10} \\
& + I_v M_{10} + v_4 u_4
\end{aligned}
$$

$$\begin{aligned}
\frac{\partial \mathcal{H}}{\partial u_5} &= -E_{kv}M_4 + E_{kv}M_{10} - I_{kv}M_7 + I_{kv}M_{10} + v_5u_5 \\
\frac{\partial \mathcal{H}}{\partial u_6} &= -P_kM_8 + v_6u_6 \\
\frac{\partial \mathcal{H}}{\partial u_7} &= -P_vM_9 + v_7u_7
\end{aligned} \tag{4.8}$$

To obtain optimal controls u_i^* $(i = 1,\ 2, \cdots, 7)$, we replace u_i in the system (4.8) with $\bar{u}_i$ and equate the right-hand side of the equations of the resulting system to zero then solve for $\bar{u}_i$. Thus, we get

$$\begin{aligned}
\bar{u}_1 &= \frac{\varpi_k P_k(-SM_1 + SM_2 - E_vM_3 + (1-q_k)E_vM_4 - I_vM_6 + q_kE_vM_7 + I_vM_7)}{v_1} \\
\bar{u}_2 &= \frac{\varpi_v P_v(-SM_1 + SM_3 - E_kM_2 + (1-q_v)E_kM_4 - I_kM_5 + q_vE_kM_7 + I_kM_7)}{v_2} \\
\bar{u}_3 &= \frac{E_kM_2 - (1-\xi_k)E_{kv}M_3 + E_{kv}M_4 + I_kM_5 - \xi_kE_{kv}M_6 - I_{kv}M_6 + I_{kv}M_7 - E_kM_{10} - I_kM_{10}}{v_3} \\
\bar{u}_4 &= \frac{E_vM_3 - (1-\xi_v)E_{kv}M_2 + E_{kv}M_4 - \xi_vE_{kv}M_5 + I_vM_6 - I_{kv}M_5 + I_{kv}M_7 - E_vM_{10} - I_vM_{10}}{v_4} \\
\bar{u}_5 &= \frac{E_{kv}M_4 - E_{kv}M_{10} + I_{kv}M_7 - I_{kv}M_{10}}{v_5} \\
\bar{u}_6 &= \frac{P_kM_8}{v_6} \\
\bar{u}_7 &= \frac{P_vM_9}{v_7}
\end{aligned}$$

Using the standard control arguments that involve the bounds of the controls, we come to the following conclusion:

$$u_1^* = \begin{cases} 0 & \text{if } \bar{u}_1 \leq 0 \\ \bar{u}_1 & \text{if } 0 < \bar{u}_1 < 1 \\ 1 & \text{if } \bar{u}_1 \geq 1 \end{cases}$$

$$u_2^* = \begin{cases} 0 & \text{if } \bar{u}_2 \leq 0 \\ \bar{u}_2 & \text{if } 0 < \bar{u}_2 < 1 \\ 1 & \text{if } \bar{u}_1 \geq 1 \end{cases}$$

$$u_3^* = \begin{cases} 0 & \text{if } \bar{u}_3 \leq 0 \\ \bar{u}_3 & \text{if } 0 < \bar{u}_3 < 1 \\ 1 & \text{if } \bar{u}_3 \geq 1 \end{cases}$$

$$
\begin{aligned}
u_4^* &= \begin{cases} 0 & \text{if } \bar{u}_4 \leq 0 \\ \bar{u}_4 & \text{if } 0 < \bar{u}_4 < 1 \\ 1 & \text{if } \bar{u}_4 \geq 1 \end{cases} \\
u_5^* &= \begin{cases} 0 & \text{if } \bar{u}_5 \leq 0 \\ \bar{u}_5 & \text{if } 0 < \bar{u}_5 < 1 \\ 1 & \text{if } \bar{u}_5 \geq 1 \end{cases} \\
u_6^* &= \begin{cases} 0 & \text{if } \bar{u}_6 \leq 0 \\ \bar{u}_6 & \text{if } 0 < \bar{u}_6 < 1 \\ 1 & \text{if } \bar{u}_6 \geq 1 \end{cases} \\
u_7^* &= \begin{cases} 0 & \text{if } \bar{u}_7 \leq 0 \\ \bar{u}_7 & \text{if } 0 < \bar{u}_7 < 1 \\ 1 & \text{if } \bar{u}_7 \geq 1 \end{cases}
\end{aligned} \tag{4.9}
$$

In compact notation, the system (4.9) can be written as

$$
\begin{aligned}
u_1^* &= \max\{0, \min\{1, \bar{u}_1\}\} \\
u_2^* &= \max\{0, \min\{1, \bar{u}_2\}\} \\
u_3^* &= \max\{0, \min\{1, \bar{u}_3\}\} \\
u_4^* &= \max\{0, \min\{1, \bar{u}_4\}\} \\
u_5^* &= \max\{0, \min\{1, \bar{u}_5\}\} \\
u_6^* &= \max\{0, \min\{1, \bar{u}_6\}\} \\
u_7^* &= \max\{0, \min\{1, \bar{u}_7\}\}
\end{aligned} \tag{4.10}
$$

□

4.1.4 Numerical Simulation

Analytical solutions to the optimality system may not always be feasible; in these cases, numerical approaches are employed to approximate the solutions and illustrate the results. The optimality system, which consists of the state system (4.1), adjoint system (4.7),

control characterization (4.10), and corresponding initial conditions, is solved iteratively to produce the numerical simulation results shown in this section. The fourth-order Runge-Kutta algorithm is used to solve the state and adjoint equations using the parameter values in Table (3.1).

The optimal strategy for considerably reducing the spread of the CBD-CLR co-infection is investigated among the following control strategies:

(i) Control with prevention of CBD and CLR infections ($u_1,\ u_2$)

(ii) Control with Treatment of CBD, CLR and CBD-CLR co-infection ($u_3,\ u_4,\ u_5$)

(iii) Control with elimination of *Colletotrichum kahawae* and *Hemileia vastatrix* pathogens ($u_6,\ u_7$)

(iv) Control with prevention of CBD and CLR infections and Treatment of CBD, CLR and CBD-CLR co-infection ($u_1,\ u_2,\ u_3,\ u_4,\ u_5$)

(v) Control with prevention of CBD and CLR infections and elimination of *Colletotrichum kahawae* and *Hemileia vastatrix* pathogens ($u_1,\ u_2,\ u_6,\ u_7$)

(vi) Control with Treatment of CBD, CLR and CBD-CLR co-infection and elimination of *Colletotrichum kahawae* and *Hemileia vastatrix* pathogens ($u_3,\ u_4,\ u_5,\ u_6,\ u_7$)

(vii) Using all interventions ($u_1,\ u_2,\ u_3,\ u_4,\ u_5,\ u_6,\ u_7$)

For the simulation of the model with optimal control, we made the following assumptions after several numerical simulations.

Coefficient	Cost value	Coefficient	Cost value
b_1	\$ 5 per plant	b_2	\$ 4 per plant
b_3	\$ 9 per plant	b_4	\$ 6 per plant
b_5	\$ 6 per plant	b_6	\$ 11 per plant
b_7	\$ 6 per plant	b_8	\$ 5 per plant

Table 4.1: Costs associated with minimizing infected plants

$v_1 = v_2 = v_3 = v_4 = v_5 = v_6 = v_7 =$ \$100 per unit of control effort squared. In addition, we used the initial: $S_0 = 10000$, $E_{k0} = 500$, $E_{v0} = 101$, $E_{kv0} = 2002$, $I_{k0} = 100$, $I_{v0} = 10$, $I_{kv0} = 12$, $P_{k0} = 1600$, $P_{v0} = 1601$, and $R_0 = 10$. The numerical simulation results are shown and discussed in in the following subsections.

4.1.4.1 Strategy 1: Control with prevention of CBD and CLR infections $(u_1,\ u_2)$

In this strategy, the objective function $\mathcal{J}$ is optimized using both prevention of CBD infection u_1 and prevention of CLR infection u_2 while other interventions $(u_3,\ u_4,\ u_5,\ u_6,\ u_7)$ are set to zero. In Figure 4.1(a), it is seen that prevention has a significant impact on controlling the emergence of new infection cases of CBD and CLR infections since the solution curve of the susceptible coffee plants S(t) without control converges to the lower bound at a higher rate than that with controls. From Figures 4.1(d), 4.1(g), 4.1(h) and 4.1(i) we observed a positive effect of prevention since the solution curves of the co-exposed coffee plants $E_{kv}(t)$, the co-infected coffee plants $I_{kv}(t)$, *Colletotrichum kahawae* pathogens $P_k(t)$ and *Hemileia vastatrix* pathogens $P_v(t)$ without control continue rising and those with controls converge to the lower bound. This implies that prevention alone is effective in reducing co-infected coffee plants $I_{kv}(t)$, *Colletotrichum kahawae* pathogens $P_k(t)$ and *Hemileia vastatrix* pathogens $P_v(t)$ as result of reduced new infection cases which in turn lead reduced shedding of pathogens. The effect of this strategy is observed in Figures 4.1(b) and 4.1(c), where the solution curves with control rise steadily to certain levels which are lower than the peaks of the solution curves without control and start falling to the lower bound. We also noticed a steady increase in the number of infection cases of CBD-infected coffee plants $I_k(t)$, the CLR-infected coffee plants $I_v(t)$ in Figure 4.1(e) and Figure 4.1(f) respectively, implying that this strategy is not effective in controlling infected coffee plants in $I_k(t)$ and $I_v(t)$ compartments. This can be related to the lack of control measures, such as treatment in these compartments.

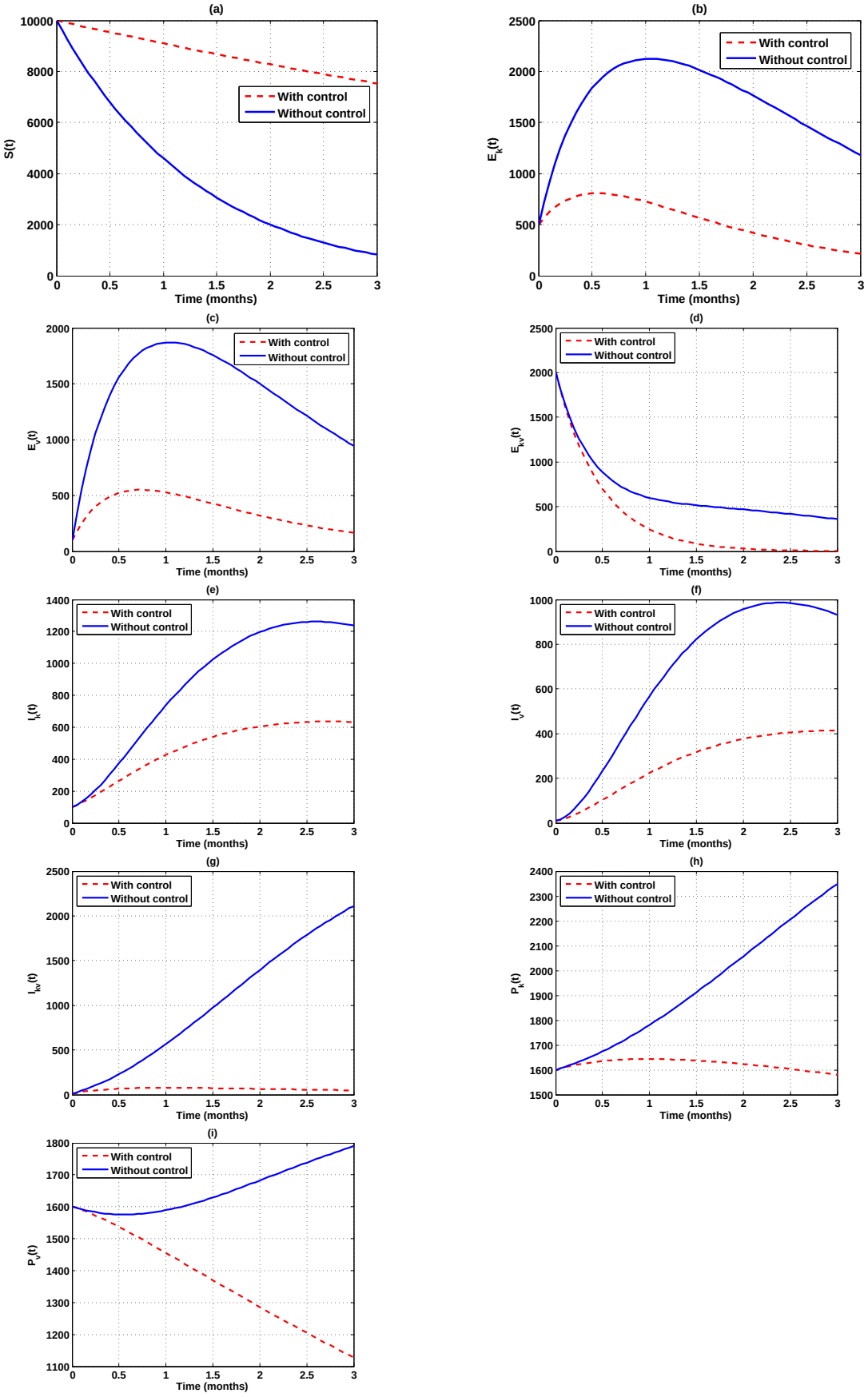

Figure 4.1: Graphs showing the effect of prevention of CBD and CLR infections (u_1, u_2) on CBD and CLR co-infection model

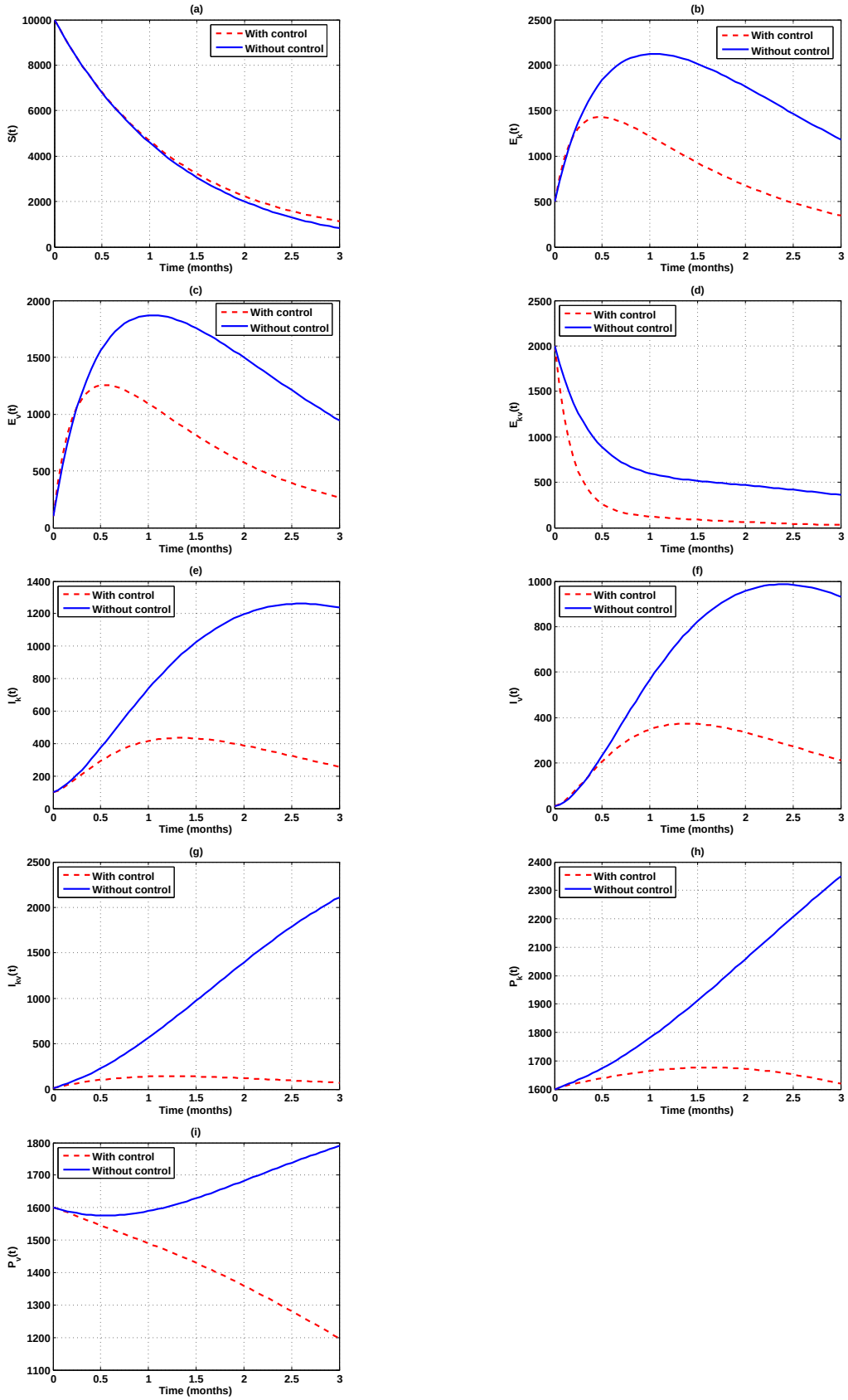

Figure 4.2: Graphs effect of treatment of CBD, CLR, and CBD-CLR co-infection (u_3, u_4, u_5) on CBD and CLR co-infection model

4.1.4.2 Strategy 2: Control with treatment of CBD, CLR and CBD-CLR co-infection ($u_3,\ u_4,\ u_5$)

In this strategy, the objective function $\mathcal{J}$ is optimized using both treatment of CBD infection u_3, CLR infection u_4 and CBD-CLR co-infection u_5 while other interventions ($u_1,\ u_2,\ u_6,\ u_7$) are set to zero. In Figure 4.2(a), we observed the solution curves of the susceptible coffee plants S(t) without controls and that of the susceptible coffee plants S(t) with controls; they almost converge to zero at the same rate whereby the S(t) with controls is slightly above that of S(t) without controls. This implies that this strategy is inefficient in reducing new CBD and CLR infection cases. From Figures 4.2(d) and 4.2(i), we observed a continuous decrease in numbers in the solution curves with controls. This is connected to the effectiveness of the strategy. In Figures 4.2(b), 4.2(c), 4.2(e), 4.2(f), 4.2(g) and 4.2(h), we noticed a slight rise of solution curves with controls to a level below that of curves without controls and followed by a steady decrease hence converging to zero. This suggests that strategy 2 effectively controls the cases at the end of the given period but not at the beginning in six compartments.

4.1.4.3 Strategy 3: Control with elimination of *Colletotrichum kahawae* and *Hemileia vastatrix* pathogens ($u_6,\ u_7$)

In this strategy, the objective function $\mathcal{J}$ is optimized by using the elimination of *Colletotrichum kahawae* pathogens u_6 and *Hemileia vastatrix* pathogens u_7. At the same time, other interventions are set to zero. The impact of eliminating pathogens is noticed in Figure 4.3(a) since the rate at which the solution curve with controls converges to zero is lower than that of the curve without control. Hence, this strategy can be used to reduce cases. Figures 4.3(d), 4.3(h), and 4.3(i) demonstrate that this strategy is effective in reducing the co-exposed coffee plants, *Colletotrichum kahawae* pathogens, and *Hemileia vastatrix* pathogens, respectively. Figures 4.3(b), 4.3(c) and 4.3(g) have shown that this strategy cannot contain the infections at the onset of the disease since the curves rise first and then fall. Also, from Figures 4.3(e) and 4.3(f), we observed that this strategy is ineffective in reducing the CBD-infected coffee plants $I_k(t)$ and the CLR-infected.

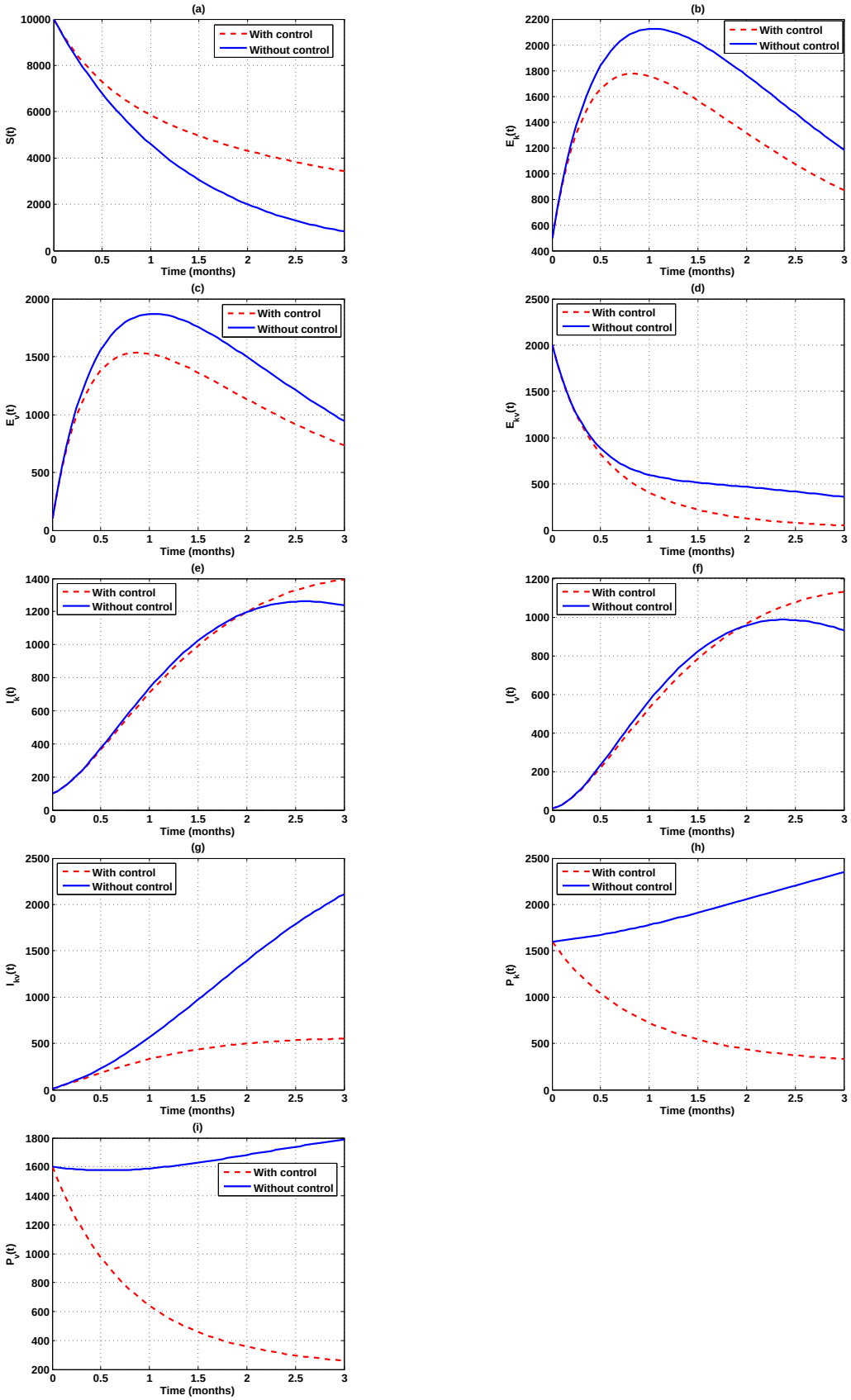

Figure 4.3: Graphs showing the elimination of *Colletotrichum Kahawae* and *Hemileia vastatrix* pathogens ($u_6,\ u_7$)

coffee plants $I_v(t)$ since their solution curves continue rising.

4.1.4.4 Strategy 4: Control with prevention of CBD and CLR infections and Treatment of CBD, CLR and CBD-CLR co-infection $(u_1,\ u_2,\ u_3,\ u_4,\ u_5)$

Prevention of CBD and CLR infections and Treatment of CBD, CLR, and CBD-CLR co-infection $(u_1,\ u_2,\ u_3,\ u_4,\ u_5)$ are used to optimize the objective function $\mathcal{J}$ while u_6 and u_7 are set equal to zero. In Figures 4.4(a), we observed that this strategy has a positive impact on controlling the emergence of new infection cases of CBD and CLR infections since the solution curve of the susceptible coffee plants S(t) with control converges to zero at a lower rate. We observed positive results in Figures 4.4(d), 4.4(g), 4.4(h), and 4.4(i) since the solution curves with controls steadily converge to zero. From Figures 4.4(b), 4.4(c), 4.4(e) and 4.4(f), we observed a slight increase of cases for the solution curves with controls at the beginning of a given infection period followed by a decrease which converges to zero. This suggests that this strategy effectively controls infection cases since the cases increase slightly and eventually converge to zero.

4.1.4.5 Strategy 5: Control with prevention of CBD and CLR infections and elimination of *Colletotrichum kahawae* and *Hemileia vastatrix* pathogens $(u_1,\ u_2,\ u_6,\ u_7)$

Prevention of CBD and CLR infections and elimination of *Colletotrichum kahawae* and *Hemileia vastatrix* pathogens $(u_1,\ u_2,\ u_6,\ u_7)$ are used to optimize the objective function $\mathcal{J}$ while $(u_3,\ u_4,\ u_5)$ are set to zero. We observed positive results in Figure 4.5(a) since this strategy significantly reduced the number of new infection cases. We also observed positive results in Figures 4.5(d), 4.5(g), 4.5(h) and 4.5(i) since this strategy is effective in reducing the numbers of the co-exposed coffee plants $E_{kv}(t)$, the co-infected coffee plants $I_{kv}(t)$, *Colletotrichum kahawae* pathogens $P_k(t)$ and *Hemileia vastatrix* pathogens $P_v(t)$ respectively. In Figures 4.5(b), 4.5(c), 4.5(e) and 4.5(f), we noticed an increase of cases for the solution curves with controls at the beginning of a given period followed by a decrease.

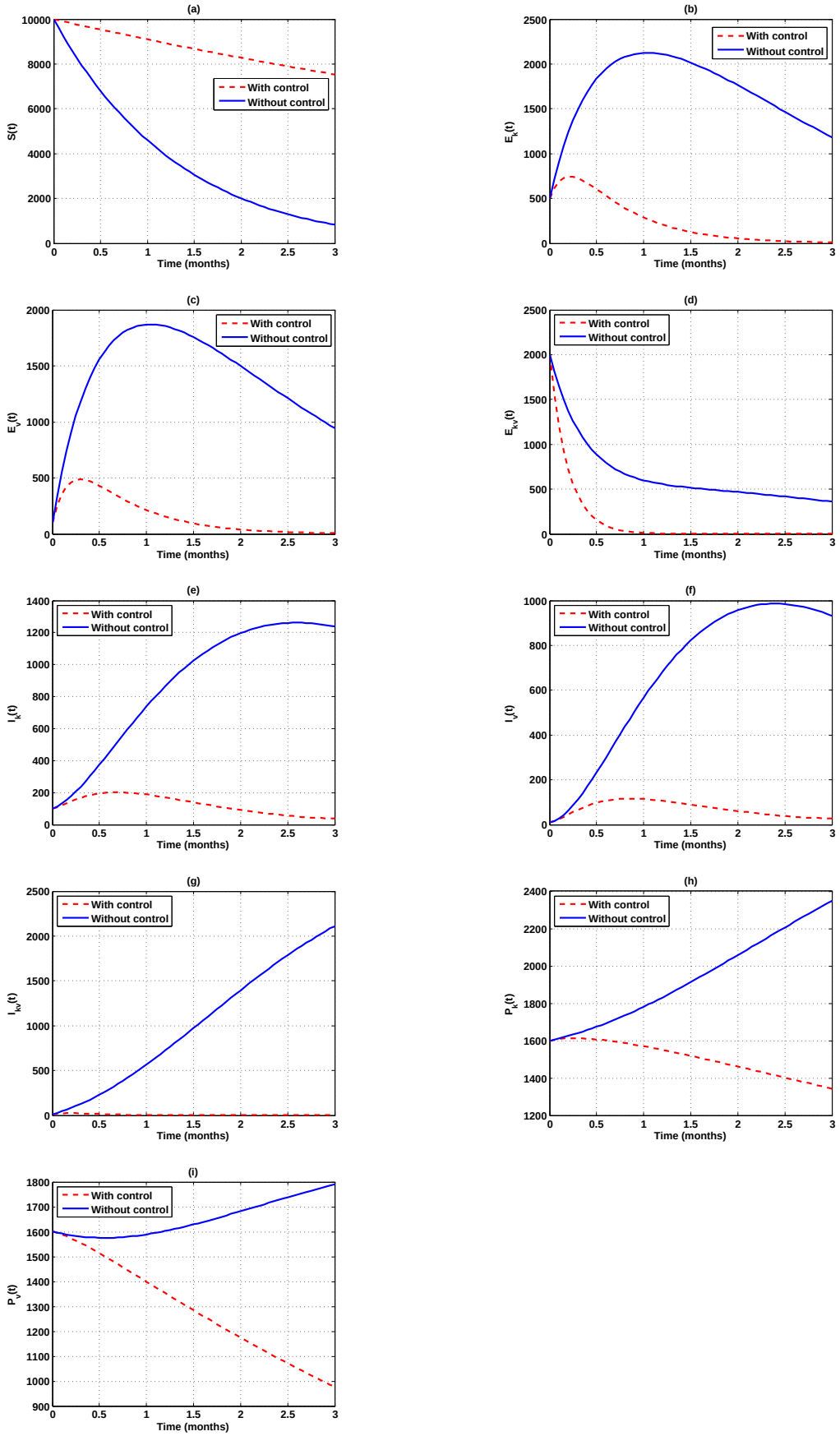

Figure 4.4: Graphs showing the effect of prevention of CBD and CLR infections and Treatment of CBD, CLR, and CBD-CLR co-infection (u_1, u_2, u_3, u_4, u_5) on CBD and CLR co-infection model

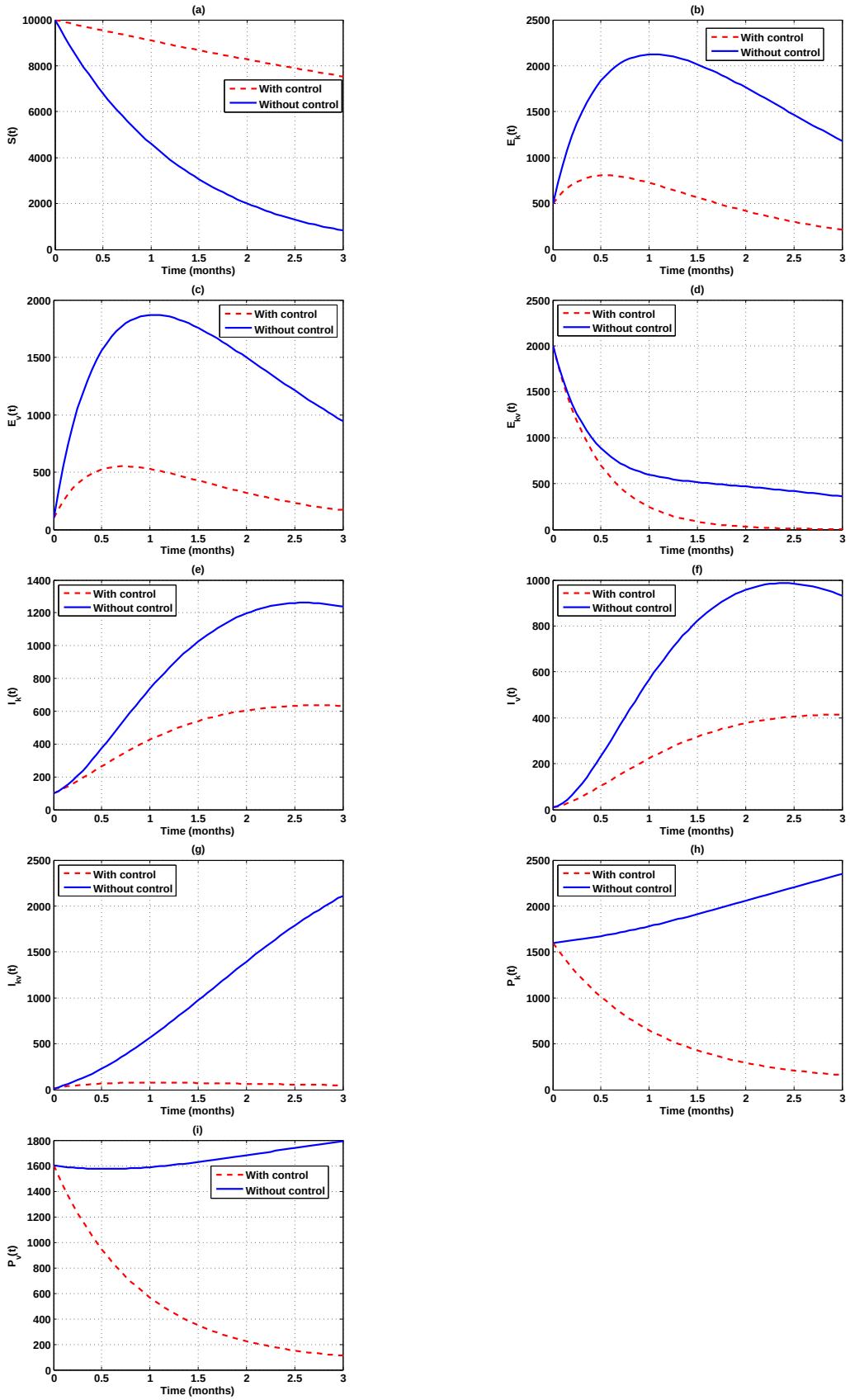

Figure 4.5: Graphs showing the effect of prevention of CBD and CLR infections and elimination of *Colletotrichum kahawae* and *Hemileia vastatrix* pathogens (u_1, u_2, u_6, u_7) on CBD and CLR co-infection model

4.1.4.6 Strategy 6: Control with the treatment of CBD, CLR and CBD-CLR co-infection and elimination of *Colletotrichum kahawae* and *Hemileia vastatrix* pathogens ($u_3,\ u_4,\ u_5,\ u_6,\ u_7$)

In this strategy, treatment of CBD, CLR and CBD-CLR co-infection and elimination of *Colletotrichum kahawae* and *Hemileia vastatrix* pathogens ($u_3,\ u_4,\ u_5,\ u_6,\ u_7$) are used to optimize the objective function $\mathcal{J}$ while ($u_1,\ u_2$ are set to zero. From Figure 4.6(a), we noticed that this strategy is moderately able to reduce the number of new infection cases since the solution curve of S(t) with controls is slightly above that of S(t) without controls. This may be connected to treating CBD, CLR, and CBD-CLR co-infection and eliminating pathogens. We noted positive results in Figures 4.6(d), 4.6(g), 4.6(h), and 4.6(i) since the solution curves with controls steadily converge to zero. In Figures 4.6(b), 4.6(c), 4.6(e), and 4.6(f), we observed that the solution curves with controls rise to certain levels and then fall as they converge to zero. This suggests that this strategy is ineffective in controlling the cases at the beginning of a given infection period.

4.1.4.7 Strategy 7: Using all interventions ($u_1,\ u_2,\ u_3,\ u_4,\ u_5,\ u_6,\ u_7$)

The objective function $\mathcal{J}$ is optimized using all control mechanisms ($u_1,\ u_2,\ u_3,\ u_4,\ u_5,\ u_6,\ u_7$) in this strategy. We observed that Figures 4.7(a), 4.7(b), 4.7(c), 4.7(d), 4.7(e), 4.7(f), 4.7(g) are similar to the corresponding figures in Figure 4.4. This suggests that the effectiveness of strategies 4 and 7 is almost the same. The only difference is that Figures 4.7(h) and 4.7(i) are not similar to the corresponding figures in Figure 4.4. This is because the solution curves with controls in Figures 4.7(h) and 4.7(i) converge to zero at a higher rate than those of Figures 4.4(h) and 4.4(i). This suggests that strategy 7 is more effective in reducing the pathogens than strategy 4.

4.2 Cost effectiveness analysis

This section determines the cost-effective control strategy for CBD and CLR co-infection. The Incremental Cost-Effectiveness Ratio (ICER), also referred to as an additional cost per additional health outcome, is used in this scenario. This provides a mechanism to

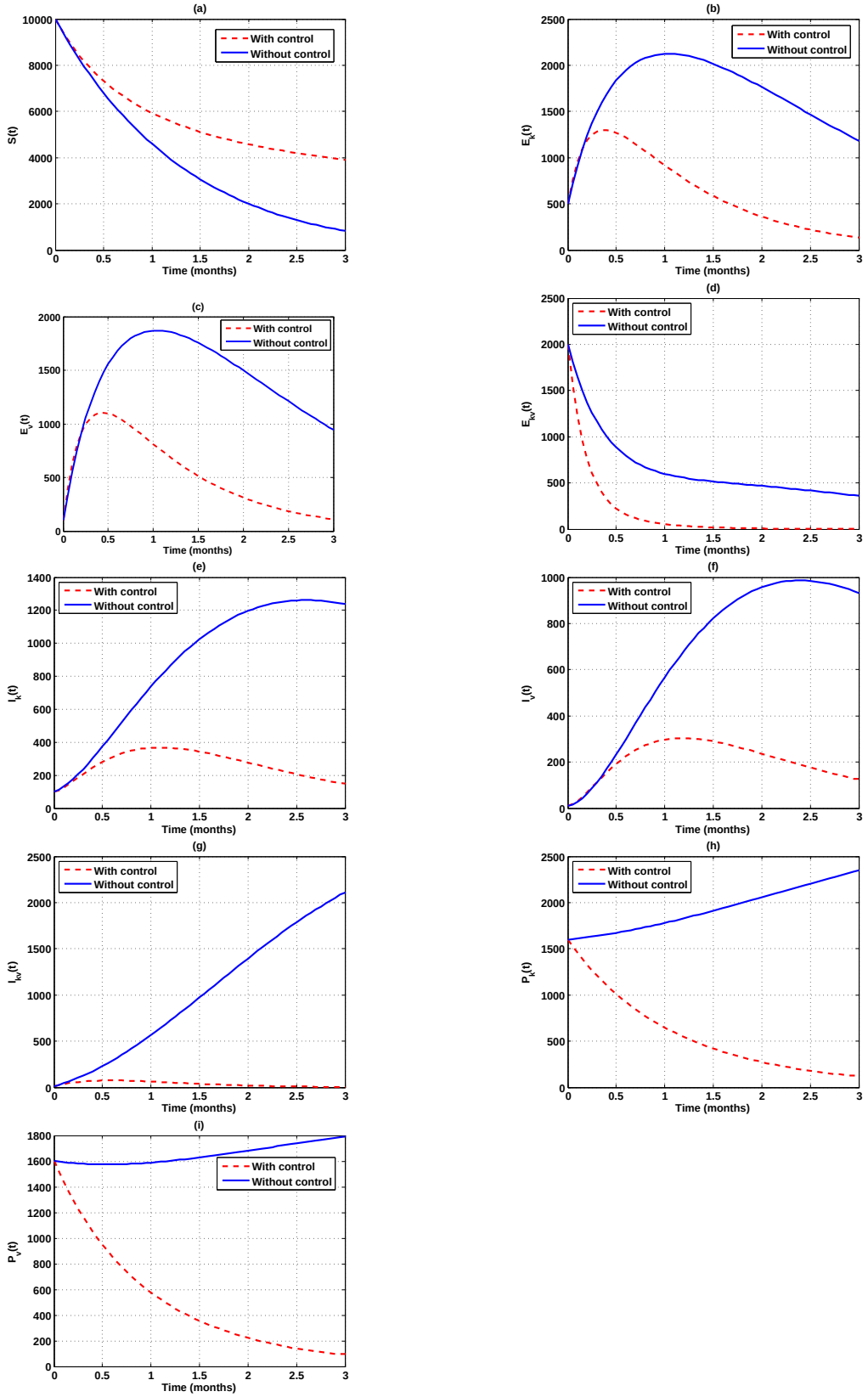

Figure 4.6: Graphs showing the effect of treatment of CBD, CLR and CBD-CLR co-infection and elimination of *Colletotrichum kahawae* and *Hemileia vastatrix* pathogens ($u_3,\ u_4,\ u_5,\ u_6,\ u_7$) on CBD and CLR co-infection model

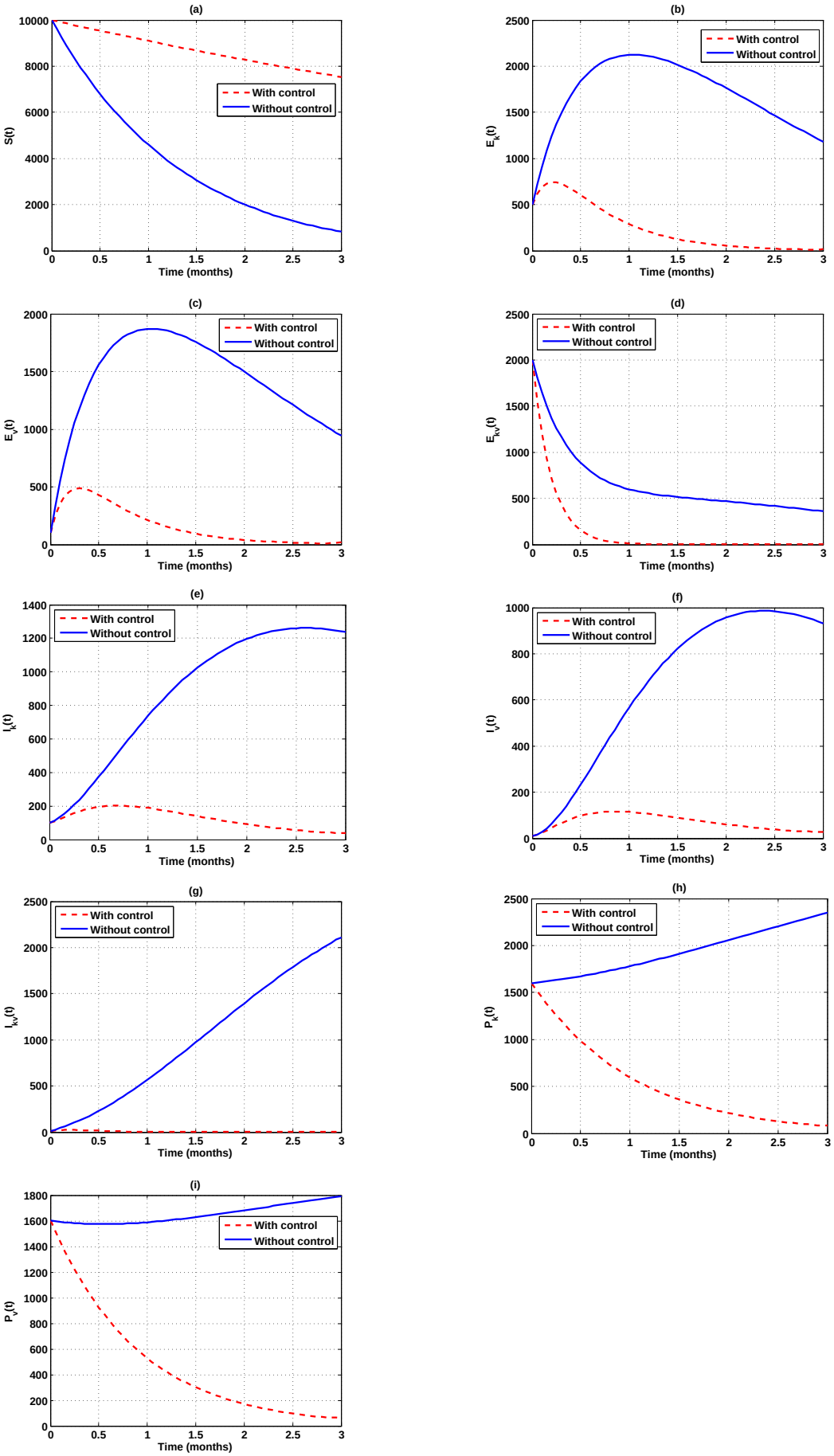

Figure 4.7: Graphs showing the effect of all interventions (u_1, u_2, u_3, u_4, u_5, u_6, u_7) on CBD and CLR co-infection model

compare the costs and outcomes of two distinct intervention strategies competing for the same resources (Okosun *et al.*, 2011). The Incremental Cost-Effectiveness Ratio (ICER) is defined by the formula:

$$\text{ICER} = \frac{\text{difference in intervention costs}}{\text{difference in the total number of infections averted}} \tag{4.11}$$

where "the total number of infections averted" is the difference between the total infectious coffee plants and pathogens without control and the total infectious infectious coffee plants and pathogens with control.

Based on the numerical simulation of the model using the parameters in Table (3.1), we have the following table:

Table 4.2: Number of infections averted and total cost of each strategy

Strategy	Total infection averted	Total cost (USD)
1	983	600.0
2	250,710	900.0
3	128,660	750.0
4	92,028	1,365.4
5	117,420	1,200.0
6	315,000	1,492.1
7	202,320	1,964.8

By using (4.11), we have

Table 4.3: First iteration for ICER Computations

Strategy	Total infection averted	Total cost (USD)	ICER
1	983	600.0	$\text{ICER}(1) = \frac{600}{983} = 0.6104$
2	250,710	900.0	$\text{ICER}(2) = \frac{900-600}{250,710-983} = 0.00120$
3	128,660	750.0	$\text{ICER}(3) = \frac{750-600}{128,660-983} = 0.00117$
4	92,028	1,365.4	$\text{ICER}(4) = \frac{1,365.4-600}{92,028-983} = 0.00841$
5	117,420	1,200.0	$\text{ICER}(5) = \frac{1,200-600}{117,420-983} = 0.0052$
6	315,000	1,492.1	$\text{ICER}(6) = \frac{1,492.1-600}{315,000-983} = 0.00284$
7	202,320	1,964.8	$\text{ICER}(7) = \frac{1,964.8-600}{202,320-983} = 0.00678$

When strategies 1 and 4 (two strategies with maximum ICER) are compared, strategy 4

saves approximately \$0.00841 more than strategy 1. The lower ICER for strategy 4 shows that strategy 1 is heavily dominated. In other words, strategy 1 is less effective and more expensive than strategy 4. To prevent strategy 1 from using up scarce resources, it is therefore removed from the list of strategies. Now we recalculate the ICER.

Table 4.4: Second iteration for ICER Computations

Strategy	Total infection averted	Total cost (USD)	ICER
2	250,710	900.0	$\text{ICER}(2) = \frac{900}{250,710} = 0.00359$
3	128,660	750.0	$\text{ICER}(3) = \frac{750-900}{128,660-250,710} = 0.00123$
4	92,028	1,365.4	$\text{ICER}(4) = \frac{1,365.4-900}{92,028-250,710} = -0.00293$
5	117,420	1,200.0	$\text{ICER}(5) = \frac{1,365.4-900}{92,028-250,710} = -0.00293$
6	315,000	1,492.1	$\text{ICER}(6) = \frac{1,492.1-900}{315,000-250,710} = 0.00921$
7	202,320	1,964.8	$\text{ICER}(7) = \frac{1,964.8-900}{202,320-250,710} = -0.02200$

Similarly, we can observe that strategy 2 saves \$0.00921 more than strategy 6 based on ICER (2) and ICER (6). As a result, we drop strategy 6 because it is somewhat expensive. Recalculating the ICER, we have

Table 4.5: Third iteration for ICER Computations

Strategy	Total infection averted	Total cost (USD)	ICER
2	250,710	900.0	$\text{ICER}(2) = \frac{900}{250,710} = 0.00359$
3	128,660	750.0	$\text{ICER}(3) = \frac{750-900}{128,660-250,710} = 0.00123$
4	92,028	1,365.4	$\text{ICER}(4) = \frac{1,365.4-900}{92,028-250,710} = -0.00293$
5	117,420	1,200.0	$\text{ICER}(5) = \frac{1,200-900}{117,420-250,710} = -0.00225$
7	202,320	1,964.8	$\text{ICER}(7) = \frac{1,964.8-900}{202,320-250,710} = -0.02200$

When strategies 2 and 3 are compared, Strategy 3 saves approximately \$0.00123 more than Strategy 2 based on ICER (2) and ICER (3). Thus, we exclude Strategy 2 from the list of strategies. We recalculate ICER as shown in the following table

Table 4.6: Fourth iteration for ICER Computations

Strategy	Total infection averted	Total cost (USD)	ICER
3	128,660	750.0	ICER(3) $= \frac{750}{128,660} = 0.00583$
4	92,028	1,365.4	ICER(4) $= \frac{1,365.4-750}{92,028-128,660} = -0.01680$
5	117,420	1,200.0	ICER(5) $= \frac{1,200-750}{117,420-128,660} = -0.04004$
7	202,320	1,964.8	ICER(7) $= \frac{1,964.8-750}{202,320-128,660} = 0.01649$

We can see that strategy 3 saves \$0.00583 more than strategy 7 based on ICER (3) and ICER (7). As a result, Strategy 7 is eliminated in the subsequent calculation of ICER because it is a bit expensive. Recalculating the ICER, we have

Table 4.7: Fifth iteration for ICER Computations

Strategy	Total infection averted	Total cost (USD)	ICER
3	128,660	750.0	ICER(3) $= \frac{750}{128,660} = 0.00583$
4	92,028	1,365.4	ICER(4) $= \frac{1,365.4-750}{92,028-128,660} = -0.01680$
5	117,420	1,200.0	ICER(5) $= \frac{1,200-750}{117,420-128,660} = -0.04004$

By comparing strategies 3 and 4, it can be seen that strategy 3 is strongly dominated based on ICER(3) and ICER(4). This implies that strategy 3 is less effective and more expensive than strategy 4. Thus, we exclude strategy 3 from the list of strategies in the next calculation of ICER.

Table 4.8: Sixth iteration for ICER Computations

Strategy	Total infection averted	Total cost (USD)	ICER
4	92,028	1,365.4	ICER(4) $= \frac{1,365.4}{92,028} = 0.01484$
5	117,420	1,200.0	ICER(5) $= \frac{1,200-1,365.4}{117,420-92,028} = -0.00651$

When ICER(4) and ICER(5) are compared, strategy 5 is found to save \$0.00651 in comparison to strategy 4. Likewise, strategy 5's negative ICER suggests that strategy 4 is "strongly dominated." In other words, strategy 4 is less effective and more expensive than strategy 5. Consequently, the strongly dominated approach 4 is not included. Based on this finding, strategy 5 is the most cost-effective for controlling CBD-CLR co-infection.

Chapter 5: Conclusion and Recommendations

5.1 Conclusion

A mathematical model illustrating the dynamics of the co-infection between CBD and CLR is developed in this thesis. The CBD-CLR co-infection model was analyzed in section 3.2 by determining the feasible region, the positivity of the solution set, the equilibria points, and the reproduction number, which is the maximum of the reproduction numbers of the CBD and CLR alone models. Moreover, the model's potential for bifurcation is examined using the Castillo-Chavez and Song (2004) theorem. We investigated the impact of the two diseases on one another, and the findings show that both CBD and CLR cases augment one another. We analyzed the CBD-only model in section 3.3 by determining the reproduction number, equilibrium points, and their stability. In section 4.1.2, the time-dependent control variables are added to the CBD-CLR co-infection model, then the optimal control problem is formulated, the optimality system is created, and the existence requirements for optimal control are identified. The elimination of CBD-CLR co-infection is recommended using seven strategies (see section 4.1.4).

The recommended strategies are numerically examined, and the outcomes are graphically presented in section 4.1.4. The graphs indicate that strategy 7 (combination of all interventions ($u_1,\ u_2,\ u_3,\ u_4,\ u_5,\ u_6,\ u_7$)) is the best strategy for slowing the spread of the CBD-CLR co-infection. In section 4.2, Cost-effectiveness analysis is carried out. The computations revealed that strategy 5 (control with prevention of CBD and CLR infections and elimination of *Colletotrichum kahawae* and *Hemileia vastatrix* pathogens ($u_1,\ u_2,\ u_6,\ u_7$)) is the most cost-effective of all strategies for controlling CBD-CLR co-infection. This implies that for coffee farmers to achieve better results in controlling the CBD-CLR co-infection, they must incur more.

5.2 Recommendations

1. **Recommendations from the Study**

   From the findings of this thesis, we recommend that coffee farmers, the Coffee Research Institute, and the Ministry of Agriculture, Livestock, and Fisheries allocate sufficient resources to control the co-infection and implement strategy 7, the optimal control.

2. **Recommendation for Further Research**

   CBD and CLR are highly dependent on climatic factors, yet this thesis has not incorporated these factors into the developed model. Therefore, further research can also incorporate the climatic factors in the CBD-CLR co-infection model.

References

Agrios, G. N. (2005). Plant Pathology (5th ed.). Academic Press.

Anco, D. J. (2018). Continuing consideration of co-infection and multiple pests. *APS Features*. doi:10.1094/APSFeature-2018-4.

Alworah G. and Gichuru E.(2014). Advances in the Management of Coffee Berry Disease and Coffee Leaf Rust in Kenya. *Journal of Renewable Agriculture* 2(1):5 DOI: 10.12966/jra.03.02.2014

Avelino, J., Zelaya, H., Merlo, A., Pineda, A., Ordóñez, M., and Savary, S. (2006). The intensity of a coffee rust epidemic is dependent on production situations. *Ecological modelling*, 197(3-4), 431-447.

Bebber, D. P., Castillo, Á. D., and Gurr, S. J. (2016). Modelling coffee leaf rust risk in Colombia with climate reanalysis data. *Philosophical Transactions of the Royal Society B: Biological Sciences,* 371(1709), 20150458. https://doi.org/10.1098/rstb.2015.0458

Beards, C. (1995). Engineering vibration analysis with application to control systems. Elsevier.

Castillo-Chavez, C. and Song, B. (2004). Dynamical models of tuberculosis and their applications. Math. Biosci. Eng., 1(2):361404.

Chan, M., and Jeger, M. (1994). An Analytical Model of Plant Virus Disease Dynamics with Roguing and Replanting. *Journal of Applied Ecology*, 31(3), 413–427. https://doi.org/10.2307/2404439

Coffee and Health (2021) available at: https://www.coffeeandhealth.org/all-about-coffee/coffee-production-today/ [accessed on 13th May 2021]

Condliffe, K., Kebuchi, W., Love, C., and Ruparell, R. (2008). Kenya coffee: a cluster analysis. *Professor Michael Porter, Microeconomics of Competitiveness. Harvard Business School*, 2.

Diekmann, O., Heesterbeek, J.A.P. and Metz, J.A.J (1990). On the definition and the computation of the basic reproduction ratio R in models of infectious diseases and heterogenous populations. J. Math. Biol. 28:365-382

Djuikem, C., Grognard, F., Wafo, R. T., Touzeau, S., and Bowong, S. (2021). Modelling coffee leaf rust dynamics to control its spread. *Mathematical Modelling of Natural Phenomena*.

Djuikem, C., Yabo, A. G., Grognard, F., and Touzeau, S. (2021). Mathematical modelling and optimal control of the seasonal coffee leaf rust propagation. *IFAC-PapersOnLine*, 54(5), 193-198.

Fairtrade (2021). Coffee farmers and workers. Retrieved May 13, 2021, from http://www.fairtrade.org.uk/Farmers-and-Workers/Coffee

Ferreira, S. A., and Boley, R. A. (1991). Hemileia vastatrix: coffee leaf rust. Crop Knowledge Master. University of Hawaii, College of Tropical Agriculture and Human Resources, Hawaii Department of Agriculture. Retrieved May 13, 2021, from http://www.extento.hawaii.edu/kbase/crop/Type/h_vasta.htm.

Gichimu, B. M., and Omondi, C. O. (2010). Early performance of five newly developed lines of Arabica Coffee under varying environment and spacing in Kenya. *Agriculture and Biology Journal of North America*. 1(1), 32

Gichuru, E. K., Ithiru, J. M., Silva, M. C., Pereira, A. P., and Varzea, V. M. (2012). Additional physiological races of coffee leaf rust (Hemileia vastatrix) identified in Kenya. *Tropical Plant Pathology*, 37(6), 424-427.

Gichuru, E., Alwora, G., Gimase, J., & Kathurima, C. (2021). Coffee leaf rust (Hemileia vastatrix) in Kenya—A review. Agronomy, 11(12), 2590. doi.org/10.3390/agronomy11122590

Giddisa, G. (2016). A review on the status of coffee berry disease (Colletotrichum kahawae) in Ethiopia. J. Biol. Agric. Healthcare, 6, 140-151.

Hoffman, D.G. (1981). Packing Problems and Inequalities. In: Klarner, D.A. (eds) The Mathematical Gardner. Springer, Boston, MA. https://doi.org/10.1007/978-1-4684-6686-7_19

ICO (2019). Coffee production in Kenya. Retrieved May 13, 2021, from http://www.ico.org/documents/cy2018-19/icc-124-7e-profile-kenya.pdf

Kar, T. K., and Jana, S. (2013). A theoretical study on mathematical modelling of an infectious disease with application of optimal control. Biosystems, 111(1), 37-50.

LaSalle J. P. (1976). The stability of dynamical systems. Regional Conference Series in Applied Mathematics, SIAM, Philadelphia, PA.

Latif, A., and Syaza, N. (2014). Mathematical modelling of induced resistance to plant disease : a thesis presented in partial fulfilment of the requirements for the degree of Doctor of Philosophy in Mathematics at Massey University, Albany campus, New Zealand.

Lebesgue, H. (1902). Intégrale, longueur, aire. Annali di Matematica Pura ed Applicata (1898-1922), 7(1), 231-359.

Masaba, D. M., and Van Der Vossen, H. A. H. (1982). Evidence of cork barrier formation as a resistance mechanism to berry disease (Colletotrichum coffeanum) in arabica coffee. *Netherlands Journal of Plant Pathology*, 88(1), 19-32.

Melese, A. S., Makinde, O. D., & Obsu, L. L. (2022). Mathematical modelling and analysis of coffee berry disease dynamics on a coffee farm. Mathematical Biosciences and Engineering, 19(7), 7349-7373.

McDonald, J (1926). A preliminary account of a disease of green coffee berries in Kenya. *Transactions of the British Mycological Society*. 11 (1–2): 145–154. doi : 10.1016/S0007-1536(26)80033-6

Mouen, J. A., Bieysse D., Nyassé, S., Nottéghem J. and Cilas C. (2010). Role of rainfall in the development of coffee berry disease in Coffea arabica caused by Colletotrichum kahawae, in Cameroon. *Plant Pathology*. 59. 324 - 329. 10.1111/j.1365-3059.2009.02214.x.

Muhumuza, C. (2018). A mathematical model for the transmission dynamics and optimal control strategy of Coffee Wilt disease (Doctoral dissertation).

Mussatto, S., Ballesteros, L., Martins, S. and Teixeira, J. (2011). Extraction of antioxidant phenolic compounds from spent coffee grounds. *Separation and Purification Technology-SEP PURIF TECHNOL*. 83: 173-179, doi:10.1016/j.seppur.2011.09.036

Nannyonga, B., Luboobi, L. S., Tushemerirwe, P.,& Jabłońska-Sabuka, M. (2015). Using contaminated tools fuels outbreaks of Banana Xanthomonas wilt: An optimal control study within plantations using Runge–Kutta fourth-order algorithms. *International Journal of Biomathematics*, 8(05), 1550065.

Nthiiri, J. K., Lawi, G. O. and Manyonge, A. (2015). Mathematical modelling of tuberculosis as an opportunistic respiratory co-infection in HIV / AIDS in the presence of protection. *Appl. Math. Sci.* 9(105): 5215–5233.

Nutman, F. J., and Roberts, F. M. (1964). Coffee Berry Disease and Coffee Leaf Rust in Kenya. *Outlook on Agriculture*, 4(2), 72–79.

Okosun, K.O. , Ouifki, R. and Marcus, N. (2011). Optimal control analysis of a malaria disease transmission model that includes treatment and vaccination with waning immunity. *Biosystems*, 106,(2), 136-145,

Pontryagin, L. S., Boltyanskii, V. G., Gamrelidze, R. V., and Mishchenko, E. F. (1962). The Mathematical Theory of Optimal Processes. *John Wiley, New York*

Rutherford, M. A. (2006). Current Knowledge of Coffee Wilt Disease, a Major Constraint to Coffee Production in Africa. *Phytopathology™*, 96 (6): 663-666, https://doi.org/10.1094/PHYTO-96-0663.

Schumann, G. L., & D'Arcy, C. J. (2012). Essential Plant Pathology (2nd ed.). APS Press.

Silva, D. N. (2010). Analysis of the neutral and adaptive genetic variation of Colletotrichumkahawae and its relationship with the C. gloeosporioides complex. Lisbon: *University of Lisbon*. p. 102.SSN 0032-0862

Smith, R. F. (1985). A History of Coffee. *Springer US*, Boston, MA. 1–12, https://doi.org/10.1007/978-1-4615-6657-1_1

Souza, R. M. (Ed.). (2008). Plant-parasitic nematodes of coffee. *Springer Science and Business Media*.

Strange, R. N. (2003). Introduction to Plant Pathology. Wiley.

Suryaningrat, W., Anggriani, N., Supriatna, A. K. and Istifadah ,N. (2020). The optimal control of rice tungro disease with insecticide and biological agent. *AIP Conference Proceedings* 2264, 040002 https://doi.org/10.1063/5.0023569

Szenthe, A. (2019). Top Coffee Producing Countries . WorldAtlas. Retrieved May 13, 2021, from https://www.worldatlas.com/articles/top-coffee-producing-countries.html

Van den Driessche, P. and Watmough, J.(2002). *Reproduction numbers and sub-threshold endemic equilibria for compartmental models of disease transmission.* Mathematical Biosciences, 180, 1-2, 29-48. DOI:10.1016/s0025-5564(02)00108-6.

Vandermeer, J., and Rohani, P. (2014). The interaction of regional and local in the dynamics of the coffee rust disease. *arXiv preprint arXiv*:1407.8247.

Vandermeer, J., Hajian-Forooshani, Z., and Perfecto, I. (2018). The dynamics of the coffee rust disease: an epidemiological approach using network theory. *European journal of plant pathology*, 150(4), 1001-1010.

Waller, J.M. (1985). Control of Coffee Diseases. In: Clifford M.N., Willson K.C. (eds) Coffee. *Springer*, Boston, MA https://doi.org/10.1007/978-1-4615-6657-1_9